A METHODOLOGY FOR USING BLUETOOTH TO MEASURE REAL-TIME WORK ZONE TRAVEL TIME

A Thesis
Presented to
The Academic Faculty

by

Stephanie Zinner

In Partial Fulfillment
of the Requirements for the Degree
Master of Science in the
School of Civil & Environmental Engineering

Georgia Institute of Technology
December 2012

A METHODOLOGY FOR USING BLUETOOTH TO MEASURE REAL-TIME WORK ZONE TRAVEL TIME

Approved by:

Dr. Michael Hunter, Advisor
School of Civil & Environmental Engineering
Georgia Institute of Technology

Dr. Randall Guensler
School of Civil & Environmental Engineering
Georgia Institute of Technology

Dr. Angshuman Guin
School of Civil & Environmental Engineering
Georgia Institute of Technology

Date Approved: November 12, 2012

Acknowledgements

The completion of this thesis would not have been possible without the constant support and guidance of several individuals with whom I have worked closely throughout my time at Georgia Tech. I was fortunate to be a part of great group of researchers in my lab, and under the guidance of several competent research engineers and professors whose input was invaluable throughout the development of this thesis.

I would like to especially thank Kathryn Colberg, my close friend and research partner, whose help and support through the last year and a half made my data collection efforts possible. Wonho Suh also deserves many thanks for his great knowledge of Bluetooth technology and his efforts in composing the scripts necessary to collect and process much of the Bluetooth data. I could not have completed this thesis without his constant support and encouragement and willingness to always provide assistance.

Many thanks also to Dr. Angshuman Guin for his willingness to provide input and advice concerning the development of my thesis topic, the design of the Bluetooth system, and also for his review of this thesis. Dr. Randall Guensler also played an important role in helping me cultivate my research interests, providing very important direction to this thesis, and deserves thanks for the review of this thesis. Finally, many thanks go to Dr. Michael Hunter, my advisor, who challenged my assumptions and provided beneficial viewpoints and feedback which led to the generation of a sound research focus. He also deserves thanks for his review of this thesis.

Table of Contents

List of Tables

List of Figures

List of Abbreviations

AFH	Adaptive Frequency Hopping
ALPR	Automated License Plate Recognition
BD_ADDR	Bluetooth Device Address
CMS	Changeable Message Signs
.csv	Comma Separated Value
dB	Decibel
DAC	Device Access Code
DIAC	Dedicated Inquiry Access Code
DOT	Department of Transportation
EB	Eastbound
EDR	Enhanced Data Rate
EST	Eastern Standard Time
FCC	Federal Communication Commission
FHS	Frequency Hopping Synchronization
FHSS	Frequency Hopping Spread Spectrum
FHWA	Federal Highway Administration
FS	Frequency Synchronization
GDOT	Georgia Department of Transportation
GHz	Gigahertz
GIAC	General Inquiry Access Code
GPS	Global Positioning System

GRA	Graduate Research Assistant
Hz	Hertz
IAC	Inquiry Access Code
IrDA	Infrared Data Association
ISM	Industrial, Scientific, and Medical
Kbps	Kilobits per second
km	kilometers
MAC	Media Access Control
Mbps	Megabits per second
MHz	Megahertz
ms	millisecond
mph	Miles per hour
µs	Microsecond (10^{-6} seconds)
MTO	Ministry of Transportation
mW	milliwatt
NTS	Not to scale
RTMS	Radar Traffic Microwave Sensors
TIPS	Travel Time Prediction System
URA	Undergraduate Research Assistant
WB	Westbound

Summary

The importance of accurately capturing travel time in a work zone corridor is twofold. On one hand, the communication of real-time travel time gives travelers the confidence to make informed travel decisions, and divert from the corridor when appropriate direction is given. Secondly, drivers remaining on the corridor including benefit from the ability to prepare for potential congestion ahead, and may reduce speeds and stay alert to unpredictable vehicle stops and starts. Technologies used for travel time measurement include microwave radar sensors, automated license plate recognition, video camera capture, global positioning system probe vehicle tracking, radio frequency identification, Bluetooth technology, etc. Bluetooth is the focus of study in this thesis, selected for its low capital and operational costs, and the ever-increasing presence of Bluetooth devices in the vehicle stream.

This thesis seeks to provide guidance on the deployment of Bluetooth sensors for travel time measurement in work zone corridors. The investigation focuses on the detection characteristics of Class 1 and Class 2 Bluetooth devices, and how cultivating an understanding of these characteristics together with the effect of the sensor inquiry cycle length can suggest a more precise method of travel time measurement. This thesis also explores the range of detection location around a Bluetooth sensor in order to recommend a minimum corridor separation of Bluetooth sensors, and to ascertain the best method of Bluetooth travel time derivation. Finally, this thesis investigates these principles further through multiple side-fire deployments on the I-285 corridor in Atlanta, Georgia; as well as two deployments capturing several hours of active work zone travel time.

Chapter 1: Introduction

Work zones provide several challenges to transportation agencies with respect to traffic management and monitoring, protection of worker and driver safety, maintenance of traffic flow, communication of existing conditions, and suggestion of alternative routes to drivers. Many work zone corridors feature the integration of changeable message sign (CMS) to inform drivers of expected delays and alternative routes; and an array of vehicle detection technologies to capture and transmit vehicle speeds, volumes, and travel times to a central database for disbursement to the traveling public.

The ability to transmit real-time speeds and travel times is of high importance in a work zone because the drivers approaching and traversing the corridor are making route choices based on the information provided to them. Delays associated with the capture and transmission of vehicle travel time translate to a less accurate representation of the current work zone corridor travel time (i.e. “stale” data), and thus less ideal driver decisions. Furthermore, evidence shows that with the presentation of potential alternative routes along with travel time data, motorists are more likely to divert their travel away from the work zone corridor. Evidence on the I-65 work zone in Indiana showed a diversion of 30% when alternative routes were displayed [30], along with 10% diversion in a Texas work zone [34], and 53% responsiveness in Washington D.C [34].

Common intelligent transportation systems deployed in work zone corridors include inductive loop sensors installed in pavement, microwave and radar sensors, and video imaging. Vehicle detection systems on the rise include cell phone tracking,

automatic license plate capture, and wireless Bluetooth sensors, each with their own benefits and drawbacks.

Bluetooth in particular has been rising in popularity due to its comparatively low capital and operational costs, and the proliferation of Bluetooth-enabled (and thus potentially discoverable) devices in the vehicle stream. This growing presence of Bluetooth devices has been encouraged by laws prohibiting the use of hand-held devices while driving. As of 2012, ten states have enacted bans on hand-held cell phone use, and 39 states have banned text messaging for all drivers (including the previous ten) [25, 24]. In addition to cellular accessories, a report released by Strategy Analytics in 2010 claims that by 2015 Bluetooth technology will be a standard component in 85% of all new vehicles, and in over 90% by 2016 [24]. While the penetration rate of Bluetooth devices is higher, a 2008 study conducted by the University of Maryland reports that the current detectable (i.e. set to discoverable, in range for a sufficient time, etc.) Bluetooth prevalence in the vehicle stream is approximately 5% [9]. Other sources rate the Bluetooth sensor sampling rate relative to traffic volume at 1.2% [27], between 2.0% and 3.4% [21], about 4% [23], and 8% [30] Voigt finds that the detection rate changes between freeways and arterial roadways, from 5%-20% to 3%-15%, respectively [18].

Bluetooth also alleviates many driver concerns of perceived privacy invasion associated with other detection modes (such as license plate matching) by detecting the 48-bit Media Access Control (MAC) address tied to devices such cell phones, global position systems (GPS), laptops, Bluetooth-enabled vehicles, and other additional wireless-communication devices, which do not include personally identifiable information [27, 29]. The MAC address is a hexadecimal code, with six sets of two

alpha-numeric pairs (i.e. a1:b2:c3:d4:e5:f6). The first three pairs provide information regarding the device manufacturer, and can be used in identifying the type of Bluetooth device, but there is no direct link available to the user [39]. One way that commercial Bluetooth sensor developers respond further to the privacy concern is to only store the last half of the MAC address, and encrypt the remainder of the address code.

A drawback to Bluetooth device detection for travel time calculation is the range of error associated with location of the device relative to the sensor. Thus, the Bluetooth sensors are not able to pinpoint the location of a device, and thus the exact location of flow breakdown or any important information about individual vehicles in the traffic stream. Although Bluetooth is a formidable technology for travel time measurement, by itself it is unable to alleviate the additional concerns of work zone traffic management.

1.1 Problem Statement

The use of Bluetooth for measuring travel times in work zones is a relatively new practice. Therefore, further investigation is needed as to the placement, spacing, and design of Bluetooth sensors along a work zone corridor to provide the most accurate, real-time measure of travel time possible within the limits of a construction project. The issue of placement refers to where to position the sensors along a work zone corridor to detect the greatest number of devices, most significantly the position relative to corridor entrance and egress points. The issue of spacing refers to the distance separating the Bluetooth sensors, and how shortening or widening the distance impacts the travel time measurement error. Lastly, the design of Bluetooth sensors refers to the sensor inquiry cycle impact on device detection along a corridor.

1.2 Objective

This objective of this thesis is to answer questions regarding the placement, spacing, and design of Bluetooth sensors in a work zone corridor by specifically exploring (1) how best to maximize the number of devices detected by a Bluetooth sensor, with an understanding that more device detections will narrow the confidence bounds surrounding the average travel time output; (2) how best to space the devices along the corridor to minimize the effect of the range of detection location around a Bluetooth sensor; and (3) how best to program the inquiry cycle period to achieve the most accurate measure of real-time travel time. This thesis explores these parameters by studying the detection characteristics of Class 1 and Class 2 Bluetooth devices; the characteristics of Class 1 Bluetooth sensors; and the location where detection is occurring around a Bluetooth sensor. The research then takes these lessons and applies them to a side-fire deployment along a freeway, and finally to a live work zone setting.

1.3 Overview

This thesis begins by providing a review of the literature available pertaining to Bluetooth technology, as well as a discussion of the current practice of travel time measurement in work zones. Next, the thesis delves into the selection and configuration of Bluetooth devices and equipment integrated into these research studies. Following the discussion of equipment, the thesis describes the experimental design, an overview of the parameters for data processing and analysis, and presents the results. The thesis wraps up with concluding thoughts and the recommended next steps to expand the research focus.

Chapter 2: Literature Review

2.1 Overview of Work Zone Travel Time Applications

2.1.1 Methods of Measuring Travel Time in Work Zones

There are several alternative methods of measuring travel time in work zones, and this thesis provides a brief introduction to the current work zone practice for microwave radar sensors, automated license plate recognition (ALPR), and Bluetooth technology, the latter of which is the focus of investigation in this thesis.

2.1.1.1 Microwave Radar Sensors

Microwave radar sensors operate by emitting an energy signature in the direction of the traffic from the side of the road or directly facing the traffic. When a vehicle passes through the energy signal, the signal is reflected back to the sensor, and a time stamp is recorded, along with the parameters listed previously [35]. Each vehicle has a signal derived from the frequency shift between the transmitted and returned signal, which allows for signal matching at two or more stations along the corridor and a travel time calculation. Microwave radar sensors have the ability to transmit across several lanes, and collect parameters such as volume, speed, and occupancy. A drawback to microwave sensors is the poor performance when detecting vehicles at rest.

In 2002, the Ohio Department of Transportation (DOT) deployed the Travel Time Prediction System (TIPS), developed by P.D. Pant of the University of Cincinnati, along a 13 mile work zone corridor on I-75 northbound near Dayton, Ohio. TIPS calculates travel time between stations through an algorithm relating velocity and roadway speed, rather than through vehicle re-identification. The Ohio DOT system consisted of three

CMSs, and microwave radar sensors placed at five stations along the roadway ranging from 5.6 miles to 12.5 mile apart. The TIPS system displayed travel time in four minute increments. For the 119 completed runs, the predicted travel time for the system ranged from eight minutes to 36 minutes. The system reportedly had 88% of travel times accurate to within four minutes, and a 65% to 71% of travel times accurate to within two minutes [33].

During the same time period in summer 2001, a TIPS system was deployed in a Wisconsin work zone on I-94 southbound. The traffic management system consisted of two CMSs and five microwave radar sensors. The CMSs were placed three miles apart, starting six miles before the start of the work zone. The first microwave radar sensor was placed with the first CMS, with the next three placed in two mile increments up to the construction taper, and last placed three miles into the work zone corridor for a total corridor length of about 10.3 miles. This system displayed the travel time in four minute increments, with the range of predicted travel times falling between 16 and 48 minutes depending on the level of congestion. The results of this travel time output show that travel times were within four minutes of the actual travel time 46% and 66% of the time for the two CMSs used; and within 30% of actual travel times for 85% and 86% of all observations for the two CMSs [36].

The Arkansas State Highway and Transportation Department also featured four radar traffic microwave sensors (RTMS), each on the eastbound and westbound approach ends of a 6.3 mile long work zone corridor, in the summer of 2002. The eastbound sensors were placed along 7.8 miles before the east end of the work zone, and the westbound sensors along 12.8 miles before the west end of the work zone. The RTMS

system proved difficult to calibrate due to the variable changing lane closure schedule, so the RTMS was replaced by Doppler radar units to solve the calibration issues [28]. The average free flow work zone travel times for the eastbound and westbound directions were 12 minutes and 47 seconds, and 16 minutes and 50 seconds, respectively. The displayed travel times were within five minutes of the actual travel time 90% of the time, out of 144 total records.

2.1.1.2 Automated License Plate Recognition

ALPR devices operate by taking a picture of the license plates of passing vehicles with either color, black-and-white, or infrared cameras. Each image capture is associated with a time stamp and the GPS coordinates of the ALPR camera. The plate processing follows the four steps: image acquisition, license plate extraction, license plate segmentation, and character recognition. After the character recognition step the plate has been transformed into a usable format (i.e. text file output) and may be matched at various locations along the corridor to generation travel time measurements [37]. ALPR cameras are typically used by law enforcement agencies, but have been on the rise as a method of travel time measure. A drawback is the expense of the ALPR equipment and processing system. One example of ALPR travel time collection in a work zone was in Arizona in 2004. The Federal Highway Administration (FHWA) released a case study following the use of a license plate matching system to manage traffic during the reconstruction of 13.5 miles of Arizona State Route 68 [16]. The system was able to successfully read 60% of the license plates and match 11% of the plates for travel time readings. The system also immediately encrypted the license plates before archiving them to allay the privacy concerns of the public.

2.1.1.3 Bluetooth Sensor Technology

The basic tenets of Bluetooth sensor operation include the sensor transmission of an "inquiry" signal on an unlicensed radio frequency, and the simultaneous "scanning" of radio frequencies by Bluetooth-enabled devices such as cell phones or navigation systems within vehicles. Detection occurs when a Bluetooth-enabled device receives the message from the Bluetooth sensor and responds with its unique MAC identifier, to which the sensor attaches a time stamp and records in a log. Travel time is generated by matching the MAC address of a Bluetooth-enabled device at different points along the corridor, and taking a difference of the time stamps to derive a travel time measure. The details of current Bluetooth practices in work zones, and an in-depth description of the Bluetooth detection process and related properties are discussed in the following sections, and lay the groundwork for the research presented in this thesis.

2.1.2 Previous Applications of Bluetooth to Measure Work Zone Travel Time

Bluetooth has become a prevalent technology for work zone travel time measure due to its low capital and operational costs, a steadily increasing Bluetooth device population, and Bluetooth's ability to transmit over long-range distances of approximately 100 meters (330 feet). There have been several cases of successful Bluetooth travel time application in active work zones, such as in 2009 when the Indiana DOT placed semi-permanent Bluetooth sensors along a ten mile work zone corridor on I-65 atop CMSs, and portable units along alternative diversion routes around the work zone (indicated to motorists through the CMSs) [30]. The Bluetooth sensors installed on the CMSs provided a direct uplink in near-real-time to Indiana DOT's Advanced Traveler Information System; and the portable units stored data internally for later download and

post-processing. The processing of Bluetooth travel times enabled Hasemen, et al., in 2010, to note where the delay exceeded ten minutes, and to relate this to the development of a queue [30].

In 2010, the Ontario Ministry of Transportation (MTO) in Canada deployed the BluFax Bluetooth system to monitor traffic delay during the Fairchild Creek culvert replacement project. Two BluFax units were placed 3 kilometers (km) on either side of the bridge under construction for point to point travel time readings [17]. The findings of travel time accuracy were not available for this study.

In 2010, Illinois DOT installed 22 Bluetooth sensor boxes designed by Trafficast in a 27 mile work zone corridor along the Eisenhower Expressway [29]. The Bluetooth sensors were employed to provide travel time information to motorists when the roadway resurfacing impaired the in-pavement sensors that were the previous source of travel time and congestion data. All accounts of this work zone are present in media records. Thus, travel time accuracy results are not available for this study

Currently in 2012 the Texas A&M Transportation Institute designed and monitors a travel information system for the I-35 expansion project; a 96 mile stretch from Hillsboro to Salado in Texas. The traffic monitoring includes the integration of Bluetooth sensors for travel time, Wavetronix systems for volume, and radar systems for speed measurement to judge the build-up of queues before the work zone entrance [32]. As this study is currently underway, findings are not available at this time.

2.1.3 Advantages and Disadvantages of Bluetooth in Work Zones

A Portland, Oregon Pilot Study recognizes several advantages of Bluetooth including its ability to provide accurate ground truth data without having to add probe

vehicles into the system, the ability to provide a wireless communication link between the Bluetooth system and an online server for real-time travel data transmission, and the relative low cost of Bluetooth technology compared to the alternative license plate readers and in-road loop detectors [5]. A study by the University of Maryland in 2008 estimated that Bluetooth technology was 500 to 2500 times more economical (i.e. less expensive) than equipping probe vehicles to obtain the same number of data points [9]. Hasemen, et al., similarly finds that alternatives to Bluetooth such as license plate matching and probe vehicles are "prohibitively expense" [30]. Furthermore, Bluetooth detection does not require a direct line of sight from the sensor to the device, and can also travel through most physical barriers, according to a 2001 study by Bringham Young University [10]. However, limited research by Kittelson and Associates, Inc. finds that despite being penetrable, the presence of a car door may decrease the detection radius of the sensor by as much as half due to interference [5].

Some disadvantages of Bluetooth technology include the need for an exterior power source for extended periods of operation, as well as the inability of Bluetooth to detect vehicle trajectories and point speeds [5]. Additional obstacles of Bluetooth system operation identified in a Portland, Oregon Pilot Study include the interference from stationary nearby devices, devices traveling on alternative routes, as well as complications that arise from the internal computer clock drift and detection ping cycles [5].

2.2 Overview of Bluetooth Technology

Bluetooth is a method of wireless device communication operating on the Industrial, Scientific, and Medical (ISM) unlicensed radio frequency band of 2.4000

Gigahertz (GHz) to 2.4835 GHz, which is the same frequency band for the communication of wireless cordless phones and other wireless devices [12]. The 2.4 GHz frequency band consists of 79 1-Megahertz (MHz) channels from 2402 to 2480 MHz, across which a Bluetooth signal will "hop" in a randomly defined order, making changes up to 1,600 times per second (or once every 625 micro-seconds (μs)) [6, 13]. The hopping sequence of Bluetooth transmission, formally called the Frequency Hopping Spread Spectrum (FHSS), occurs to minimize the likelihood of interference with other Bluetooth signals competing for communication along the same 2.4 GHz frequency band [6].

According to the Federal Communication Commission (FCC) sections 15.247 and 15.249 there are certain criteria that frequency hopping on the 2.4 GHz band must meet. These include a random hopping pattern across at least 15 non-continuous frequency channels, and being stationary at a given frequency no longer than 0.4 seconds multiplied by the number of frequency channels [7]. Of the 79 hopping frequencies available on the unlicensed spectrum, 32 are used for inquiry (called "wake-up frequencies"), and another 32 are used for inquiry response based on the Bluetooth versions for the United States and most European countries [3, 2, 14].

2.2.1 Sensor-Device Inquiry Protocol

2.2.1.1 Procedure

The inquiry protocol establishing the sensor-device interaction is initiated by a *master* device, and received by a *slave* device. The master device sends out an inquiry packet of information on the 2.4 GHz frequency band in search of Bluetooth-enabled devices, or slaves. The protocol established the master and slave because one device is

controlling the communication (the master) and other device is responding to and following the directions of the master device (the slave). The roles may also be reversed at any time.

There are two major states and are seven substates that devices can fall under during the device connection process. The two major states are standby and connection. The substates vary depending on whether a device is a master device or a slave device, and consist of the following: (1) inquiry (*master*); (2) inquiry scan (*slave*) (3) inquiry response (*slave*); (4) page (*master*); (5) page scan (*slave*); (6) slave response (*slave*); (7) master response (*master*) [1, 2, 10, 12]. Following the final master and slave responses, a connection is initiated between the two devices.

The first initiation of connection protocol is when a master device enters the inquiry substate. The inquiring device generates a hopping sequence based on an inquiry access code (IAC), and the inquiring device's internal clock, which determines the phase in the hopping sequence [10, 12]. The IAC may be general (GIAC) if the inquirer wishes to discover all devices in range, or dedicated (DIAC) if the inquirer wishes to find specific types of devices (or different device classes) [11, 12]. The inquiring device then broadcasts a message or ID packet over the 32 wake-up frequencies of the 2.4 GHz frequency band in the pre-determined hopping sequence, which is simply a packet containing an access code, packet header, and payload [11]. Every time the inquiry hops to the next frequency it transmits two ID packets, one of which the receiving device should register when it hops to the same frequency. Each ID packet is 625 μs in length, or one time slot. During the inquiry phase the ID packet lengths are reduced to 312.5 μs half slots.

The 32 inquiry channels are separated in two unique 16 channel trains, and there must be two iterations of each train during the inquiry process. The inquiry message first transmits over the first set of 16 frequencies, repeating 256 times, and then transmits over the second set of 16 frequencies. During the inquiry state the hopping rate increases from 1600 hops per second to 3200 hops per second for the inquirer to increase the likelihood of a connection [12]. The faster inquiry rate is what allows for the 312.5 half-slot during frequency hopping. The inquiry substate proceeds continuously until it receives a response from a potential slave device.

The second substate for a device to enter is the inquiry scanning substate, which a device must be in to receive the inquiry packet transmitted from the master device. The potential slave device is not always active, but rather is in the standby state and will periodically enter the inquiry scan state and hop on the 32 wake-up frequencies. The scanning frequency hopping sequence takes place at a much slower rate, changing frequencies every 1.28 seconds (remaining for 2048 time slots on each frequency band) [12, 14, 15]. The inquiry scanning substate follows the same frequency hopping mechanism described above, which is determined instead by the internal clock of the scanning device, and the device access code. Just as for the inquiring device, the scanning device hops across the 32 frequencies between two sets of 16-frequency trains.

The third substate is the inquiry response substate, which a device enters after scanning the frequencies and receiving an ID packet from the master device. The device then sends an inquiry response message, or Frequency Hopping Synchronization (FHS) packet, which includes the device's native clock and a 48-bit Bluetooth Device Address (BD_ADDR). Once again, this packet covers a single time slot, or 625 μs. The FHS

packet informs the potential master device what hopping sequence the local device is following, so the master device can use that sequence for the next communication. However, the receiving device does not send the FHS packet right away. Instead, the device halts the inquiry process for a time period of x time slots, randomly selected from 0 to 1023 (a maximum of 639.375 milliseconds (ms)) [3]. This period is called the back-off limit, and adds to the average total delay in device discovery [14]. This back-off time minimizes the potential for a signal collision with other devices that may be responding to the same master inquiry ID packet. After this random interval expires, the local device sends the FHS packet when it receives the next inquiry message from the master device [12, 3].

After the receiving device sends the FHS packet to the inquiring device, there is a period of delay, referred to as frequency synchronization (FS) delay, before the potential master begins to transmit using the frequency hopping sequence delivered in the FHS packet. Once the potential master receives the FHS packet, it enters the page substate. In the page substate, the potential master sends a Device Access Code (DAC) packet to the potential slave, which should be in the page scan substate. The inquirer sends the DAC packet using a frequency hopping sequence determined by the FHS packet sent by the potential slave, which is based off the local device's address and local clock. The DAC packet contains unique information about the master device, allowing the potential slave device to request access to the master device.

Meanwhile, the potential slave device entered the page scan substate after sending the first FHS packet response to the potential master device. In the page scan substate,

the potential slave device hops according to the internal clock and local device address [1].

When the potential slave device receives the DAC packet from the master device, it responds with a DAC packet, or page response packet. Immediately upon receiving the return DAC packet from the potential slave device, the master device sends an FHS packet to the local device, which contains the master device's native clock and BD_ADDR. After receiving the FHS packet, the potential slave device adjusts its hopping frequency to match that of the master device, and sends an additional reply DAC packet. After receiving the final DAC packet, a connecting is initiated and the master device controls the communication with the slave device. This connection is called a piconet, which can be point to point, or point to multipoint [19]. Multiple piconets together make up a scatternet. Now that the inquiry has completed, the master device reduces its hop rate from 32000 hops per second to 1600 hops per second, and the slave device increases its hop rate the same rate for matching communication [10, 3, 12]. Figure 1 below provides a summary of the device-sensor inquiry process.

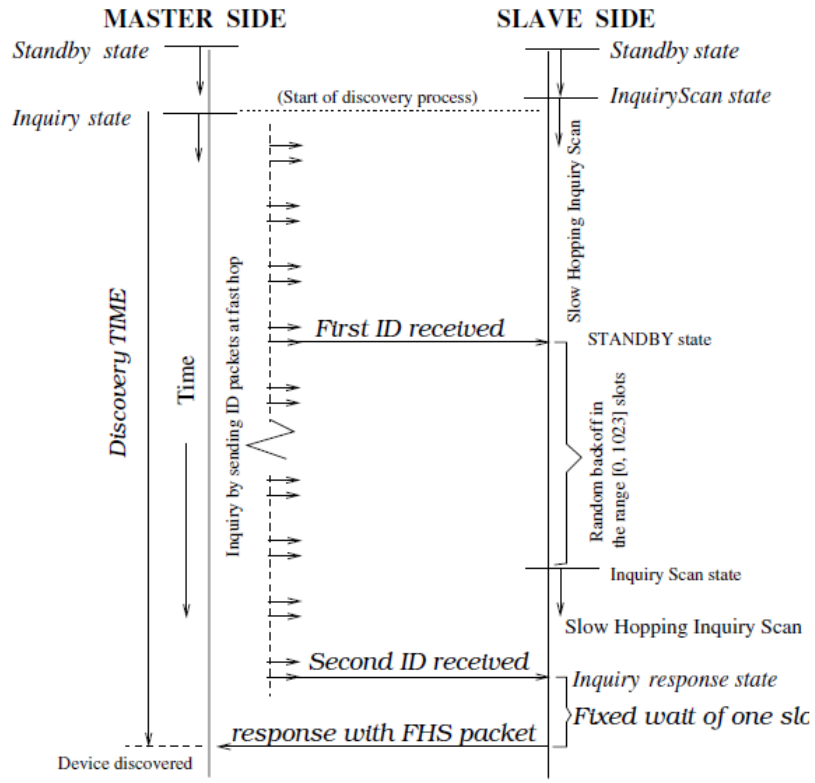

Figure 1 Device-Sensor Inquiry Protocol Procedure [14]

2.2.1.2 Inquiry Cycle Length

There are many elements that contribute to the industry standard, and Bluetooth-recommended specification of a 10.24 second inquiry cycle. The inquiry cycle is designed as the optimal time needed to detect all discoverable Bluetooth devices within range. The Bluetooth specifications recommend completing two iterations of each 16-frequency train, and repeating the entire inquiry process 256 times. The 256 repetitions come from 16 multiplied by 16, to cover all frequency pairings between the potential master and slaves alternating between the two 16-frequency trains. The 10.24 second

inquiry cycle is derived from the following formula: 2 trains × 0.01 second/train × 2 iterations × 256 repetitions = 10.24 seconds [10].

A study by Peterson, et al., in 2006 recommends that an inquiry cycle should be limited only to detect an "acceptable number of devices" [15]. Their study suggests that a single sensor will detect 98.95% of scanning devices in 5.12 seconds. The study further suggests that the inquiry method can be reduced to 3.84 and 1.28 seconds using standard and interlaced inquiry modes [15]. Figure 2 below provides a summary of Peterson, et al.'s inquiry length investigation. Chakraborty, et al., also finds that two devices typically take 5.76 seconds to establish a connection [14]. Another component to device inquiry is the capacity of a sensor for detection. Voigt identifies a limit of eight MAC address reads per second [18].

Inquiry_Length	Inquiry Duration	% Discovered
1	1.28 s	36.71
2	2.56 s	48.96
3	3.84 s	86.71
4	5.12 s	98.95
5	6.4 s	99.98

Figure 2 Summary of Inquiry Duration Investigation by Peterson, et al. [15]

An additional factor influencing the total detection time is the delay inherent in the detection process. Zaruba, et al., identifies the total inquiry delay as a function of the FS delay and random back-off delay. The first FS delay occurs in the initial inquiry substate when the master sends the first IAC to the potential slave. The second FS delay is the time it takes after the potential slave wakes up from its back-off, to when it receives

and responds to the final inquiry message. These delays cause together a total potential inquiry delay of 679.375 ms [3]. A study by Woodings, et al., proposes the addition of Infrared Data Association (IrDA) to reduce the device discovery time to 1.12 seconds [10]. Chakraborty, et al., discuss how eliminating the repetitions of the two separate 16-frequency trains, as well as reducing the back-off limit to between 200 and 300 time slots (from the current 1023) will reduce the inherent delay in device discovery [14]. Figure 3 below is graphic from the Chakraborty report. In addition to decreasing the inquiry delay, only requiring one run of each train would cut the inquiry time in half to 5.12 seconds.

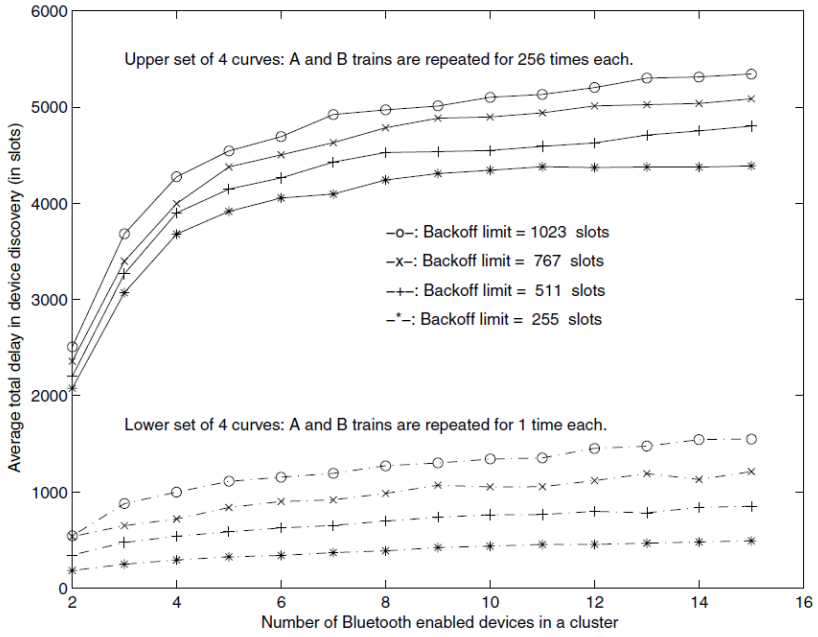

Figure 3 Average delay as a function of the number of discoverable devices [14]

2.2.2 Bluetooth Class and Model Specifications

Since the first Bluetooth specifications released in 1999 there have been many new standards created for the development of Bluetooth-enabled products. Over the years, Bluetooth has seen the addition of the adaptive frequency hopping (AFH) feature, which allows the Bluetooth inquiry frequency hopping pattern to avoid frequencies with a fixed interference stream. Additional features include an enhanced data rate (EDR) transfer, which increases the base information transfer speed from 1 Megabit per second (Mbps) to 3 Mbps. The more realistic data transfer rate for Class 1 and Class 2 devices is 721 Kilobits per second (kbps) and 2.1 Mbps, respectively [4]. The EDR feature is present in Bluetooth model specifications 2.0 and forward, with version 1.2 and prior having the slower data transmission speed of 1 Mbps [22, 6]. The most recent Bluetooth model specifications allow for a data transfer rate upwards of 10 Mbps.

Bluetooth-enabled devices also fall under a power class of 1, 2, or 3, with Class 1 being the highest power class and Class 3 being the lowest power class. The power class represents the amount of power draw the device requires for operation, measured as 1milliwatt (mW) (0 decibels (dBm)) for Class 3 devices, 2.5 mW (4 dBm) for Class 2 devices, and 100 mW (20 dBm) for Class 1 devices. The dBm represents the power ratio in decibels to mW. A compliance overview published by Texas Instruments in 2005, and SEMTECH International's overview of FCC regulations for ISM Band devices, list that FCC sections 15.247 and 15.249 put the maximum power at +21 dB with 15 to 75 frequency hopping channels [7, 8]. However, with frequency hopping in place, and greater than 75 hopping channels, power can be a maximum of +30 dB.

The power requirements for the different Bluetooth classes correlate with the transmission range of the power class. Class 1 Bluetooth-enabled devices experience the greatest transmission range of approximately 100 meters (330 feet), followed by Class 2 at 10 meters (33 feet), and Class 3 at 1 meter (3 feet) [19]. Higher power devices such as laptops, tablets, and specially designed adaptor plug-ins typically fall under the Class 1 rating and allow for transmission of data over a much farther range than their Class 2 counterparts found in Bluetooth headsets, hand-held GPS devices, et cetera. Class 3 Bluetooth devices are much less common, and therefore the focus of the research investigation in this thesis revolves around Class 1 and Class 2 devices.

Therefore, the performance and characteristics of any Bluetooth-enabled device within the discoverable population of a Bluetooth sensor is defined by the Bluetooth specification guidelines, which determines the transmission speed and adaptability; and the Bluetooth power class, which determines the transmission range. Knowing the range of properties a detectable population is expected to exhibit allows for the proper design of a Bluetooth sensor system.

2.2.3 Bluetooth Detection Range

The typical range of Class 1 Bluetooth sensor is approximately 330 feet. As such, a Bluetooth-enabled device must be within the 330 foot radius surrounding a Bluetooth sensor if it is to be detected. The detection between device and sensor can be likened to two men standing on a football field; one at an end zone and one at midfield [19]. If the two men are both Class 1 devices then as one man shouts to the other across a 330 foot distance, the sound will make it to the second man, and he will be able to detect the communication and return a shout back across the field for the first man to receive.

However, if the first man is a "Class 2 device" then when he attempts to shout to the second man down the field, the shout will only travel approximately 33 feet (not far enough for the second man to receive the communication and respond). This analogy helps explain the boundaries of the communication between Class 1 and Class 2 Bluetooth-enabled devices, and that the communication range is limited by the weaker power class [19]. As an example, the XRange2000 Bluetooth transmitter product has an advertised range of 1000 to 2000 meters, but a real-application communication range of up to 250 meters, limited by the capabilities of the cell phones on the receiving end [20].

A study completed by Motorola on Bluetooth radio performance in 2008 describes an alternative view of the real Bluetooth device range. The Motorola Technical Brief states that the Bluetooth device range is a combination of the radio frequency (RF) power of the transmitter, the receiver sensitivity, and the absorption rate of the medium the transmission is attempting to travel through [6]. According to this analysis, detection range is function of the maximum allowable path loss, which is the difference between the maximum device power, and the maximum device sensitivity, which is independent of whether the Bluetooth device is power class 1 or 2. Note Figure 4 below, from the Motorola Technical Brief, which provides a visual representation of the principle just described. This shows that Class 1 and Class 2 Bluetooth devices can theoretically have the same transmission range. Thus, by supplying a Class 2 device with a greater sensitivity, the maximum power loss is increased, thus increasing the transmission range.

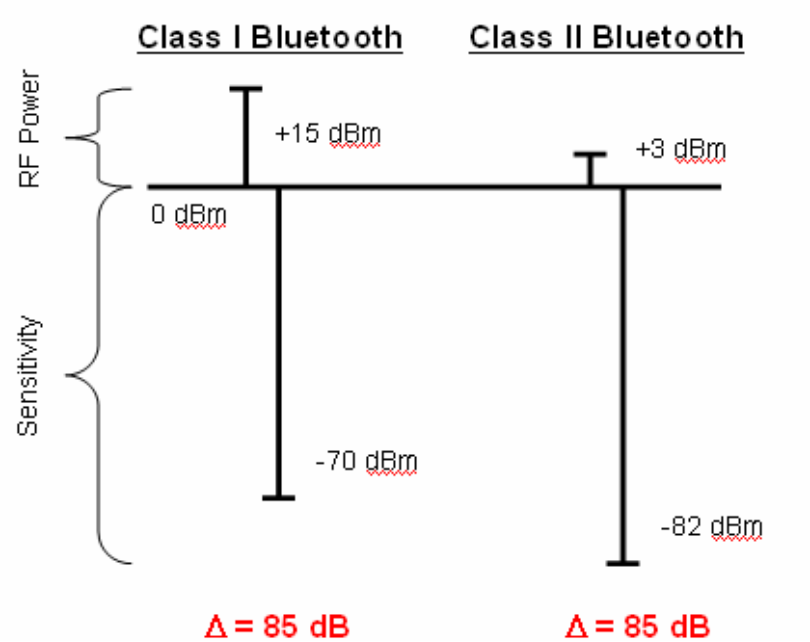

Figure 4 Class 1 and Class 2 Bluetooth Radio Performance [6]

2.2.4 Bluetooth Travel Time and Speed Error

J. Porter, et al., cites the result of a Virginia DOT study that capturing between 2% and 3% of the total roadway traffic volume (three samples every five minutes) is acceptable for generation of a meaningful travel time measure [23]. Monsere, et al., reports that travel time estimates that fall within 20% of the actual travel time can still provide useful information to motorists, and that this error value is deemed acceptable by the FHWA [26]. Tudor, et al., finds that a travel time delay error of five minutes was acceptable for a 7.8 and 12.8 mile work zone corridor in the study of smart work zone technology in Arkansas (with approximate 13 minute and 17 minute respective free flow travel times). Several motorists still filed complaints that this margin was too great [28]. Malinovskiy, et al., conducted a field test on a 0.98 mile corridor comparing the performance of Bluetooth and ALPR technologies for time travel measurement.

Malinovskiy, et al., find that although Bluetooth sensors are out-detected by ALPR cameras by about 25 times, and show a prejudice towards picking up slower moving devices (and generating longer travel times) they are still a viable alternative to ALPR for travel time measurement [38].

A study by Haghani, et al., at the University of Maryland derived a method for calculating the error in Bluetooth speed derivation, which they define as a function of the segment length, and the real vehicle speed (i.e. corridor design speed). The function is an expansion of the Speed = Distance/Time equation, with each speed, distance, and time component having a built in error. Haghani, et al., assumes a maximum possible distance error of 600 feet (from the designed range of the Bluetooth sensor), and a minimum possible time error of five seconds (from the scan period of the Bluetooth sensor). A simplified formula for the maximum possible speed error finds that error increases with vehicles speeds from 15 miles per hour (mph) to 45 mph, and decreases as speed increases above 45 mph. Haghani, et al., uses a first-to-first travel time calculation method. The findings also show that as the corridor length shortens below one mile, the speed error increases from below 2.5 mph to 3.5 to 4.5 mph for speeds ranging from 30 to 60 mph [21]. Wasson, et al., similarly finds that the error associated with the spatial location of Bluetooth detection decreases as larger, two to three mile segments separate Bluetooth sensors [27]. J. Porter, et al., also cites the findings from a Washington DOT study of omnidirectional and directional antennae, which states that shorter corridors have inherently higher errors in travel time measurement [23].

2.3 Summary

The literature discusses how Bluetooth is an up-and-coming technology for travel time measurement in work zone corridors. There are several advantages of Bluetooth technology such as the low cost and the proliferation of discoverable Bluetooth devices. Some disadvantages include the inability to detect point speeds and the potential interference from devices on adjacent corridors. A Bluetooth connection consists of a master device, which initiates device communication through an inquiry process and controls the communication; and a slave device, which response to the commands of the master device. The roles may be reversed at any time. The Bluetooth specification states that an inquiry cycle length of 10.24 seconds is necessary to detect all discoverable devices within range of a Bluetooth sensor, but additional sources comment that a cycle as short as 5.12 seconds is adequate. Furthermore, Bluetooth devices fall under different power class ratings, which correspond to the speed and distance over which devices can communicate. Higher power class devices (Class 1) have a greater transmission speed and range than lower class devices (Class 2), by about three times. The properties of detection range influence the error associated with a Bluetooth travel time measurement. To reduce this travel time measurement error, many sources concur that a sensor separation of greater than one mile, preferably two to three miles, should be maintained along a corridor.

The following chapters of this thesis explore Bluetooth technology further in multiple deployments in a live work zone environment on I-285 in Atlanta Georgia, as well as in several comparison deployments along I-285 in a non-active work zone. This thesis also investigates the 10.24 cycle length to assess whether the length is adequate to

detect a sufficient number of devices entering a sensor's field of view. Furthermore, the following chapters examine the detection properties of Class 1 and Class 2 devices, as well as the detection range trends of these two power classes, and finally the resulting error in Bluetooth travel time associated with this range error. The next chapter, Chapter 3, provides details on the devices and equipment selected for this research study, and their method of configuration.

Chapter 3: Device and Equipment Selection and Configuration

3.1 Selection of Bluetooth Enabled Devices

Bluetooth-enabled devices played a large role in the research contained within this thesis. They were first used as subjects in a controlled indoor test measuring sensor capacity, cycle detection pattern, and detection headway by device power class. Their second use was to serve as components of a known device population within probe vehicles during field deployments. Details of the test deployments are described in Chapter 4. The selection of Bluetooth-enabled devices to include in this study was driven by the need to provide a realistic representation of the devices existing in a typical device population. The knowledge that both Class1 and Class 2 devices are present in the traffic stream underscored the importance of investigating their properties and detection behavior in separate groups.

3.1.1 Class 1 Bluetooth-Enabled Devices

The research presented in this thesis includes four different Class 1 Bluetooth-enabled devices. The devices are Asus Eee PC Netbooks, Toshiba Thrive AT-100 Tablets, and IOGear USB Bluetooth Adapters (plugged into Asus Netbooks to provide a power source). An additional device used for the indoor control test series is an Apple Mac Mini, Model #A1347, © 2010, referred to as rg49mac1. Table 1 provides a summary of the Class 1 Bluetooth specifications and anticipated transmission range and speed. Figure 5 and Figure 6 also show images of the Asus netbook and Toshiba Thrive AT-100 tablet, respectively.

Table 1 Summary of Class 1 Device Specifications

	Bluetooth Version	Power Class	Frequency	Data Transfer Rate	Transmission Range (anticipated)
IOGear USB Bluetooth Adapter	2.0 + EDR	Class 1	2.4 GHz	2.1 Mbps	330 feet
Asus Eee PC Netbook	2.1 + EDR	Class 1	2.4 GHz	2.1 Mbps	330 feet
Toshiba Thrive AT-100 Tablet	2.1 + EDR	Class 1	2.4 GHz	2.1 Mbps	330 feet
Apple Mac Mini, Model #A1347, © 2010	2.1 + EDR	Class 1	2.4 GHz	3.1 Mbps	330 feet

(a) (b)

Figure 5 (a) IOGear Adapter connected to Asus netbook and (b) close-up of IOGear adapter with MAC ID stamp

Figure 6 Toshiba Thrive AT-100 Tablet

3.1.2 Class 2 Bluetooth-Enabled Devices

The Class 2 Bluetooth devices selected for this study include handheld QStarz (models BT-1000eX and BT-1000XT) GPS units and Ikross FM transmitter car-adaptors. Table 2 provides a summary of the Class 2 device specifications and anticipated transmission range and speed. Figure 7 also shows an image of the Ikross FM Transmitter. The QStarz GPS devices are described in more detail in Section 3.5.1.

Table 2 Summary of Class 2 Device Specifications

	Bluetooth Version	Power Class	Frequency	Data Transfer Rate	Transmission Range (anticipated)
QStarz BT-1000eX	1.2	Class 1	2.4 GHz	721 kbps	33 feet
QStarz BT-1000XT	1.2	Class 1	2.4 GHz	721 kbps	33 feet
Ikross FM Transmitter	1.2	Class 1	2.4 GHz	721 kbps	33 feet

Figure 7 Ikross FM Transmitter

3.2 Bluetooth Sensor Configuration

This thesis discusses the configuration of both a custom Bluetooth sensor developed for this effort and commercial Bluetooth sensors. The custom Bluetooth sensor system was developed by the Georgia Tech research team early in 2011. The commercial Bluetooth system was purchased from Digiwest in summer 2012, and operates using BlueMAC software with a wireless uplink to an online tracking database. Digiwest was deployed in all Bluetooth deployments in hopes of providing a commercial ruggedized alternative for travel time measurement in a work zone. However, at the time of deployment the system did not perform as expected, so a travel time comparison was not possible. Additional efforts are underway to determine if the commercial deployment issue was related to user error or equipment malfunction.

3.2.1 Custom Class 1 Bluetooth Sensor

The custom sensor configuration is comprised of five components: (1) one IOGear universal serial bus (USB) Bluetooth adaptor, (2) one ASUS netbook running a

Ubuntu Linux operating system, (3) one 32 foot USB extension cable providing a connection between the IOGear adaptor and ASUS netbook, (4) one ten foot tall tripod assembly consisting of a vertical body shaft and a three foot long perpendicular arm, and (5) one 3/4 inch male PVC adaptor providing a secure, immobile connection between the tripod arm and adaptor/extension cable joint. The sensor is designed to be mounted at a ten foot height, based on the findings presented in Box's 2011 thesis that a ten foot antennae height will have the greatest detection rate [40]. Below, Figure 8 shows the custom sensor configuration and Figure 9 shows a close-up of the PVC adaptor connection to the tripod arm with the attached IOGear USB Bluetooth adapter.

Figure 8 Typical custom Bluetooth sensor configuration

Figure 9 PVC adapter connection to tripod arm and USB extension cable

As Chapter 2 discusses, a Bluetooth-enabled device can act as either a master or a slave in the device communication protocol. The roles are established when one device, in this case the IOGear ISB adaptor, is instructed to send an inquiry message to Bluetooth-enabled devices within a detectable range. The IOGear USB Bluetooth adapter also acts as a discoverable device in other applications in this research, exemplifying the versatility in Bluetooth technology.

3.2.1.1 Custom Sensor Time Sync

An important component of the custom Bluetooth sensor configuration is syncing the internal Bluetooth clocks to Eastern Standard Time (EST). This time sync ensures that at the start of a data collection period all sensors are detecting in the same time frame. With the sync to EST, the time of the detection can then also be linked to the time stamps retrieved from other vehicle tracking methods such as GPS systems and license plate capture.

The time sync proceeds by powering on the netbook and loading the Windows XP operating system. Once the netbooks have loaded, the user selects the clock in the lower right hand corner of the display and selects “change date and time settings”. Once all the

netbooks are on this page, the user changes the netbook time according to the known EST obtained via a cell phone or network-connected computer, with accuracy to the nearest second. Software has since been developed to sync the netbooks with greater accuracy, but was not available for the data collection efforts undertaken in this research. Conducting a time sync before every Bluetooth deployment is recommended because the internal netbook clock experiences a positive drift in time as the netbook is in operation. The internal drift is small, observed as a drift of four seconds over an eight hour period of operation (or 0.5 seconds per hour).

3.2.2 Digiwest Commercial Sensor

The Digiwest Bluetooth system is designed as a pole mount system. For the purpose of this thesis, the pole mounting system was not possible, due to the long time necessary to process an approval for access to a pole, the temporary nature of the deployments, and the poor chance of a pole existing where the deployment was to take place. Therefore, a tripod mounting system was designed to accommodate the Digiwest Bluetooth sensor. With the battery installed in the unit, the weight of a single system is approximately 15 pounds, so a very sturdy system was needed to support the unit at a ten foot height and insure that the vertical arms do not sway. Figure 10 shows the front and back views of the final configuration, which consists of two three-legged tripods with ten foot vertical body shafts connected by two PVC arms onto which the Digiwest unit is secured.

Figure 10 Digiwest system deployment configuration showing the full front view (left) and a close-up view of the back configuration (right).

3.3 Custom Sensor Inquiry Cycle

The Class 1 IOGear USB Bluetooth adaptor described in Section 3.2.1 is the sensor that initiates the detection of Bluetooth-enabled devices. The Class 1 adapter follows an inquiry cycle initiated by two PERL functions which run on the ASUS netbook Ubuntu platform. The first function, or loop function, continuously scans the vicinity for other Bluetooth-enabled devices within range, and is continuously submitting the inquiry message to surrounding devices.

The second function, or scan_id function, monitors the result of the inquiry process and writes an entry into a .log file for every device detected including the UNIX time stamp (column A) obtained from the netbook, MAC Address (column G) obtained

from the inquiry response data, and date. A sample of the output .log file, once imported into Microsoft Excel for analysis, is shown in Figure 11. The PERL scripts do not filter out repeat detections, but provide all the raw data associated with the deployment. This allows for filtering during the post-processing stage according to the objective of the analysis.

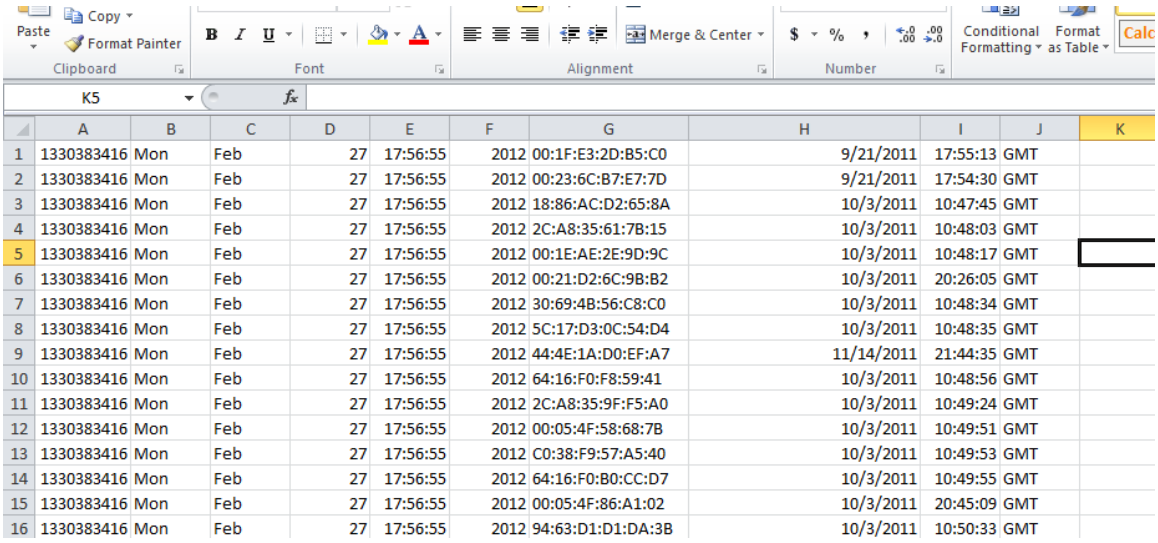

	A	B	C	D	E	F	G	H	I	J	K
1	1330383416	Mon	Feb	27	17:56:55	2012	00:1F:E3:2D:B5:C0	9/21/2011	17:55:13	GMT	
2	1330383416	Mon	Feb	27	17:56:55	2012	00:23:6C:B7:E7:7D	9/21/2011	17:54:30	GMT	
3	1330383416	Mon	Feb	27	17:56:55	2012	18:86:AC:D2:65:8A	10/3/2011	10:47:45	GMT	
4	1330383416	Mon	Feb	27	17:56:55	2012	2C:A8:35:61:7B:15	10/3/2011	10:48:03	GMT	
5	1330383416	Mon	Feb	27	17:56:55	2012	00:1E:AE:2E:9D:9C	10/3/2011	10:48:17	GMT	
6	1330383416	Mon	Feb	27	17:56:55	2012	00:21:D2:6C:9B:B2	10/3/2011	20:26:05	GMT	
7	1330383416	Mon	Feb	27	17:56:55	2012	30:69:4B:56:C8:C0	10/3/2011	10:48:34	GMT	
8	1330383416	Mon	Feb	27	17:56:55	2012	5C:17:D3:0C:54:D4	10/3/2011	10:48:35	GMT	
9	1330383416	Mon	Feb	27	17:56:55	2012	44:4E:1A:D0:EF:A7	11/14/2011	21:44:35	GMT	
10	1330383416	Mon	Feb	27	17:56:55	2012	64:16:F0:F8:59:41	10/3/2011	10:48:56	GMT	
11	1330383416	Mon	Feb	27	17:56:55	2012	2C:A8:35:9F:F5:A0	10/3/2011	10:49:24	GMT	
12	1330383416	Mon	Feb	27	17:56:55	2012	00:05:4F:58:68:7B	10/3/2011	10:49:51	GMT	
13	1330383416	Mon	Feb	27	17:56:55	2012	C0:38:F9:57:A5:40	10/3/2011	10:49:53	GMT	
14	1330383416	Mon	Feb	27	17:56:55	2012	64:16:F0:B0:CC:D7	10/3/2011	10:49:55	GMT	
15	1330383416	Mon	Feb	27	17:56:55	2012	00:05:4F:86:A1:02	10/3/2011	20:45:09	GMT	
16	1330383416	Mon	Feb	27	17:56:55	2012	94:63:D1:D1:DA:3B	10/3/2011	10:50:33	GMT	

Figure 11 Sample of ouput .LOG file imported into Microsoft Excel

The PERL loop function leading the device inquiry is divided into cycles. The Bluetooth sensor inquiry process contains a 10.24 second inquiry cycle duration, followed by a one second period of reset time to clear the buffer, comprising a total approximate 11.24 second cycle length. The research team chose the 11.24 second cycle length pursuant to the recommendation of current Bluetooth design specifications. Although designed to be an 11.24 second cycle, in deployment the cycle is an average of 11.28 seconds +/- 0.27 seconds, with the maximum and minimum cycle lengths observed at 16.5 seconds and 1.1 seconds, respectively. The cycle lengths are derived from the

cyle_start.log and cycle_end.log files, which contain the time stamps of the start and end of each cycle, respectively; and are written by the loop script. The cycle_start.log and cycle_end .log files allow for the research team to observe where a device-detection is occurring within a cycle, and the cycle detection count, which becomes important when trying to maximize the number of detections through the investigation of cycle detection patterns.

3.4 Probe Vehicles

Probe vehicles provide a way to include a controlled set of Bluetooth-enabled devices with known performance characteristics in the traffic stream. The devices placed in the probe vehicles during the field tests are a combination of Class 1 and Class 2 Bluetooth-enabled devices, which have MAC addresses known to the research team. An additional device present in the probe vehicles during every deployment is a handheld QStarz GPS device which monitors the carrier's speed, acceleration, and location with one record every second. The GPS raw data output is compatible with ArcGIS, allowing for a spatial analysis of the detections relative to the location of the sensor. This feature allows the research team to investigate where in space device detection occurs, from which the research team can derive an average expected offset, or range of offsets, that the device will be from the sensor when the time stamp is recorded.

The probe vehicles devices are placed around the interior of a vehicle either on the floor in front of the front passenger seat, on the front passenger seat, plugged into the center console, or on a rear seat of the vehicle. The placement of Bluetooth-enabled devices at various, pre-selected locations in the probe vehicles are intended to be representative of the placement of similar devices in the vehicle population to be

detected. The probe vehicles used for the test deployments are a 1998 Toyota Avalon and a 2002 Honda CRV. The Bluetooth-enabled devices, GPS devices and their locations within the probe vehicles are listed in Table 3 below. Details on the probe vehicle use during deployments can be found in Chapter 4 of this thesis.

Table 3 Placement of Devices within Probe Vehicle

Device Class	Bluetooth-enabled Device	Vehicle Location
1	Netbook & IOGear Adapter	Back Right seat
1	Toshiba Thrive AT-100 Tablet	Front Right seat floor
2	QStarz GPS BT-1000eX/XT	Front Right seat
2	Ikross FM Transmitter	Cigarette lighter

3.5 Ground Truth Data

When using Bluetooth sensors to collection travel time data along a corridor, it is essential for the research team to provide a method of verifying the Bluetooth records. Sources of ground truth data explored during the research undertaken for this thesis are handheld GPS units and overpass video cameras for manually capturing time stamped vehicle license plates. ALPR devices are also present during the freeway travel time deployments, to provide an alternative measure of travel time when other methods are not available. For the research conducted, pairing license plated numbers and timestamps manually read from video cameras at the Bluetooth reader locations serve as ground truth during freeway data collection, whereas the GPS serves as ground truth for arterial data collection. The following sections describe how these technologies are used to validate the Bluetooth travel time data.

3.5.1 Global Positioning Systems

The GPS systems used in this study are the QStarz BT-1000eX and BT-1000XT models, which also act as detectable, Bluetooth-enabled probe devices as other sections of this thesis have noted. Figure 12 below shows an image of the BT-1000eX and BT-1000XT GPS models featured in this research.

Figure 12 GPS devices with BT-1000eX on the left and BT-1000XT on the right

White stickers on the devices aid the researchers in recording the device number, as well as the MAC address of the device, at the start of each experimental run. This is important during the data analysis portion of this study. The QStarz GPS tracks its position with one record every one second. The GPS also has the ability to log up to five records per second, however that precision was deemed not necessary for the purpose of this research.

With a time sync occurring between the Bluetooth sensor system and the handheld GPS device using the method described in Section 3.2.1.1, the GPS functions as a record of the ground truth for location and travel time through a corridor. The QStraz

GPS data is transferred to the computer via a USB connection using the QTravel software package. Figure 13 shows a screenshot of the QTravel software with the data logged by the GPS.

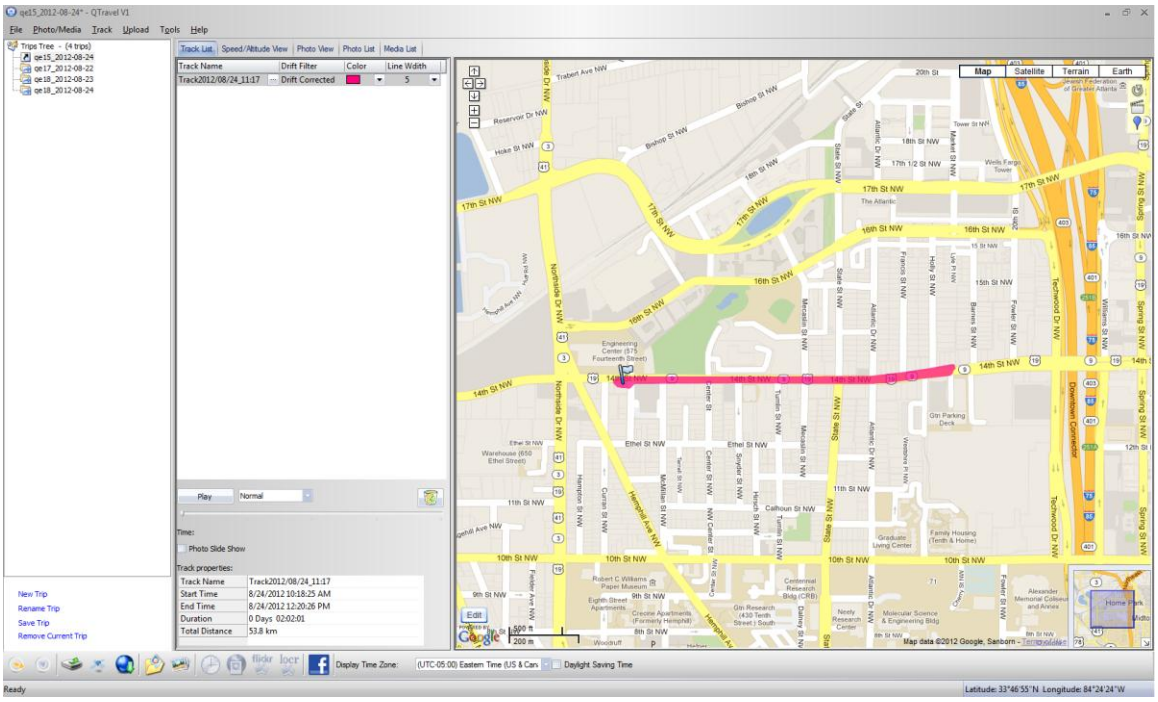

Figure 13 Screenshot of QTravel Software

The QTravel software also allows the user to insert a point, to which the program assigns geographic coordinates. This became helpful when inserting the location of the Bluetooth sensor stations along deployment routes to calculate the position offset of the device at the point of detection. The raw GPS data collected during the deployments can be exported to a comma separated value (.csv) file type which can then be converted to a Microsoft Excel file for processing. Information captured in the raw data file includes the date, timestamp, latitudinal and longitudinal coordinates, device speed, altitude, etc.

3.5.2 Video Cameras

Video cameras can also provide a way to collect ground truth travel time data when collecting Bluetooth travel time. The video cameras used during the data collection efforts are Panasonic HDC-TM700 video cameras mounted on tripods. Video cameras become an efficient ground truth data collection method when the corridor is so long that a probe vehicle would not be able to complete a sufficient number of passes through the system. The object of analysis for video ground truth data is matching the license plate detection at each site. By performing a time-sync between the video cameras and the Bluetooth system again using the process outlined in Section 3.2.1.1, the time stamps and extrapolated travel time from license plate records become a ground truth measure to compare to Bluetooth travel time. However, a drawback of this method is that the license plate data must be manually recorded from the video requiring a potential significant additional data collection effort after field data collection.

For the given study sections freeway data collection captures the morning traffic peak, where the travel time of a probe vehicle loop is upwards of 30 minutes. This is impractical because only four to five runs could be achieved during the deployment period, which is insufficient to provide a significant ground truth record. The video cameras are placed on the overpasses facing the rear of the passing vehicles to capture their license plates. The cameras must be focused through the chain-link fence present at most overpasses, so that there is no obstruction of license plates during the processing of the video. The camera view is such that each camera focuses on two lanes of traffic, with the edges of the lanes hitting the middle of the video camera view. Figure 14 below shows the typical configuration of the overpass video cameras.

Figure 14 Video Camera Configuration on Freeway Overpass

3.5.3 Automated License Plate Recognition

The ALPR technology is deployed in conjunction with the Bluetooth sensors for the I-285 travel time test series (to be discussed in Chapter 4) as an alternative method of measuring corridor travel time. Although this thesis does not directly investigate the effectiveness of ALPR technology, the simultaneous deployment of this technology alongside Bluetooth sensors warrants the inclusion of the results to provide a comparative measure of travel time. Figure 15 shows the typical setup of the ALPR units.

Figure 15 Field setup of ALPR technology on I-285 gore area

The ALPR system consists of three camera lenses each with fixed focal lengths of 25mm, 35mm, and 50mm, respectively. The different focal lengths allow the cameras to focus most effectively on different lanes of traffic to capture license plates. The cameras operate through a program called ALPR Mobile Plate Hunter installed on an Asus netbook running a Windows 7 operating system. As the camera automatically detects license plates rolling through its view scope, the program records a picture of the license plate, a text version of the license plate, as well as the time stamp associated with the detection.

Chapter 4: Experimental Design

4.1 Introduction

There are two components the research team investigated to provide guidance on how best to increase the accuracy of real-time travel time measurement in a work zone corridor. The first is developing a method to maximize the number of Bluetooth-enabled devices the Bluetooth sensor can detect with the understanding that the confidence bounds surrounding the travel time will thus decrease; and the second is optimizing the frequency of sensor placement along a corridor to account for the inherent error in detection location around a sensor and the resultant error in travel time.

To investigate how the sample size of Bluetooth sensor detection can be increased, it is important to first explore factors that influence the number of devices the sensor can detect. These factors include characteristics of the device, such as the pattern of detection, which influences the likelihood of detection; and the characteristics of the sensor, such as the sensor capacity for detection. This thesis seeks to explore these questions by investigating the device and sensor characteristics so that the most effective method of Bluetooth device detection can be employed. Because of the innate differences in Bluetooth devices present in the detectable population, this thesis investigates the detection properties of different device groups independently, as well as jointly, and observes the effect as more and different devices are brought into a sensor's field of view.

Secondly, sensor placement frequency refers to the spacing or separation of Bluetooth sensors along a travel-way. When a Bluetooth-enabled device is detected by a

Bluetooth sensor, there is a location range around the sensor from where the detection originated. Knowing this spread of detection location around a sensor is important when spacing the sensors to calculating the resulting error in speed and travel time derivation.

4.2 Bluetooth Device and Sensor Characteristics

To explore device and sensor properties the research team performed a series of tests in a controlled indoor environment in one of the lab rooms at the Georgia Institute of Technology. There was minimal noise/interference from other devices other than those tested, and the research team was able to bring a controlled group of devices into a sensors field of view for pre-determined lengths of time to observe the behavior of both the sensor and Class 1 and Class 2 devices. The research team used a combination of the Class 1 and Class 2 devices presented in Section 3.1. The two tests conducted include a single-sensor capacity test, and a multiple sensor effect test. The following sections of this thesis describe the details of the sensor and device test series.

4.2.1 Test Series 1: Single-Sensor Capacity

4.2.1.1 Overview

Sensor capacity represents the maximum number of Bluetooth-enabled devices that a Bluetooth sensor can detect during an 11.24 second cycle. The research team designed a controlled test to investigate the number of devices that a Class 1 Bluetooth sensor can detect during an 11.24 second cycle by bringing an increasing number of devices into the sensors field of view (by turning additional devices on in a controlled manner), and looking for a point where the detection rate begins to drop off. The research also focused on providing a distinction between Class 1 and Class 2 devices to

see if the sensor has a higher propensity for detection based on Bluetooth power class. The sensor used for the Single Sensor Capacity test series is Sensor 5.

4.2.1.2 Day 1: Single-Sensor and Class 2 Devices

The first day of the single-sensor capacity test series involved testing a series of 5,10,15,20, and 25 Class 2 devices, each for a ten minute period (equating to about 53 11.24 second cycles). The 25 Class 2 devices were a combination of 15 QStarz BT-1000eX devices (Number 6 through 20, in the following tables) and ten QStarz BT-1000XT devices (Number 21 through 30). All devices were placed on a conference table in rows of five devices, with about six inches of separation between each device (Figure 16). The first five devices in the closest row to the sensor were turned to the on position for the first ten minutes. Then, without the first five devices being turned off, the next five devices were turned on for the following ten minute period. The Class 2 test proceeded in this manner until all 25 devices were turned on at once. Figure 16 shows a view of the deployment configuration containing 20 devices. The final deployment configuration contained one more row of GPS units on the further side away from the sensor, following the same spacing arrangement as the first 20 devices. Figure 16 also shows the location of the Class 1 Bluetooth sensor. The sensor is at a height of approximately eight feet, and is offset horizontally by about five feet from the closest row of GPS devices.

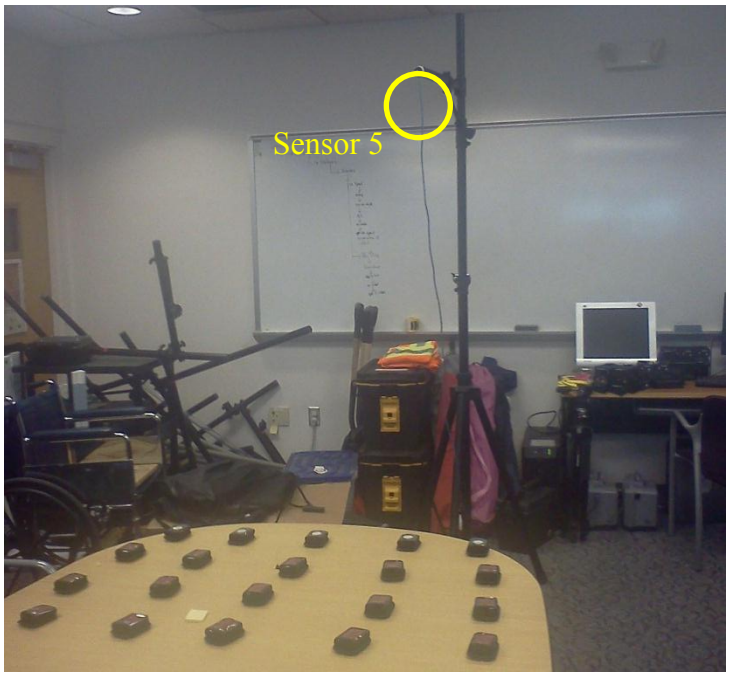

Figure 16 Set-up for Class 2 Capacity Test

4.2.1.3 Day 2: Single-Sensor and Class 1 Devices

Day 2 of the sensor capacity test series entailed placing an increasing number of Class 1 devices into the custom sensor's field of view ranging from 5, 10, 15, 20, to a final 25 devices. The test followed the same procedures as in Day 1 with respect to turning on the first five Class 1 devices for ten minutes, and then the next five for the following ten minutes, et cetera. The Class 1 devices included ten IOGear USB Bluetooth adapters connected to Asus Netbooks, nine Toshiba Thrive AT-100 Tablets, and six Asus netbooks operating on the Ubuntu Linux platform with built-in Bluetooth. Only one IOGear USB Bluetooth adapter was connected to each netbook because complications arose with the Bluetooth sensor not registering all connected devices when more than one adapter was attached. Table 4 provides a summary of the device deployment procedure.

Table 4 Summary of Class 1 Capacity Test

TEST PERIOD	TIME BEGIN	TIME END	DEVICES
1: 5 Class 1 Devices	15:12:30	15:22:30	NB16 & R2
			NB21 & R6
			NB22 & R4
			NB8 & R17
			NB17 & R 10
2: 10 Class 1 Devices	15:46:00	15:56:00	TABLET 3
			TABLET 12
			TABLET 14
			TABLET 15
			TABLET 16
3: 15 Class 1 Devices	16:06:00	16:16:00	NB3 & R3
			NB15 & R1
			NB19 & R26
			NB13 & 9
			NB7 & R11
4: 20 Class 1 Devices	16:26:07	16:36:07	NB 0
			NB 1
			NB 2
			NB 4
			NB 9
5: 25 Class 1 Devices	17:13:45	17:23:45	NB 6
			TABLET 1
			TABLET 6
			TABLET 11
			TABLET 13

4.2.1.4 Day 3: Single-Sensor and Class 1 and 2 Devices

The final day of the sensor capacity test series involved testing 25 Class 2 and 25 Class 1 devices together. Figure 17 below shows the setup configuration with all devices placed on a large conference table. The devices are a combination of all the Class 1 and Class 2 devices tested in Days 1 and 2 of the sensor capacity test series. Table 5 provides a summary of the devices in the final capacity test. In order to provide consistency with Day 1 and Day 2 of this test series, all devices were activated for a period of ten minutes,

or about 53 complete detection cycles. A separation of approximately six inches was maintained between each device for the entire deployment series to avoid direction interference between Bluetooth antennae.

Table 5 Bluetooth-Enabled Devices in Final Sensor Capacity Test

	Power Class	**Count**
IOGear USB Bluetooth Adapter	Class 1	10
Asus Eee PC Netbook	Class 1	6
Toshiba Thrive AT-100 Tablet	Class 1	9
QStarz BT-1000eX	Class 2	15
QStarz BT-1000XT	Class 2	10
	TOTAL	**50**

Figure 17 Class 1 and 2 device configuration for sensor capacity final test

4.2.2 Test Series 2: Multiple Sensor Effect

4.2.2.1 Overview

The multiple sensor test series seeks to explore how the detection rate changes when there are two sensors competing for detections. This quality is important to investigate whether the number of sensors influences the detectabilitity of a given device as well as the detection characteristics of individual sensors.

4.2.2.2 Procedure

The multiple sensor effect test series consisted of placing 20 Class 2 Bluetooth-enabled devices on the same conference table used for the sensor capacity test, but with a different orientation as shown in Figure 18. The selection of the 20 Class 2 devices was influenced by the individual device performance in the previous the sensor capacity tests. The five devices that consistently performed the worst across each day of testing (i.e. they did not experience comparable detection to other devices of the same make and model) were not included in the multiple sensor effect test series. The device mix consisted of 11 QStarz BT-1000eX GPS devices and 9 QStarz BT-1000XT GPS devices.

The two Class 1 Bluetooth sensors used in this test series are Sensor 5 and Sensor 8 (based on numbering from the capacity tests). To eliminate interference between the two sensors, the sensors are separated by 12 feet, one foot on either side of the ten foot long conference table. Sensor 5 and Sensor 8 are each connected to a single netbook operating on the Ubuntu platform, which follow the standard inquiry procedure outlined in Section 3.3.

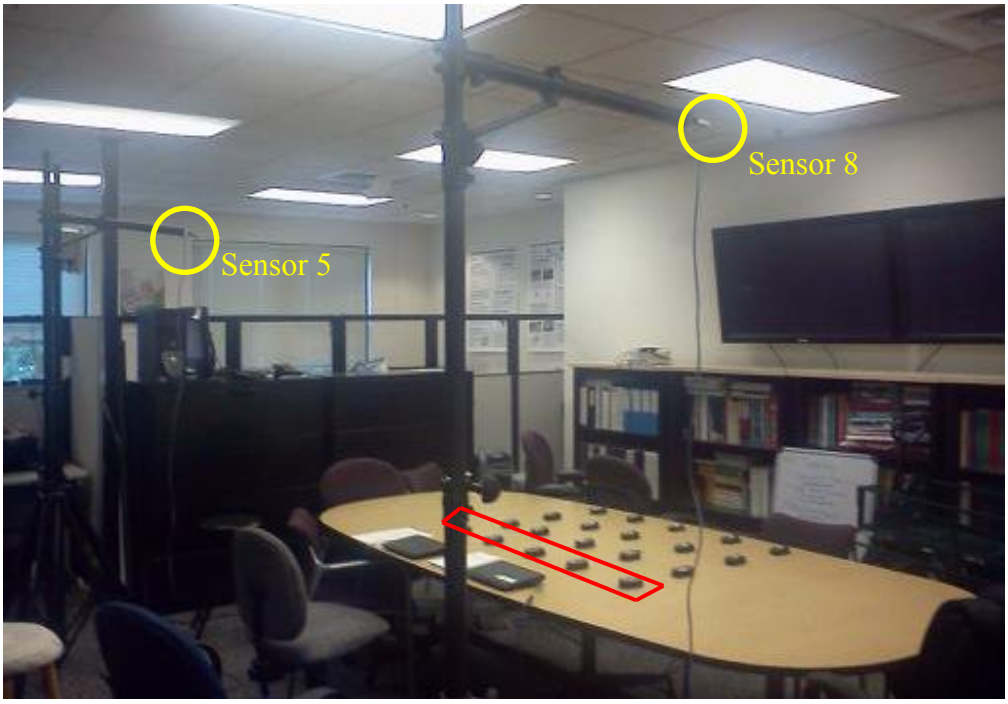

Figure 18 Device and Sensor Configuration for Multiple Sensor Test Series

The sensors are at a height of approximately eight feet above floor level, which is the same position as for the sensor capacity test series, and the table is approximately 2.5 feet high. The sensors and devices are also placed so that the devices are in the center and as a group equidistant to either sensor. The closest devices to each sensor are about four feet away (on the horizontal plane), and the farthest devices are about six or seven feet away. The devices are also separated by six inches again for this test to decrease the potential for direct signal interference.

Once the sensors and devices are positioned correctly, the first row of five devices (indicated by the red box in Figure 18) is turned on to the 1 Hertz (Hz) position to log one record per second. The first row is activated for ten minutes, and remains on while the second row is activated for the following ten minutes, until the final 40 minutes when all 20 devices are activated.

4.3 Investigation of Detection Range

4.3.1 Objective

The focus of the detection range deployment is to capture the position of Class 1 and Class 2 Bluetooth-enabled devices when they are detected by a Class 1 Bluetooth sensor as they travel through a corridor. The additional purpose of this test is to assess whether the most accurate travel time calculation uses a first-to-first detection pairing, a last-to-last detection pairing, or a combination of the two (i.e. a centroid). The assumption going into this test is that Class 1 devices will experience a larger range of detection location than will the Class 2 devices, due to Class 1 devices being of a higher power class and having the ability to communicate over roughly three times the distance as Class 2 devices.

4.3.2 Deployment Location

The research team found it important to test the device detection range on a corridor containing both a midblock location (no signal, with a stop bar on the side street), and an intersection location (with a signal). The reasoning behind this view is that an intersection location is indicative of a stop-and-go work zone corridor, where traffic must stop or move slowly because of a delay for several seconds and then resume free-flow. The midblock location represents the scenario of consistent flow through the system, where very rare stop and slowed conditions occur.

An additional consideration to site identification was the selection of a corridor where free flow speed was a slow speed (around 30 mph), so the research team could capture conditions more representative of an active work zone. Furthermore, the research team wanted to incorporate probe vehicles containing Class 1 and Class 2 Bluetooth-

enabled devices, so selecting a location that allows for quick vehicle turn-around was important. The site that met these conditions, and was also within a reasonable driving distance from the group research lab, is 14th Street, west of the I-75/85 downtown connector. Figure 19 below shows an aerial view of the corridor, with the Bluetooth sensor locations denoted by a yellow triangle, and the turnaround (TA) locations denoted by a red circle and labeled TA 1 and TA 2.

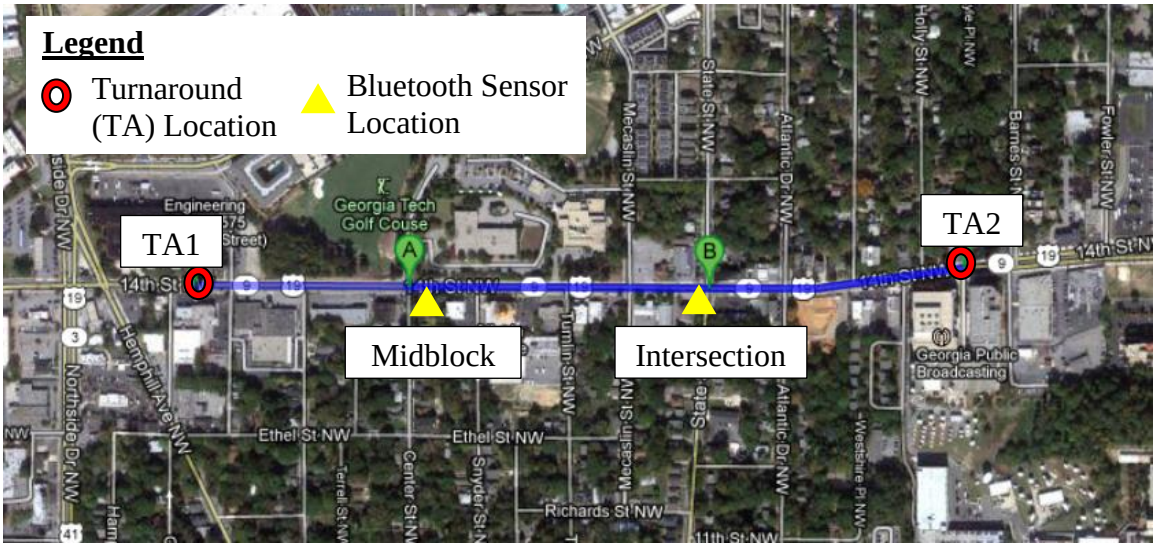

Figure 19 Aerial view of 14th Street Deployment Corridor

The Bluetooth sensors were placed on the right side of the eastbound traffic. Each site features one custom Bluetooth sensor, and one Digiwest Bluetooth sensor, configured using the method described in Section 3.2. Site A is the midblock location at the intersection of 14th Street and Center Street (on the east corner of the intersection), and Site B is the intersection location at the crossing of 14th Street and State Street (at the west corner of the intersection). TA 1 and TA 2 were the turnaround locations. Table 6 provides the geographic coordinates for each sensor station and turnaround location.

Table 6 Geographic Coordinates for 14th Street Corridor

	Latitude	Longitude
TA 1	33.786110°N	84.405278°W
Site A (Midblock)	33.786111°N	84.402778°W
Site B (Intersection)	33.786111°N	84.398889°W
TA 2	33.786389°N	84.395278°W

The geographic coordinates are essential to the range calculation for this test. Site A and Site B are approximately 1,418 feet apart. The offset from TA1 to Site A is approximately 911 feet, and from Site B to TA2 is about 1,320 feet. The expectation is that the range of detection should not significantly exceed 300 feet for the probe vehicle devices (based on the accepted properties of Class 1 devices presented in Section 3.1.1), so separating each of the sensors and the turnaround locations by a minimum of 600 feet was deemed sufficient to eliminate any dual sensor-device interference.

4.3.3 Deployment Procedure

This deployment series consisted of three consecutive days of data collection for two hours each day from approximately 11:30am to 1:30pm. The data collection was conducted on Tuesday August 22nd, Wednesday August 23rd, and Friday August 24th. This allowed the collection period to fall during the lunch hour and increased the likelihood of detectable vehicles and devices on the corridor. The setup for Site A and Site B took approximately 30 minutes in total. The personnel requirements were minimal, with one Undergrad Research Assistant (URA) stationed at each site, and two or three Graduate Research Assistants (GRA) overseeing the deployment and also driving the probe vehicles. The next section describes the details of the probe vehicle setup.

4.3.4 Probe Vehicles

The research team used probe vehicles to bring a controlled set of pre-determined Class 1 and Class 2 Bluetooth-enabled devices into the detection range of the Bluetooth sensors along the 14th Street corridor. The summary of the devices in each probe vehicle are listed in Table 7 below. The same devices were present in the same vehicles, in the same vehicle position, on all three days to allow for a level of consistency and to eliminate any potential for overlapping error if certain devices didn't function properly. The reason for including probe vehicles in the 14th Street test is to provide ground truth data for the location of each device along the corridor when it is detected by the custom Bluetooth sensor. This generation of the device (and thus the vehicle) location is possible because each probe vehicle is outfitted with a QStarz GPS device that tracks the location of the vehicle, and thus all devices within that vehicle.

Table 7 Summary of Probe Vehicle Devices for 14th Street Test

Vehicle	Device Class	Transmitter ID	Vehicle Location
Honda CRV	1	Netbook 16 & Reader 2	Back Right seat
	1	Toshiba Tablet #1	Front Right seat floor
	2	QStarz GPS BT-1000eX #15	Front Right seat
	2	Ikross emitter #5	Car DC Power Adapter
Toyota Avalon	1	Netbook 17 & Reader 10	Back Right seat
	1	Toshiba Tablet #3	Front Right seat floor
	2	QStarz GPS BT-1000eX #18	Front Right seat
	2	Ikross #6	Car DC Power Adapter

The probe vehicles drove on a pre-determined route along the 14th Street corridor. The probe vehicles stayed in line for the entire deployment, and began each run segment as a group. The data from all of the probe vehicles is defined as the data for that run. The first run began at TA1, where the vehicles pulled out of the lot and drove eastbound down the 14th Street corridor, passing the sensors at Site A and Site B along the way. The vehicles were always driving in the right lane when traveling eastbound, unless an obstruction presented itself on the roadway. If a stopping sequence was imminent at the intersection of State Street and 14th Street, the lead car would make an effort to stop and keep the probe vehicles grouped together. This did not happen in every case. Once passing Site B, the vehicles would move to the left lane of the eastbound corridor and prepare to turn left into the parking lot of TA2. This completes the eastbound leg of the run.

The lead car would then remain at TA2 until all probe vehicles entered the parking lot, and then turn right out of TA2 to begin the westbound leg of the same run at the start of the next minute. In this way, the eastbound and westbound legs of each run began at the start of a minute. When driving westbound the vehicle was most often in the right lane of westbound traffic when passing Site B and in the left lane when passing Site A, in preparation to turn left into TA1. After all the probe vehicles completed the westbound leg of the first run, the second run started in the same manner as the first. This sequence continued for the entire two hour data collection period, allowing for the completion of 27 to 29 complete runs through the system (i.e. 28 runs on day 1, 29 runs on day to, and 27 runs on day 3). The driver of the lead probe vehicle also recorded the

time when each eastbound/westbound leg of each run began, for reference during the data processing.

4.4 Freeway Side-Fire Travel Time

4.4.1 Objective

The objective of the freeway side-fire test is to apply the lessons learned in the Sensor and Device Characteristics tests and the Detection Range test to measuring real-time travel time. The research team chose to position the Bluetooth sensors in side-fire mode because this is most available and accessible position along a typical work zone corridor, and does not require the construction of additional mounting mechanisms needed for overhead positioning. An additional focus of this test is comparing the detectability of devices traveling in the direction adjacent to the Bluetooth sensor to those traveling in the opposite direction with greater sensor separation, and cultivating an understanding for the different detection rates of the two groups.

4.4.2 Deployment Location

The research team selected a section of the I-285 eastbound corridor around Atlanta ten miles in length, from Paces Ferry Road to Ashford Dunwoody Road, as the location for the freeway side-fire travel time test series. The research team selected this corridor because it was an active work zone on the weekends (with partial lane closures along corridor), and an inactive work zone on the weekdays (with all lanes open). This travel time test series featured weekday deployments in the non-active work zone in preparation for the following test series, which consists of travel time measurement in an active work zone. By deploying several times along the I-285 corridor, the research

team was able to become familiar with the test sites, as well as generate a control dataset for the active work zone travel times.

4.4.2.1 Site Selection Process

There were several considerations that were accounted for when selecting the sites for Bluetooth deployment along the I-285 corridor. First, the Bluetooth sites selected should minimize interference from surrounding objects and devices. Examples of object interference include vegetation cover and obstructing wall, signs, and fences. Proximity to stationary or nearby corridors can lead to the detection of unwanted Bluetooth-enabled devices that can complicate the travel time calculation, or reduce the number of unique detections of strictly corridor devices. Therefore, selecting sites that would minimize interference is important.

The accessibility of the site location is also important so that the equipment can be safely and easily transported, setup, and broken down. Therefore, the sites must be accessible via a sidewalk and crosswalk from a nearby parking area, or have a wide protected shoulder adequate for temporarily parking a vehicle to unload equipment. The temporary vehicle pull-off is only considered safe when in the gore area of a freeway overpass where passing vehicles are entering or exiting the corridor at slower speeds. The site must also have level ground to support the Bluetooth tripod configuration, and feature a wall or guardrail to protect the personnel and equipment. The constraints were generally imposed for the safety of the data collection team, who were not part of the construction site personnel. Future efforts could employ and instrumented work zone truck. It is anticipated that when deployed by a contractor additional sites would be available that were not considered in this effort.

Another important consideration for site selection is the availability of an overpass to place cameras to capture license plates of passing vehicles along the corridor. The cameras are necessary to the study because they provide the method of ground truth travel time data collection. Finally, because the purpose of this data collection is to collection travel times, selecting work zone segments not including a major interchange was desirable to maximize the likelihood of vehicles traversing the entire work zone. Otherwise, a great portion of the vehicles traveling between two points may exit at a major interchange and not generate travel time measurements.

Although all of these considerations are important when selection the optimal locations to station the Bluetooth sensors, the consideration of safety and accessibility are of greatest importance in this research effort. This puts the site location options at freeway interchanges in the gore area of an overpass where there is protection behind a wall or a guardrail. The gore area between the freeway exit ramp is most ideal, because even if a device is detected exiting the freeway, the assumption is that the vehicle will not be directly re-entering the freeway, and thus will not provide a significant measure of error in the travel time.

4.4.2.2 Site Identification

The research team identified three feasible sites for data collection on the eastbound section of the I-285 corridor to use for measuring eastbound morning peak corridor travel times. One custom Bluetooth sensor was stationed at each site and one ALPR system was also stationed at two sites on each day of deployment. Figure 20 below shows an aerial view of the deployment corridor for the freeway side-fire travel time measure.

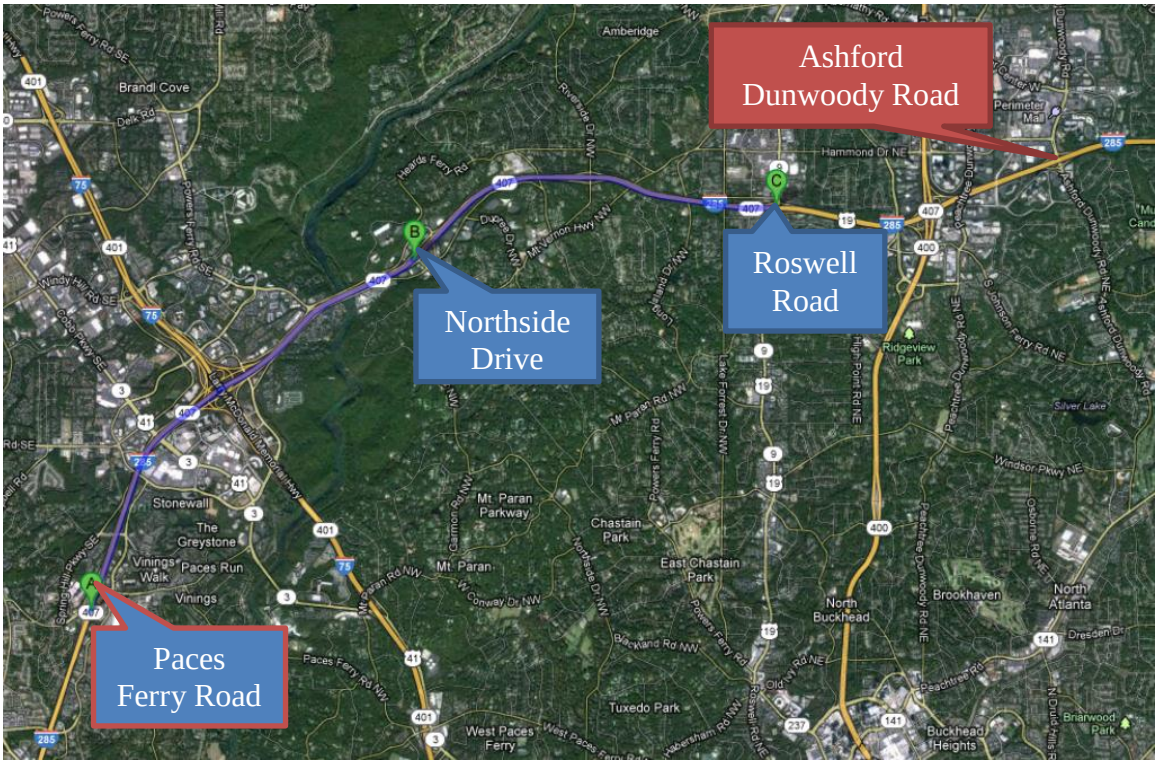

Figure 20 Aerial View of I-285 Eastbound Deployment Locations

Site A is located at the intersection of I-285 and Paces Ferry Road, Site B is located at the intersection of I-285 and Northside Drive, and Site C is located at the intersection of I-285 and Roswell Road. The location of Ashford Dunwoody Road is also shown on the corridor for spatial reference. Paces Ferry Road is shown with a red box to highlight that it is at the end of the work zone corridor, and also the first eastbound corridor location. The distance between Paces Ferry Road and Northside Drive is approximately 4.3 miles, and between Northside Drive and Roswell Road is approximately 3.3 miles. Figure 21, Figure 22, and Figure 23 show aerial views of the Paces Ferry Road, Northside Drive, and Roswell Road sites, respectively. The Paces Ferry Road site is approximately 175 feet from the overpass, the Northside Drive site is approximately 175 feet, and the Roswell Road site is about 150 feet from the overpass.

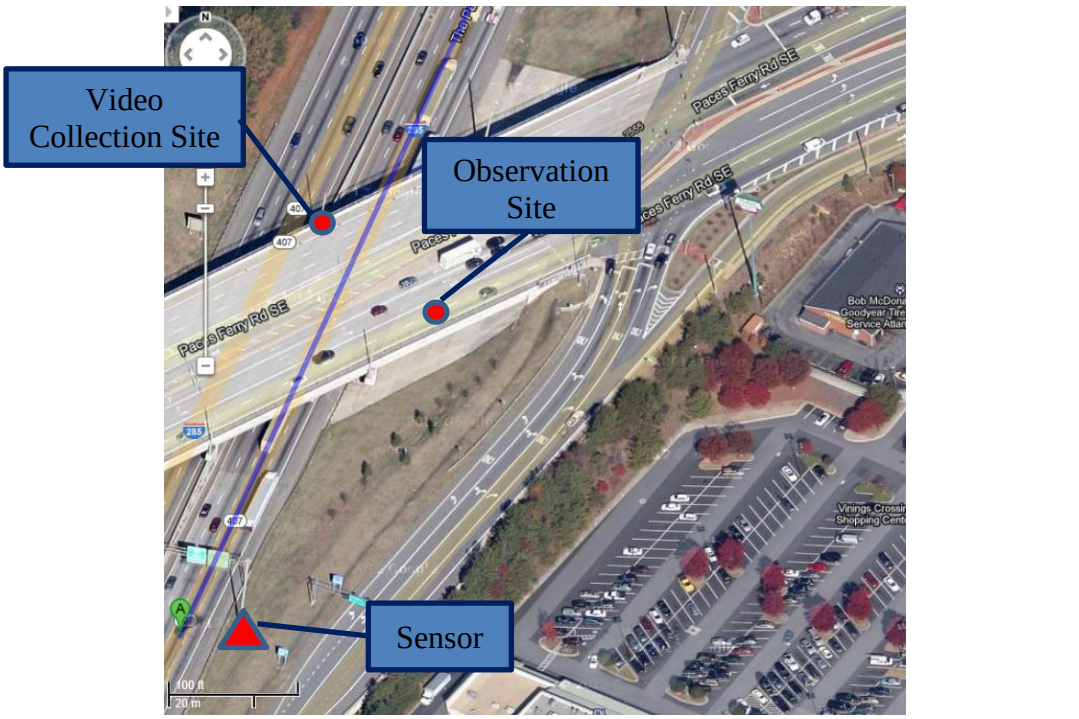

Figure 21 Aerial View of Paces Ferry Road

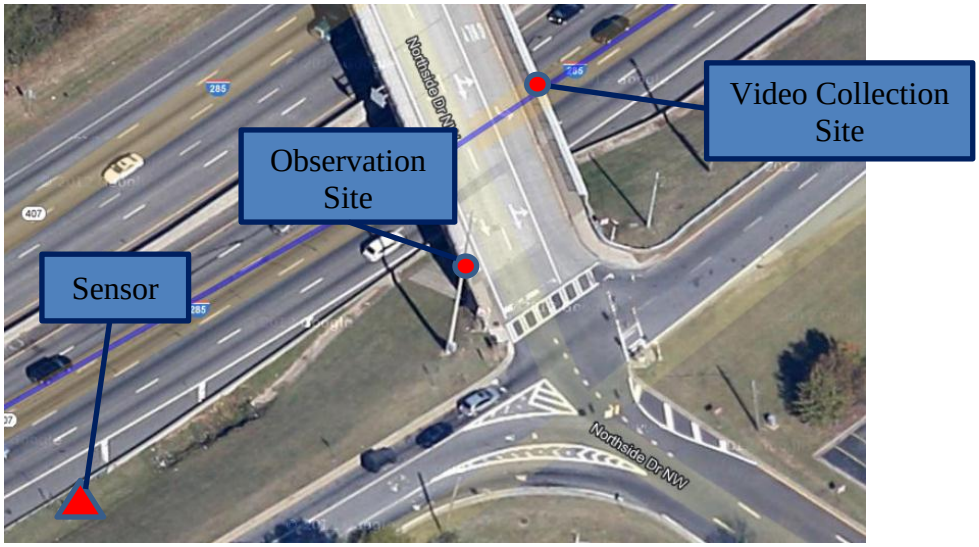

Figure 22 Aerial view of Northside Drive

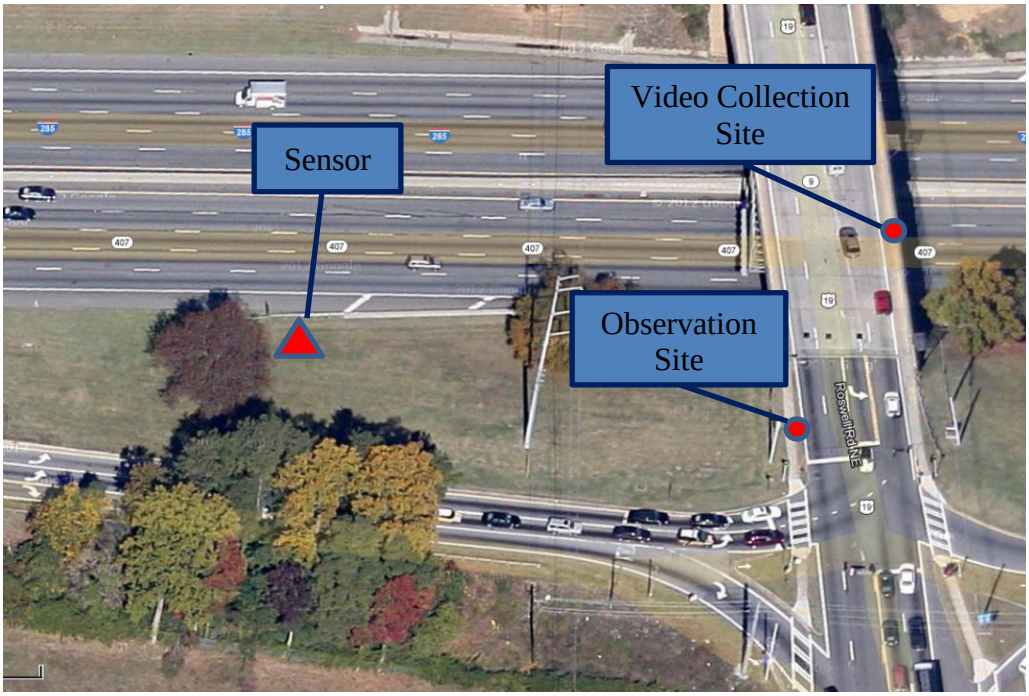

Figure 23 Aerial View of Roswell Road

4.4.3 Deployment Procedure

Before every data collection field deployment, the research team provided a plan to the Georgia Department of Transportation (GDOT), which in all cases had to be approved before collection began. Furthermore, the research team contacted the local law enforcement personnel for each data collection site to advise them of the location, duration, and equipment that would be present for the data collection.

4.4.3.1 Day 1: Friday, September 7th, 2012

For the first day of data collection, the research team deployed to two sites, Paces Ferry Road and Northside Drive. There were two data collection teams at each site, each with three URAs and one GRA. The Bluetooth sensors were assembled at both sites by 8:05 AM. The planned end of data collection for Paces Ferry Road was 10:25 AM, and

for Northside Drive was 10:35 AM, to allow ample time for vehicles to traverse the 4.3 mile corridor. However, the netbook for the custom Bluetooth sensor at Northside Drive powered off at 10:15 AM at Northside Drive due to heat exposure, which still allowed for the capture of more than two hours of travel time data. This day of data collection also featured one ALPR system at each site.

4.4.3.2 Day 2: Wednesday, September 12th, 2012

For the second day of Bluetooth data collection the research team deployed to two sites, Northside Drive and Roswell Road. Each data collection team on this day was comprised of two URAs and one GRA. The site assembly was faster for Day 2 because of the prior experience with the site, so the research team was able to begin data collection at 7:30 AM and collect data for a two hours and 20 minutes, until 9:50 AM at Northside Drive, and 10:00 AM at Roswell Road (to allow for vehicles observed at Northside Drive to reach Roswell Road). Data collection also featured one ALPR system at each data collection site.

4.4.3.3 Day 3: Friday, September 14th, 2012

On the third day of I-285 travel time data collection the research team deployed to all three sites: Paces Ferry Road, Northside Drive, and Roswell Road. This allowed for capturing the entire corridor with an intermediate travel time station. The Bluetooth collection for Day 3 began at 7:20 AM and lasted for about two hours until 9:32 AM at Paces Ferry Road, 9:36 AM at Northside Drive, and 9:40 AM at Roswell Road. A full ten minutes was not allotted for travel between each site at the close of the collection period because the findings from Day 1 and Day 2 of the travel time test series did not show any significant increase in data resulting from this staggered turn-off procedure.

On this third day of data collection Bluetooth sensors were placed at all three data collection sites, and ALPR systems were stationed at Northside Drive and Roswell Road. These two sites were used to maximize the potential for plate matches as any site pair containing Paces Ferry Road tended to lose significant number of potential matches due to the I-75/I-285 interchange.

4.4.4 Ground Truth

Given the route length, and the potential for a 30-minute driving loop for the probe vehicles, it was determined that probe vehicles data would not provide a sufficient travel time sample for the freeway studies. Therefore, the method of ground truth for the I-285 data collection series is license plate matching, as described in Section 3.5.2. Paces Ferry Road has four lanes of eastbound traffic, so two video cameras were necessary for this site. Northside Drive and Roswell Road each have five lanes of eastbound traffic, so three video cameras were necessary to capture no more than two lanes of traffic a piece. (Previous efforts under different projects conducted at Georgia Institute of Technology have shown limiting video capture to two lanes per camera allows for optimal manual license plate data collection [42].) Section 5.5.2 of this thesis summarizes the processing method for matching license plates captured by the overpass video cameras.

4.5 Work Zone Travel Time

4.5.1 Objective

The objective of the work zone travel time test is to assess the effectiveness of using Bluetooth to measure travel time through an active work zone corridor. The research team again placed the Bluetooth sensors in side-fire locations, comparable to the

locations discussed in the previous section. An additional focus of this study is the effectiveness of measuring both eastbound and westbound travel times from a single sensor positioned on one side of the road.

4.5.2 Deployment Locations

As was discussed on Section 4.4.2, the research team selected the ten-mile I-285 corridor from Ashford Dunwoody Road to Paces Ferry Road for the side-fire travel time test series with the intent of deploying along the same corridor in an active work zone study. The previous side-fire travel time tests focused on the eastbound section of the work zone corridor. The active work zone corridor can consist of lane closures in varying quantity through sections of the eastbound and westbound directions. Therefore, to prepare for deploying in an active work zone the research team had to select potential sensor placement locations along the right side of the westbound travel direction of the corridor. The previously identified eastbound deployment locations are also potential work zone deployment sites, but will not be readdressed in this section of this thesis.

4.5.2.1 Site Selection Process

Consistent with the parameters of site selection used for the eastbound deployment locations, the research team selected sites that were safely accessible for parking and unloading, featured an overpass, and were in the gore area between the westbound corridor and a freeway exit ramp. Furthermore, the sites had to be flat, or have a slight slope away from the corridor protected by a guardrail to ensure the safety of the traveling public, and the safety of the research personnel during equipment setup and takedown. The initial goal of westbound site selection was to explore the westbound gore area of the previously identified eastbound sites, so this is where the research team

began the investigation. The process of site selection involved completing an initial search of the corridor area using Google Maps, and then driving along the corridor to visit and catalogue the potential sites.

4.5.2.2 Site Identification

The research team found two potential sites in the westbound direction along the ten mile work zone corridor, shown in green in Figure 24 below. Figure 24 also identifies the three eastbound data collection sites, shown in blue. The ends of the work zone corridor are indicated with boxes outlined in red.

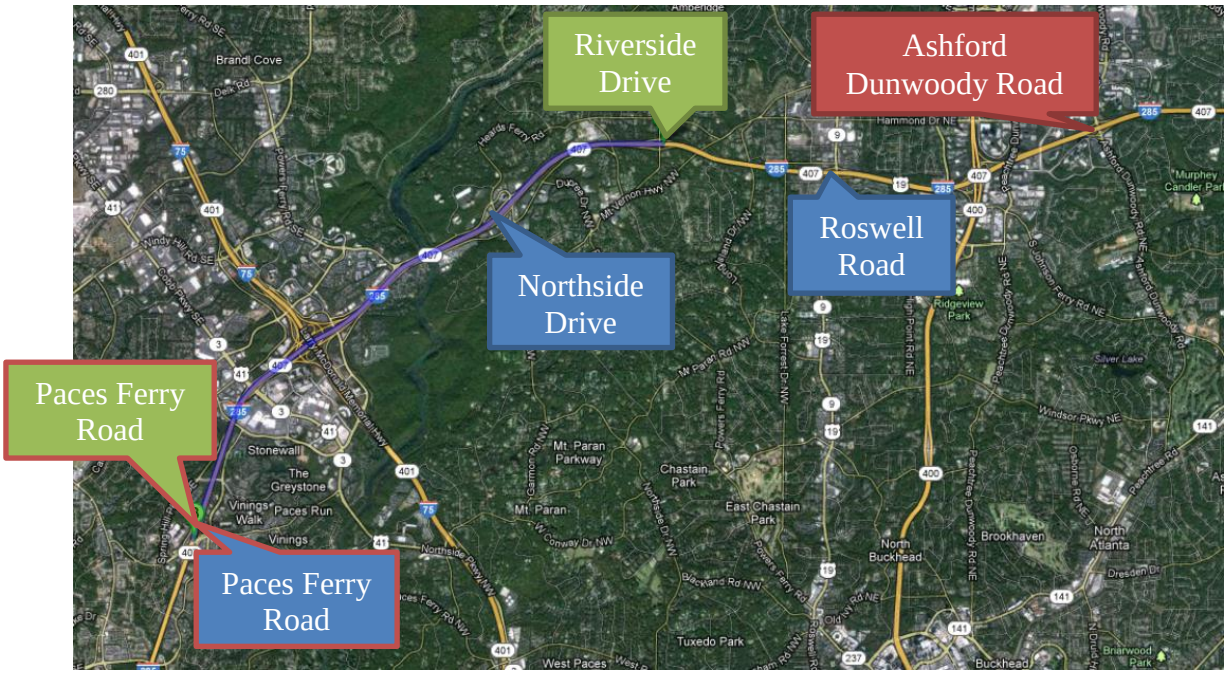

Figure 24 Aerial View of I-285 Westbound Deployment Locations

One custom Bluetooth sensor was stationed at each site during the work zone deployment and one ALPR system was at two sites on each day of deployment. The first westbound site is Riverside Drive, and the second is Paces Ferry Road, separated by a

distance of 5.9 miles, and divided by I-75, a place for major ingress/egress of vehicles and thus potential loss of many travel time pairs. Figure 25 and Figure 26 below show aerial views of the Riverside Drive and Paces Ferry Road data collection sites. The Paces Ferry Road site is approximately 75 feet from the overpass, and Riverside Drive is about 150 feet from the overpass.

Figure 25 Aerial view of Riverside Drive

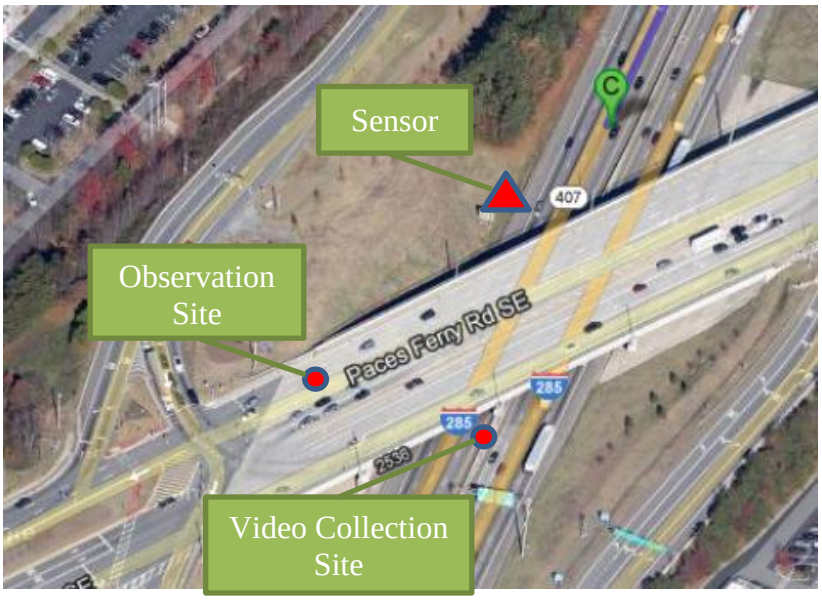

Figure 26 Aerial view of Paces Ferry Road Westbound

4.5.3 Deployment Procedure

The deployment procedure for the work zone travel time test series was dependent on the weekend lane closure plan for the active I-285 work zone. The construction plan for an upcoming weekend was not released until the Wednesday before the weekend closure. This reporting schedule required the research team to contact GDOT about the upcoming lane closures on a weekly basis, to construct a plan for deployment accordingly, and assess whether the given lane closures were consistent with the deployment capabilities of the Bluetooth (and the jointly deployed ALPR technology). All work zone data collection plans were approved by GDOT, and the research team notified the local law enforcement personnel of the planned activities prior to each deployment session.

4.5.3.1 Day 1: Saturday, September 29, 2012

The first day of active work zone deployment took place on Saturday, September 29th, 2012. The reported lane closures were the three inside lanes traveling eastbound from Roswell Road to Ashford Dunwoody Road, and the three inside lanes traveling westbound from Roswell Road to Paces Ferry Road. Based on the approved sites, the research team decided to deploy to the right side of the westbound corridor at Riverside Drive and Paces Ferry Road. Upon arrival at the work zone, the research team found the lane closure plan had been modified so that the planned deployment sites did not directly capture the active work zone. There were active work zone lane closures in the eastbound direction of travel at Riverside Drive, but no active lane closures eastbound at Paces Ferry Road. The research team proceeded with the deployment, beginning Bluetooth data collection at 7:14 AM and continuing for two hours and 25 minutes until 10:45 AM at Riverside Drive, and 10:51 AM at Paces Ferry Road.

The research team hoped that an adequate number of unique MAC addresses would be detected in the eastbound traffic in the active work zone across from the Bluetooth sensors placed on the right side of the westbound traffic at Riverside Drive. The eastbound traffic was moving considerably slower than the westbound traffic at Riverside Drive, was more condensed, and within the detection window for the Bluetooth sensors for a longer period of time than the closer, westbound traffic. However, the work zone started further eastbound than Paces Ferry Road, so eastbound traffic was in free-flow at this site, decreasing the opportunity to detect vehicles that would pass along the eastbound corridor through the active work zone.

4.5.3.2 Day 2: Saturday, October 20, 2012

The second day of active work zone data collection took place on Saturday, October 20, 2012. The targeted lane closure for this deployment was the one inside lane from Powers Ferry Road to Route 41 on I-285 westbound. The planned deployment sites were Riverside Drive and Paces Ferry Road westbound. Upon arrival at the work zone, the research team found the lane closure schedule had been modified. However, the research team was able to deploy on I-285 eastbound at Paces Ferry Road and Northside Drive to capture the closure of the two right lanes from Paces Ferry Road to I-75, including the closure of the access ramp to I-75. The data collection began at 9:25 AM and continued until 12:34 PM at Paces Ferry Road and 12:52 PM at Northside Drive to allow ample time for the vehicles to reach Northside Drive in the congested traffic. For the entire deployment period the vehicles at Paces Ferry Road eastbound were very slow moving in congestion, and the vehicles at Northside Drive eastbound were in free flow on the I-285 corridor. One complication for the Bluetooth travel time measurement may be the line of vehicles backed up about 0.5 miles waiting to access the off-ramp at Northside Drive. Instead of moving in free flow, these vehicles were moving in a stop and go pattern at a very slow rate.

4.5.4 Ground Truth

The I-285 work zone travel time test uses the same method of ground truth as the previous I-285 travel time tests, which is matching license plates drawn from overpass video recordings at the corridor sites. Paces Ferry Road has four lanes traveling westbound and eastbound, so two cameras were deployed to this site. The five lanes at

Riverside Drive and Northside Drive required the deployment of three overpass video cameras.

Chapter 5: Data Processing and Analysis Parameters

5.1 Introduction

The procedure for data processing and analysis is an important consideration of this thesis. Of main importance is discussing the parameters that were used in the data analysis to provide relevance to the results presented in Chapter 6. This Chapter provides a description of the device and sensor characteristics that are a focal point in the analysis of different device/sensor test configurations. This Chapter also discusses the method of calculating the device detection range, and finally the ground-truth travel times.

5.2 Device and Sensor Detection Properties

There are three main properties that become important when distinguishing between the device and sensor performance under different test scenarios. They are device detection pattern, device detection rate, and cycle detection pattern, which are briefly described in the following sections.

Furthermore, although the device and sensor characteristic tests were designed to be a controlled test with minimal interference from outside devices, the research team found that several devices other than those tested were present in the sensor detection log. The devices detected continuously include rg49mac1, lg101-a1, and mobile02, which are network devices present both in the Georgia Institute of Technology lab room where the tests were conducted, as well as in neighboring lab rooms. Additional devices detected included personnel computers and tablet devices.

5.2.1 Device Detection Pattern

The device detection pattern refers to the headway between same-device detection, which is the time between when a given device is detected first, and when it is detected again. Therefore, a smaller headway represents more frequent detection. The headway may be presented as a frequency, which provides a count of how many times a given detection headway range occurs. The headway may also be presented as a percentage, which provides a rate of what percentage of all headways are falling within a certain headway range. This is useful when the number of represented devices is not the same across categories.

5.2.2 Device Detection Rate

Device detection rate refers to a ratio of the number of actual detection events to the number of possible detection events. The possible detection events in the Device and Sensor Characteristics test series refers to the number of sensor inquiry cycles the device was within the range of the sensor. The detection rate is then the number of cycles out of the total number of cycles a given device detected. For instance, during each ten minute device test, there are approximately 53 cycles (derived by multiplying 10 minutes * 60 seconds per minute * 1 cycle per 11.24 seconds = 53.38 cycles).

5.2.3 Cycle Detection Pattern

The cycle detection pattern represents the relationship between the Bluetooth sensor and a Bluetooth-enabled device. When the sensor interacts with the Bluetooth-enabled devices, the sensor .log file records the MAC address and the time stamp of device detection. The cycle_start.log files record when the sensor inquiry cycles start. By pairing the MAC address time stamps with the cycle_start.log file each detection has

an associated "time after cycle start" value. The research team evaluates the experiments conducted to uncover whether a 10.24 second inquiry cycle length is the most optimal to maximize the number of unique device detections. An additional factor explored is whether the optimal inquiry cycle length changes under different levels of corridor congestion.

An additional component of the cycle detection analysis is calculating the number of detections that are occurring during the 11.24 inquiry cycle. This provides insight into the capacity that cycle has to detect unique devices, and thus the likelihood that a device traveling through a sensor's detection window will have the opportunity to be detected.

5.3 Device Detection Range Calculation

The device detection range is the distance separating the device and the sensor at the point of detection. The location of the device at the point of detection is identified by longitude and latitude coordinates (the method of derivation is described in Section 5.5.1 below). This is known for devices in probe vehicles equipped with GPS devices. The longitude and latitude coordinates for the midblock and intersection sensor locations are known (Table 6). The offset is then derived by calculating the distance between the sensor and device coordinates, while identifying for eastbound and westbound detections, first run detections, and last run detections. The identification of first detection and last detection for each eastbound and westbound run is accomplished by labeling each detection with the direction the device was traveling (known based on the times recorded for each leg of each run) and then also the order of the detection (based again on the bounds of the run, and how many detections took place in each leg of the run by device).

A simple filtering then allows for the identification of the results by direction and detection order.

Part of the analysis also included checking the GPS log file output to ensure that no GPS wandering occurred along the 14th Street corridor, and that the logged points were occurring in the correct time sequence. An additional tool used to aid in the detection range analysis was importing the GPS log file and associated device locations into ArcGIS to complete a visual check of the location of the detection around the Bluetooth sensor.

5.3.1 Built-in Error

There is a built-in error associated with the link between the GPS timestamp and the MAC address timestamp. The MAC address time stamp in the Bluetooth sensor .log file has 0.1 second in sensitivity, and the GPS time stamp has one second in sensitivity. The average vehicle speed on 14th Street is about 35 miles per hour (mph). There is as much as 0.5 seconds in error associated with this lapse, translating into a location error of about 26 feet. This error is considered of low significance because the detections are occurring in a random pattern, thus it is not anticipated that there will be a pattern (or bias) in the errors. That is, the likelihood of a location error being positive should be the same as the location error being negative, with large samples. However, this is an assumption based on current knowledge of the equipment, and future efforts will seek to confirm through measurement this non-biased behavior.

An additional error in time is the internal clock drift of the Bluetooth netbook (and thus the MAC address time stamps in the .log output file), discussed in Section 3.2.1.1. The total time drift over a two hour data collection is about 0.5 seconds. To

account for this drift, all time stamps were reduced by 0.5 seconds before processing the data. Furthermore, there is a potential error associated with the original time sync because it was completed manually. The assumption is that this error is less than one second, because there is no apparent disconnect between the netbook internal clocks at the point of time sync.

5.4 Custom Sensor Travel Time Calculation

To generate a travel time measurement, a Bluetooth sensor must detect the same device MAC address at two (or more) locations along a corridor. The travel time is then calculated by subtracting the detection time stamp of the second site from the detection time stamp of the first site. This makes not only the number of detections important along a corridor, but also the number of detection pairs between sites.

The travel time along the I-285 corridor was generated using Microsoft Excel functions. Typically, the first step was to import the .log file from the netbooks into Excel, keeping all of the data columns intact, which Figure 11 in Section 3.3 portrayed. The data were then filtered so only those records from the time of the data collection remain, eliminating the records from previous deployments that the .log file maintains for data backup purposes. The next step was to remove the duplicate MAC addresses detected at each collection site. The automatic duplicate removal function kept the first device detection, producing ultimately a "first-to-first" travel time calculation. After removing the duplicates, a COUNTIF function was performed calling on the range of MAC addresses at the first site to see if a given MAC address from the second site is present. This function was performed for all unique MAC addresses at either site. The use of the COUNTIF function also allowed the researcher to ensure that no duplicates

remain (i.e. all the count values should be 1 or 0 for each record). The final step was to filter the remaining results by those records that have a 1, indicating a MAC match is present. These filtered records were then transferred to a new sheet, labeled with the appropriate site, and then sorted by MAC address and site location. This allowed simple IF function to subtract the appropriate time stamps for each MAC address match to generate the travel time, as well as to calculate the time after the start of the data collection when the device was detected at the first site.

This method of travel time calculation allows for differentiation between eastbound and westbound devices. The positive travel times are representative of travel in the direction from the sensor designated as the first to that designated as the second, which is eastbound for all deployments except Day 1 of Work Zone Travel Time. The negative travel times represent the opposite direction, which in most instances is westbound. The majority of the records are for the eastbound traffic for the three days of I-285 travel time tests, but there are also several data points available for the westbound traffic, which allows for an interesting comparison between each direction of travel.

5.4.1 Match Rate Calculation

The I-285 travel time results contain two different match rates. The first match rate is calculated on a per site basis, and the second on an aggregate basis including all unique MAC addresses between sites. A directional aggregate match rate is then calculated for eastbound and westbound. When detection occurs, the sensor does not know whether or not the device was traveling eastbound or westbound past the sensor. The direction is only known for those devices that are matched between two locations, with the direction of the unpaired devices unknown. The following equations explain

how the site match rate and aggregate match rate are calculated for a hypothetical Site A and Site B.

$$\text{Match Rate for Site A} = \frac{\text{Site A Unique MAC Add.} \cap \text{Site B Unique MAC Add.}}{\text{Site A Unique MAC Add.}}$$

$$\text{Aggregate Match Rate} = \frac{\text{Site A Unique MAC Add.} \cap \text{Site B Unique MAC Add.}}{\text{Site A Unique MAC Add.} \cup \text{Site B Unique MAC Add.}}$$

5.4.2 Average Travel Time Calculation

For each day of I-285 travel time data collection on Friday September 7th, Wednesday September 12th, and Friday September14th, the results present a peak travel time, and an off-peak travel time value. For the I-285 work zone travel time data collection on Friday September 29th, and Saturday October 20th, the results present the work zone travel time, and a free flow travel time. For all days of travel time collection, the westbound vehicles represent the free flow, or off-peak travel time, and peak or work zone travel time is found in the eastbound travel time records. Matched points with a high likelihood of representing vehicles that have left the corridor for a period of time, and later returned are filtered from the data in the travel time analysis. For westbound, all travel times greater than 15 minutes are removed from the analysis because for every corridor length tested up to 7.6 miles, the expected travel time is less than ten minutes, based on the observed travel times. Longer travel times infer that the vehicle stopped somewhere along the corridor. Currently the peak and work zone travel time filter is implemented through visual analysis of the travel time plots. One challenge of this filter is that while easily implemented after full data collection it is not readily applicable in a real-time environment. All figures and analysis clearly indicate whether filtered or unfiltered data is utilized.

5.5 Ground Truth Calculation

5.5.1 Probe Vehicle GPS

The GPS instrumented vehicles serve as a ground truth during the 14th Street device detection range test series. The method for calculating this distance includes first importing the QStarz GPS logging data into the QTravel program. The raw data is then exported to a .csv format. The utilized headings are the timestamp, the date, and the latitude and longitude coordinates for each QStarz GPS. The GPS timestamp has one second in sensitivity as mentioned previously. The time stamp of the sensor device detection (0.1 second sensitivity) is then rounded to the nearest second for as close a time match as possible. Next, processing proceeds by manually matching the time stamps of the GPS log file with the timestamps of the device detection. The matching records are then extracted, which creates a record of latitudinal and longitudinal coordinates for detection points.

5.5.2 License Plate Matching

The manual processing of the license plates is a very time consuming and labor intensive process, requiring approximately ten hours of processing time for every hour of video data. The video is processed by running the videos through a freeware program by DVDVideoSoft called Free Video to JPG Converter [41] that extracts image frames from the video by taking a screen shot of the video every 30th frame, off of the base frame rate of two frames per second [42]. Each frame has an associated time stamp, so as the processers input the license plate, it is directly linked to a time stamp, which then allows for an easy travel time calculation.

5.5.3 ALPR Travel Time Derivation

The method for deriving the travel time collected by the ALPR system is very similar to that used for the Bluetooth sensor travel time calculation. The same filtering technique is used to gather the unique records. One difference is that there are three different ALPR cameras at each site, each with a different focal length. There are occasions where multiple cameras detected the same license plate. Only the first detection in time for each license plate was taken for each site, deriving a "first-to-first" travel time for the ALPR system as well. The more detailed analysis of ALPR license plate matching is not the focus of this thesis and will be presented in a companion thesis by Kathryn Colberg, expected Spring 2013. The exact matches are only shown as a way to verify the Bluetooth travel time calculation when the preferred video ground truth is not available due to extensive time processing requirements.

Chapter 6: Results

6.1 Bluetooth Device and Sensor Characteristics Results

6.1.1 Single Sensor Capacity

The sensor capacity test series results show the device characteristics including device detection pattern and the sensor ability to detect and increasing number of Class 1 and Class 2 Bluetooth-enabled devices. For the sensor capacity test series the script had not yet been developed that records the cycle_start and cycle_end time stamps which allow the research team to accurately count how many detections are taking place in each cycle and in what pattern. Therefore, for the sensor capacity test series, the number of cycle detections was calculated as an average based on the known cycle length of 11.24 seconds.

6.1.1.1 Class 2 Devices

First, Figure 27 below shows the number of device detections for each ten-minute period as additional Class 2 devices were turned on in the single sensor's field of view. The blue dashed lane represents the mark of 53 cycles in each ten minute detection frame. There is no noticeable decrease in the capacity of the sensor to detect the additional devices, and the individual devices don't show a trend toward decreasing detections with up to 25 Class 2 devices, indicating that the sensor capacity has not yet been saturated by the presence of 25 Class 2 Bluetooth devices. Next, Figure 28 and Figure 29 show the headway frequency trend for device increments of five devices through 25 devices in 0.5 second bins.

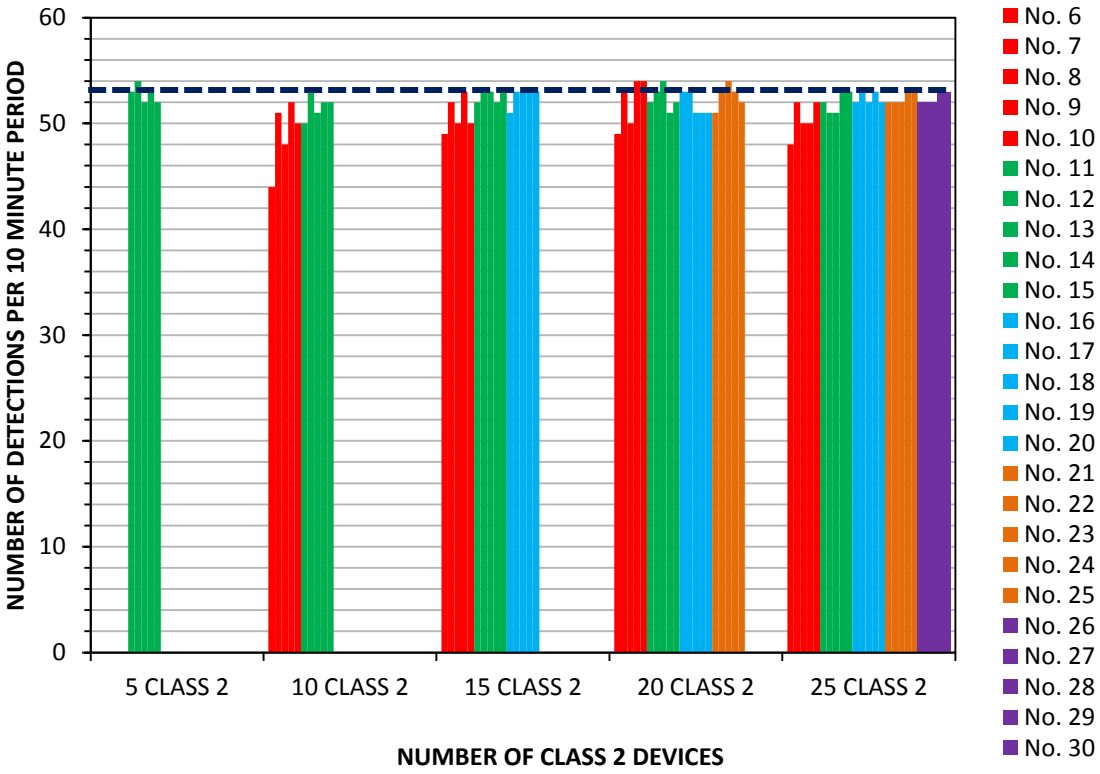

Figure 27 Class 2 Device Detection Count

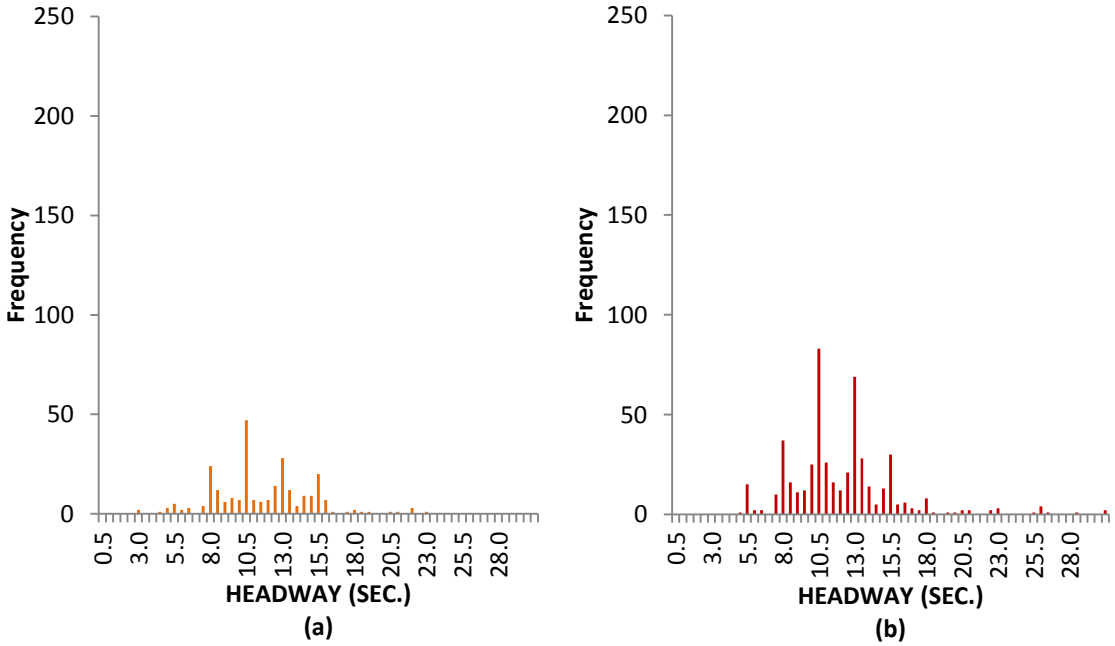

Figure 28 Headway frequency for (a) 5 and (b) 10 Class 2 devices

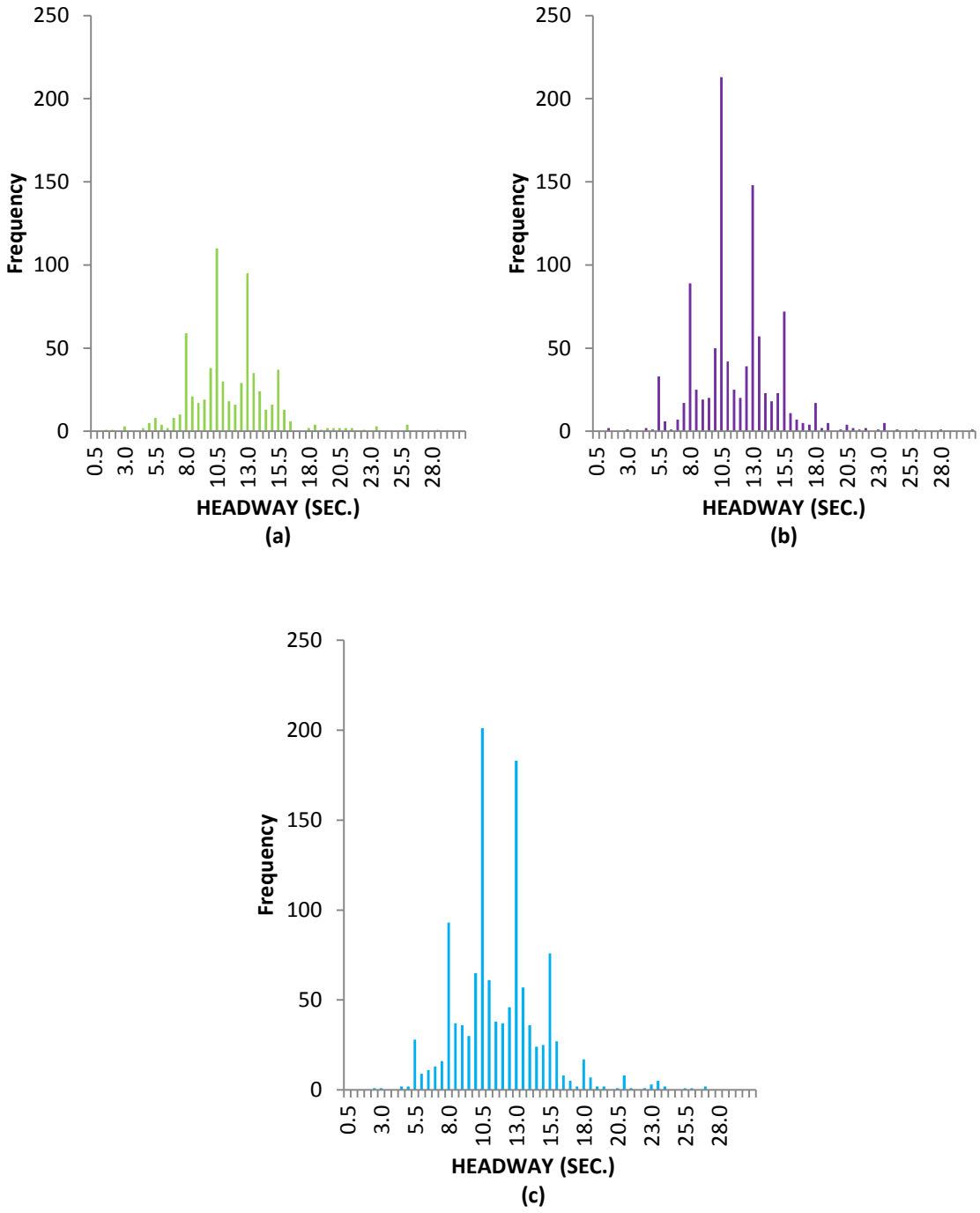

Figure 29 Headway frequency for (a) 15, (b) 20, and (c) 25 Class 2 devices

There is a common headway frequency peak trend for each set of the additional five Class 2 Bluetooth devices approximately every 2.5 seconds. Thus devices were

redetected with eight second, 10.5 second, 13 second, and 15.5 second intervals. The 2.5 second trend is likely related to the inquiry subcycle duration of 1.28 seconds, with two subcycles occurring every 2.56 seconds. The Figures show that the peak detection interval is 10.5 seconds (approximately the length of one cycle) followed closely by 13 seconds. This indicates that Class 2 devices have a likelihood of being detected approximately once per inquiry cycle.

6.1.1.2 Class 1 Devices

Figure 30 shows the detection count for each Class 1 device for the entire deployment series of five through 25 devices. The shading is by device type, not by every five device grouping as in the presentation above. Figure 30 shows that the sensor capacity is not saturated by the presence of up to 25 Class 1 devices because the detection count does not decrease with the introduction of an increasing number of Class 1 devices. Rather, the detection count for 25 Class 1 devices is greater than for the preceding grouping of 20 Class 1 devices.

Two of the Class 1 IOGear Bluetooth adaptors (R1 and R2) consistently exhibit the detection count trend of a Class 2 device. Further investigation is required to understand why Bluetooth adaptors R1 and R1 exhibit this trend. The remaining Class 1 devices have a detection count three to four times that of Class 2 devices, which is most likely indicative of the transmission speeds for Class 1 devices being three times that of Class 2 devices (3 Mbps vs. 1 Mbps).

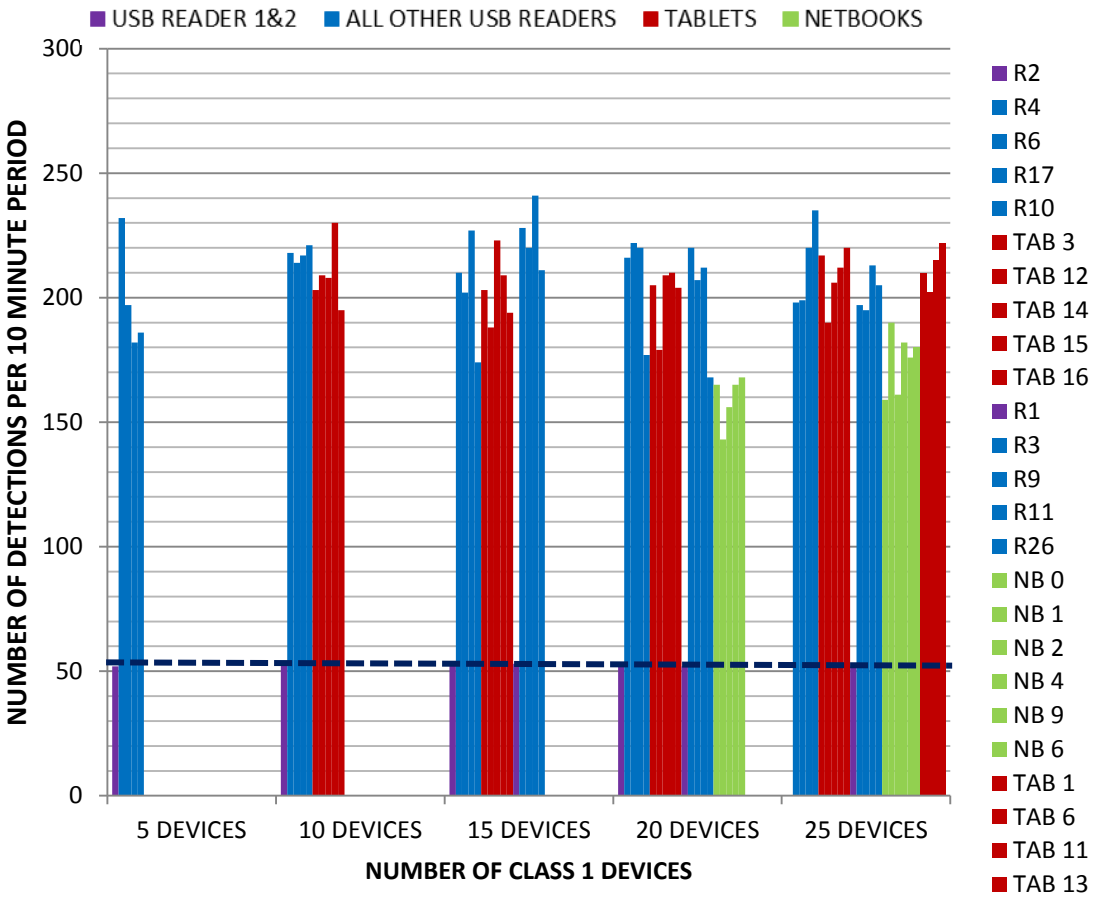

Figure 30 Class 1 Device Detection Count

Next, Figure 31 shows the headway frequency percentage trend for all sets of Class 1 devices tested from five through 25, in 0.5 second bins. The percentage value for the frequency is used to distinguish between the properties of unique device classifications that do not have an equal number of devices. Figure 31 shows that Class 1 Bluetooth-enabled devices other than R1 and R2 have bimodal headway peaks at one second and five seconds, with the R1 and R2 Bluetooth readers trending towards an average 11.3 second headway. In additional, although the peaks do not move with the addition of more Class 1 devices, the one second peak shrinks slightly from 26% to 24%, and the five second peak increases slightly, showing a bit of a "flattening" effect.

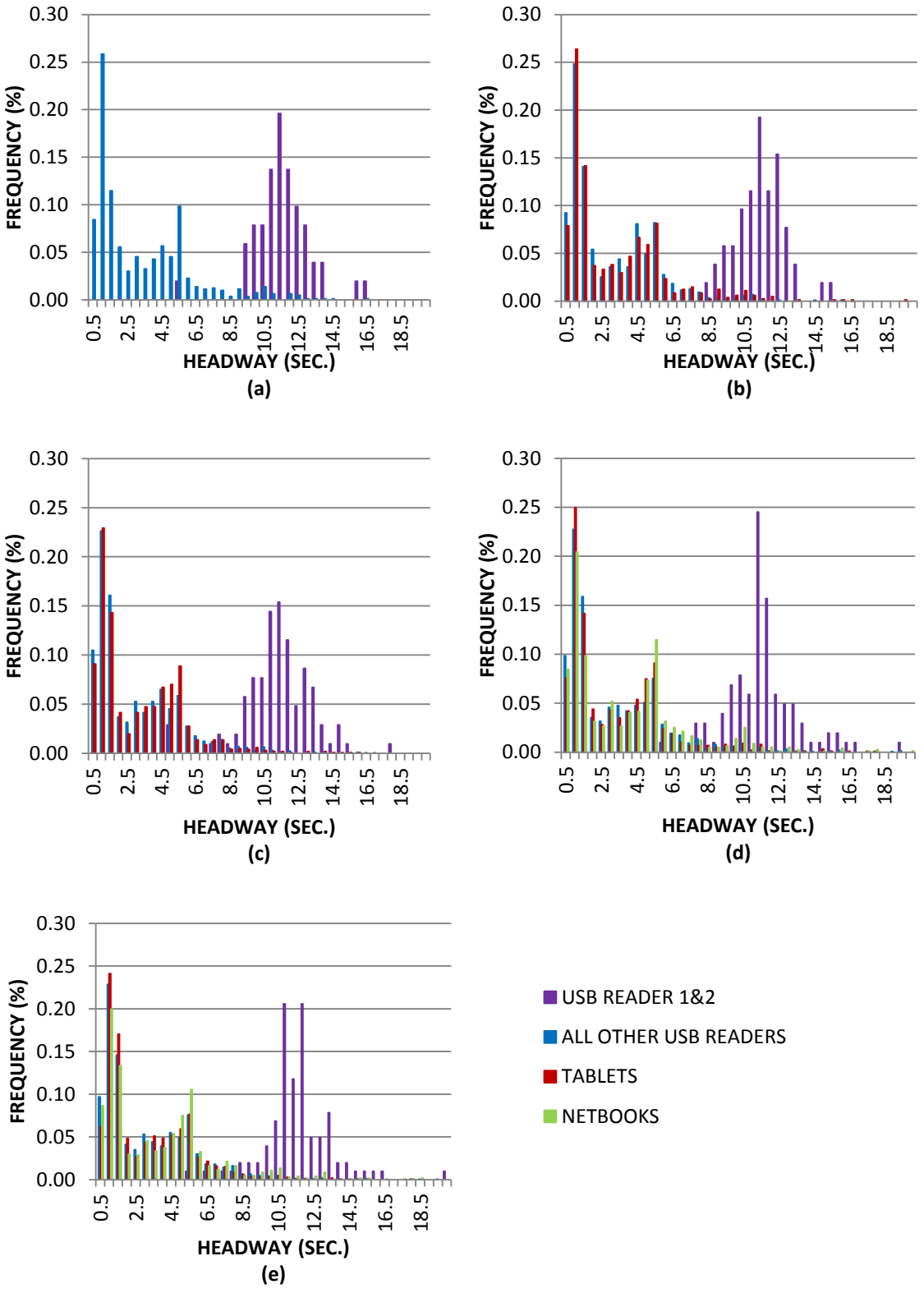

Figure 31 Headway frequency trend for Class 1 devices: (a) 5 devices, (b) 10 devices, (c) 15 devices, (d) 20 devices, (e) 25 devices

6.1.1.3 Joint Class 1 and Class 2 Devices

Figure 32 below shows the average headway trend for the individual Class 1 and Class 2 device test series, as well as the average headway for each device present in the Joint Class 1 and Class 2 test. The black dashed line represents the cycle length of 11.24 seconds to show how this value relates to the average headway of each device.

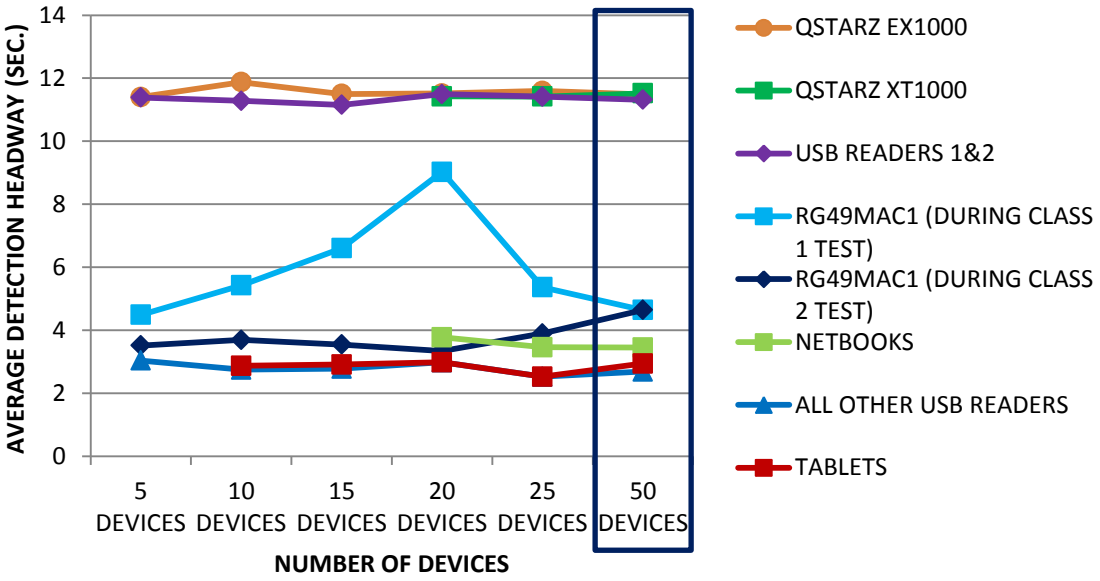

Figure 32 Joint Class 1 and 2 Device Headway trend

The headway trend remains relatively constant for the QStarz devices and USB Bluetooth readers R1 and R2 at slightly above 11.24 seconds. The headway trend for the netbooks, other USB Bluetooth readers, and tablets is unaffected by the addition of 25 additional Class 2 devices. With all 25 Class 1 and 25 Class 2 devices combined, the headway decreased for rg49mac1compared to previous Class 1 tests, but the headway increased for rg49mac1 compared to the previous Class 2 tests. This makes rg49mac1

the only device that experiences any significant change in detection characteristics with the addition of more devices in between the rg49mac1 device and the sensor. For the tests the rg49mac1 device was about 15 feet offset from the Bluetooth sensor, and the Class 1 and Class 2 devices were offset five to seven feet from the Bluetooth sensor. The closer devices experienced sustained detection while the rg49mac1 detection frequency decreased. It is not certain at this time the reason for the rg49mac1 device behavior. Future efforts will seek to explain this behavior.

Figure 33 below shows the trend of the average number of detections per cycle for the individual Class 1 and Class 2 test results, and then finally the Joint Class 1 and Class 2 results. The cycle detection count for the individual 25 device groups are not only met, but also slightly increases when the two groups of 25 devices are deployed together.

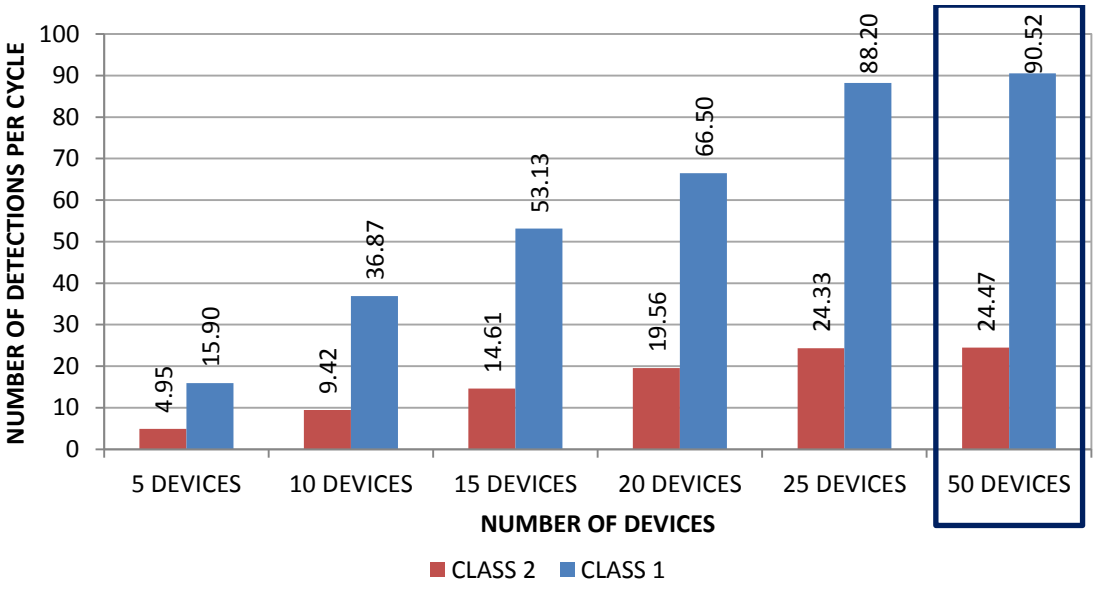

Figure 33 Joint Class 1 and 2 average detections per cycle

These results show that 50 devices is not yet the point of saturation for the Class 1 custom Bluetooth sensor. Following, Figure 34 shows the average detections per cycle separated into device type. The Class 1 devices consistently have greater detections per cycle than Class 2 devices by three to four times (again indicative of the different transmission speeds). Furthermore, there is a relative consistency of cycle detection count as more Bluetooth-enabled devices are placed in the sensor's field of view. This demonstrates further than 50 devices do not appear to reach single sensor saturation.

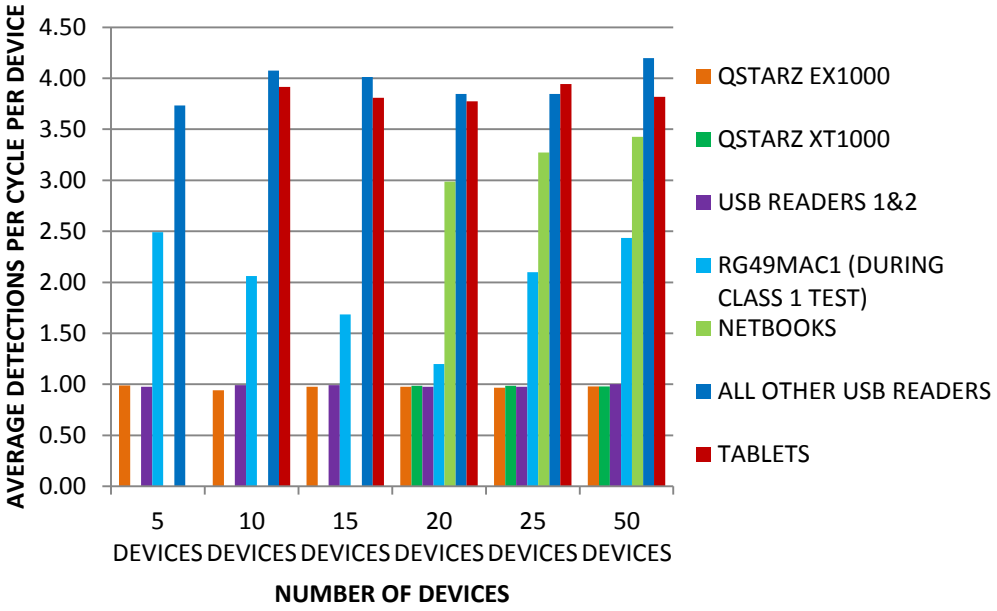

Figure 34 Joint Class 1 and 2 average detections per cycle by device type

6.1.2 Multiple Sensor Effect

Figure 35 and Figure 36 below show the detection count for each Class 2 device in each ten minute detection period incrementing from five to 20 Class 2 devices for Sensor 5 and Sensor 8, respectively.

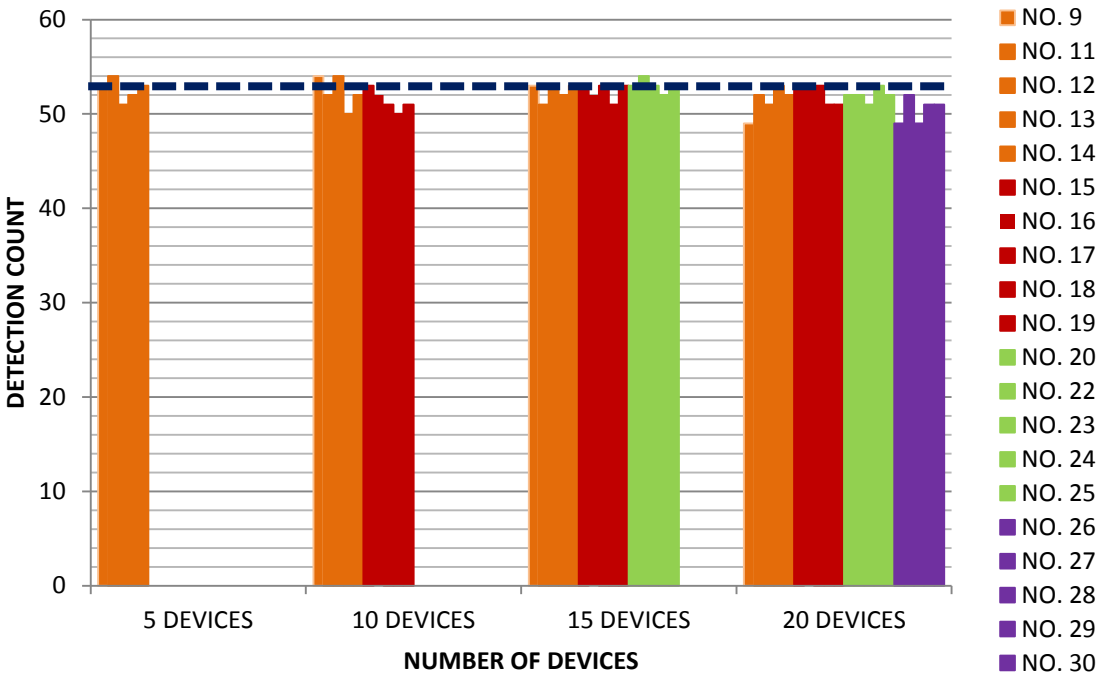

Figure 35 Dual Sensor Class 2 Device Detection Count (sensor 5)

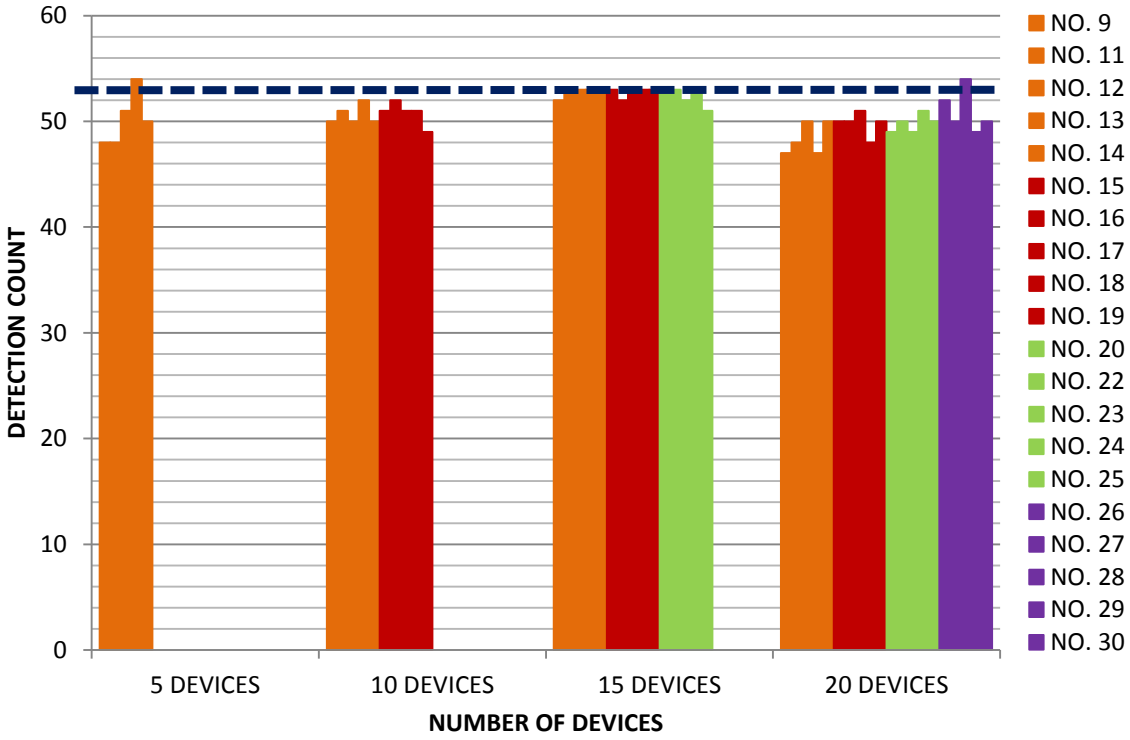

Figure 36 Dual Sensor Class 2 Device Detection Count (sensor 8)

Sensor 8 has lower overall detections than Sensor 5 for each ten minute detection period. This could be the effect of the presence of multiple sensors, or that Sensor 8 is effectively not "equal" to Sensor 5. Furthermore, the detection count shown in Figure 35 is comparable to the detection count for five through 20 devices shown in Figure 27 for the single sensor capacity test results (also Sensor 5), indicating that the presence of one additional sensor does not impact the net count of detections during each ten-minute period.

Figure 37, Figure 38, Figure 39, and Figure 40 below show the headway trends for 5, 10, 15, and 20 Class 2 Bluetooth-enabled devices, respectively, when deployed along with a dual-sensor system. Each Figure has an (a) and (b) component representing the headway trend for sensor 5 and sensor 8, respectively. The headway peaks vary across sensors, and also vary greatly from the single sensor 5 device headway trends presented in Section 6.1.1.1. There is a similar detection count trend for the single and dual Sensor 5 scenarios, with the main difference in dual sensor deployment coming down to how the detections are appropriated. Therefore, with more sensors vying for the detection of one device, the headway experiences fewer peaks.

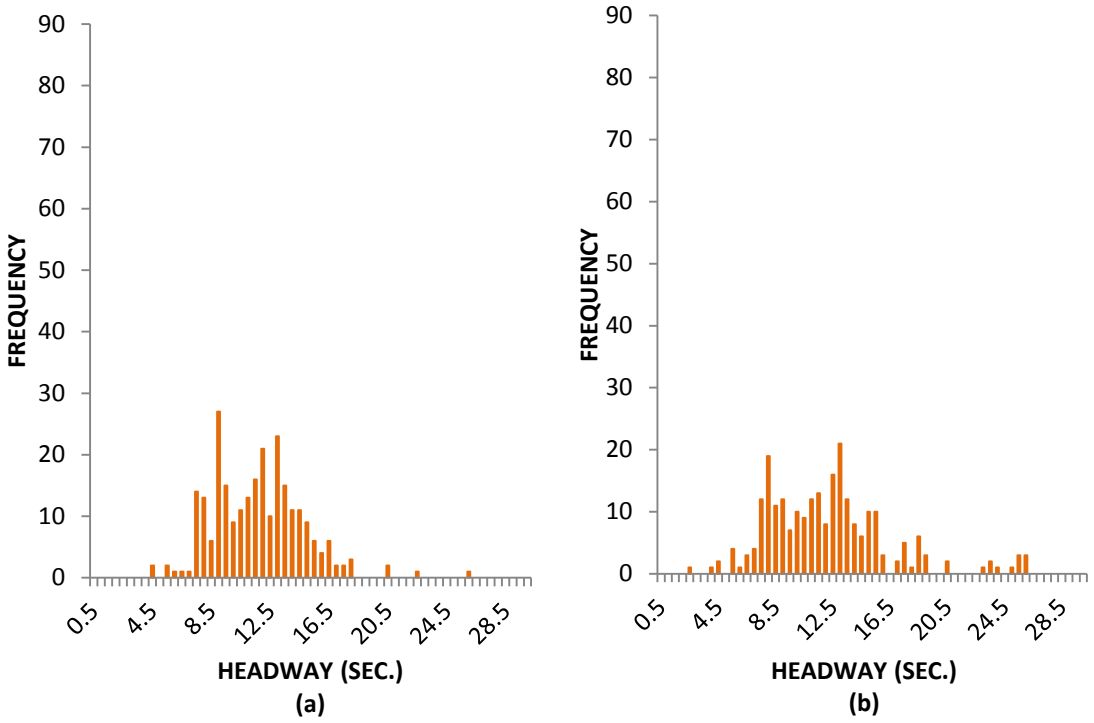

Figure 37 Headway frequency for 5 Class 2 devices for (a) sensor 5 and (b) sensor 8

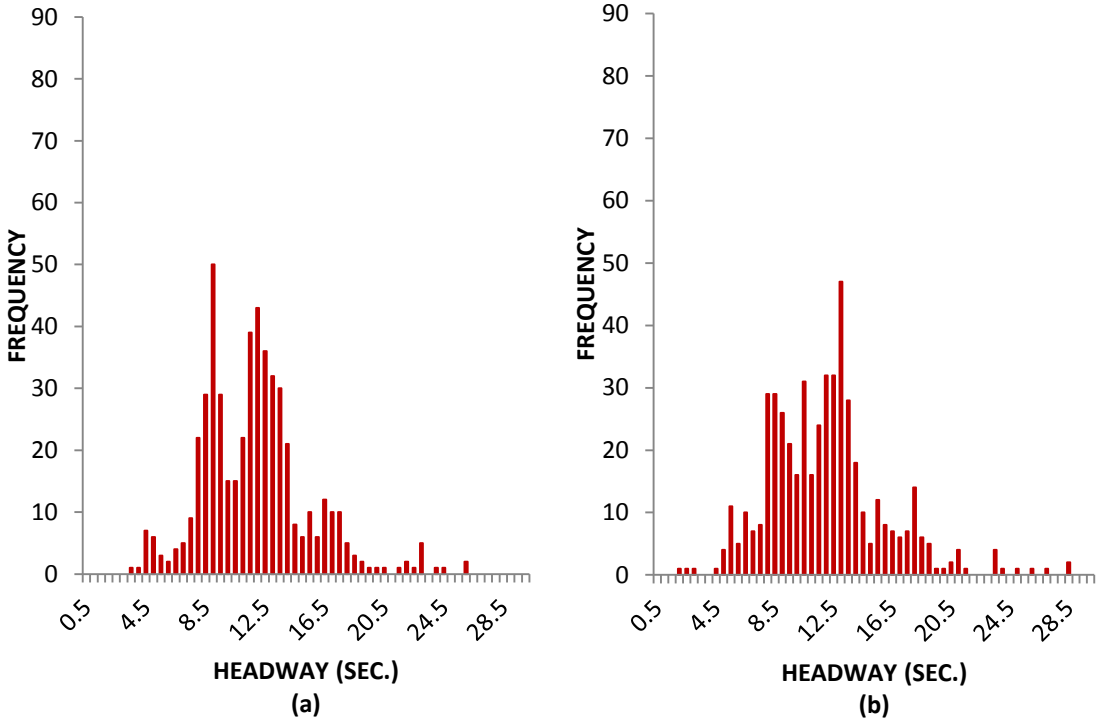

Figure 38 Headway frequency for 10 Class 2 devices for (a) sensor 5 and (b) sensor 8

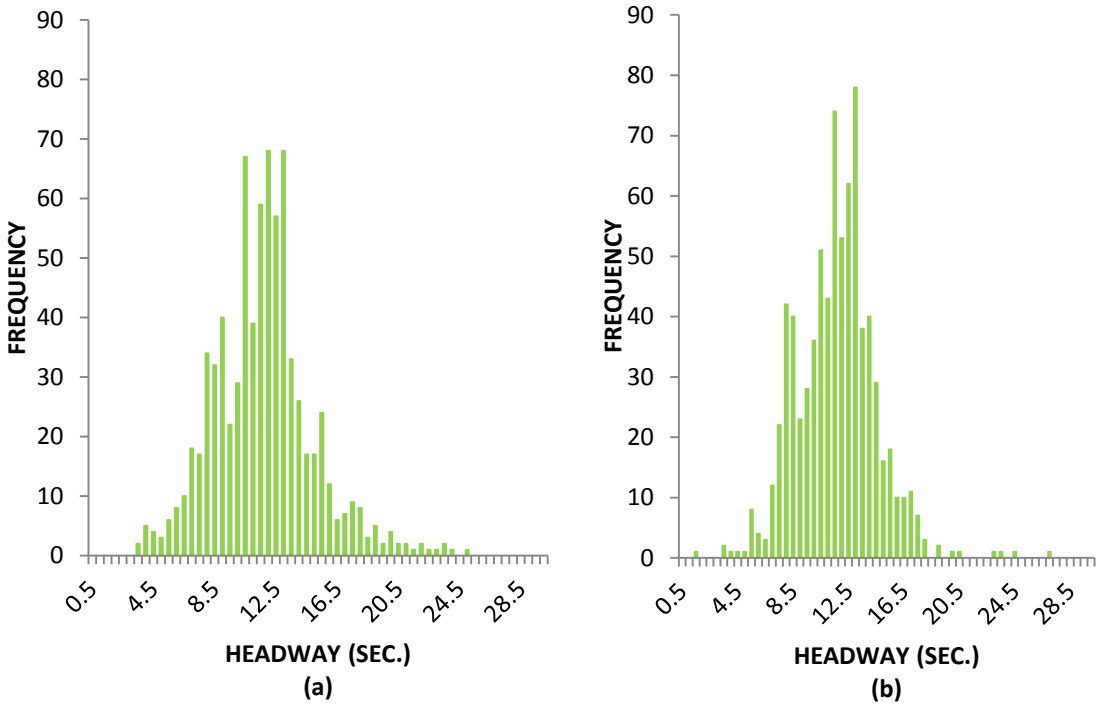

Figure 39 Headway frequency for 15 Class 2 devices for (a) sensor 5 and (b) sensor 8

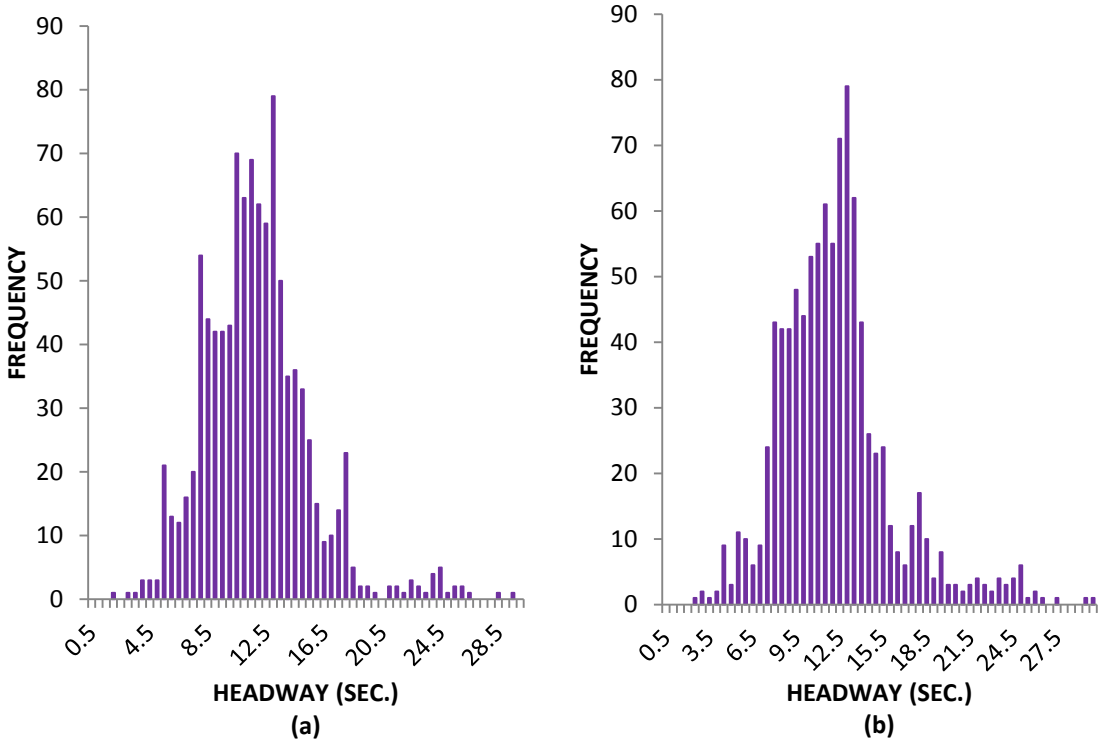

Figure 40 Headway frequency for 20 Class 2 devices for (a) sensor 5 and (b) sensor 8

Table 8 provides a comparison of the device headway averages for single and dual Sensor 5 deployment. In some cases the average detection headway increased, and in some cases the average headway decreased, but there is not a clear trend showing an impact of an additional sensor on Class 2 device headway. Therefore, these results show that there is no major net effect on detection when two sensors are put in place. Although the detection pattern changes, the aggregate detection results for the dual sensors don't show a large difference from the single sensor results.

Table 8 Average Device Headway Comparison for Sensor 5 Dual and Single

	5 Devices	**10 Devices**	**15 Devices**	**20 Devices**
QStarz 1000eX (single)	11.40 sec.	11.87 sec.	11.50 sec.	11.52 sec.
QStarz 1000eX (dual)	11.43 sec.	11.55 sec.	11.47 sec.	11.59 sec.
QStarz 1000XT (single)				11.42 sec.
QStarz 1000XT (dual)			11.31 sec.	11.71 sec.
rg49mac1 (single)	3.52 sec.	3.69 sec.	3.55 sec.	3.34 sec.
rg49mac1 (dual)	3.56 sec.	3.28 sec.	3.56 sec.	3.70 sec.
Cycle Length	11.24 sec.	11.24 sec.	11.24 sec.	11.24 sec.

6.2 14th Street Device Detection Range Results

6.2.1 Device Detection Range

The results for 14th Street device detection range are presented in a number of ways. First, the results contain a distinction between each probe vehicle device, also calling out whether the device is Class 1 or Class 2. Secondly, the results show the effect of separating the range profile up into purely eastbound and westbound direction detections, as well as the first and last detections in each run segment. Each of these

distinctions is made for the midblock and intersection sensor locations in the following sections. The reason for separating the results into these different categories is to see if a pattern arises in any category, and to assess which detection characteristic to use when calculating travel time along a corridor.

6.2.1.1 Detection Range Influencing Factors

There are two main factors that play a role in the detection range results presented in the following results. The first is how the physical boundary of the run corridor is defined, and the second is how the beginning and end of a run coincides with the beginning or end of an inquiry cycle.

6.2.1.1.1 Physical Run Boundary

After the initial analysis, the research team chose to redefine the physical limits of the run to end 100 feet before the two turnaround locations on the 14th Street corridor. The reasoning behind this decision is that the probe vehicles were stationary at the turnaround locations for anywhere from five seconds to over 60 seconds. During this time the probe vehicles were not actively on the corridor, and were also present at the same location for portions of the eastbound and westbound legs of each run. In addition, the probe vehicle devices were not in motion on the corridor, which contradicts the goal of this analysis to assess the best method of calculating real-time travel time. Furthermore, stationary Bluetooth-enabled devices do have a higher propensity for detection than devices in motion when within a sensor's field of view.

By narrowing the window of the corridor by 100 feet before each turn around location, the revised window of the detection corridor is 811 feet west of the midblock

location, and 1220 feet east of the intersection location. However, to be consistent with defining the extents of the corridor around the midblock and intersection sensor locations, the research team opted to narrow the corridor span to 800 feet on the eastbound end of the intersection sensor and 800 feet on the westbound end of the midblock sensor. Although these adjustments were made for the majority of the analysis, the initial results show the raw data including all detections occurring near-to and within TA1 and TA2.

6.2.1.1.2 Run Time and Inquiry Cycle

The results show a correlation between continued device detection and the sensor inquiry cycle. A string of detections including anywhere from two to eight detections at the midblock and up to 18 detection at the intersection occur all within the same sensor inquiry cycle. Once the sensor detects a device, a communication stream has been established between the two where ongoing detection occurs. Surprisingly, this ongoing detection continues even as the device leaves the 300 foot detection window for the Bluetooth sensor to as far out as 1000 feet, particularly for Class 1 devices, as the results of the 14th Street test show below.

6.2.1.2 Friday, August 24, 2012

6.2.1.2.1 All Detections

On Friday, August 24th, the probe vehicles completed 27 runs (each with an eastbound and westbound leg) along the 14th Street corridor. Figure 41below shows all of the detections, eastbound and westbound, including multiple detections, for the midblock Bluetooth sensor. The black dashed line shows the location of the sensor of

focus, the red dashed line shows the location of the other sensor, and the gold dashed line shows the location of the turnaround locations (labeled appropriately).

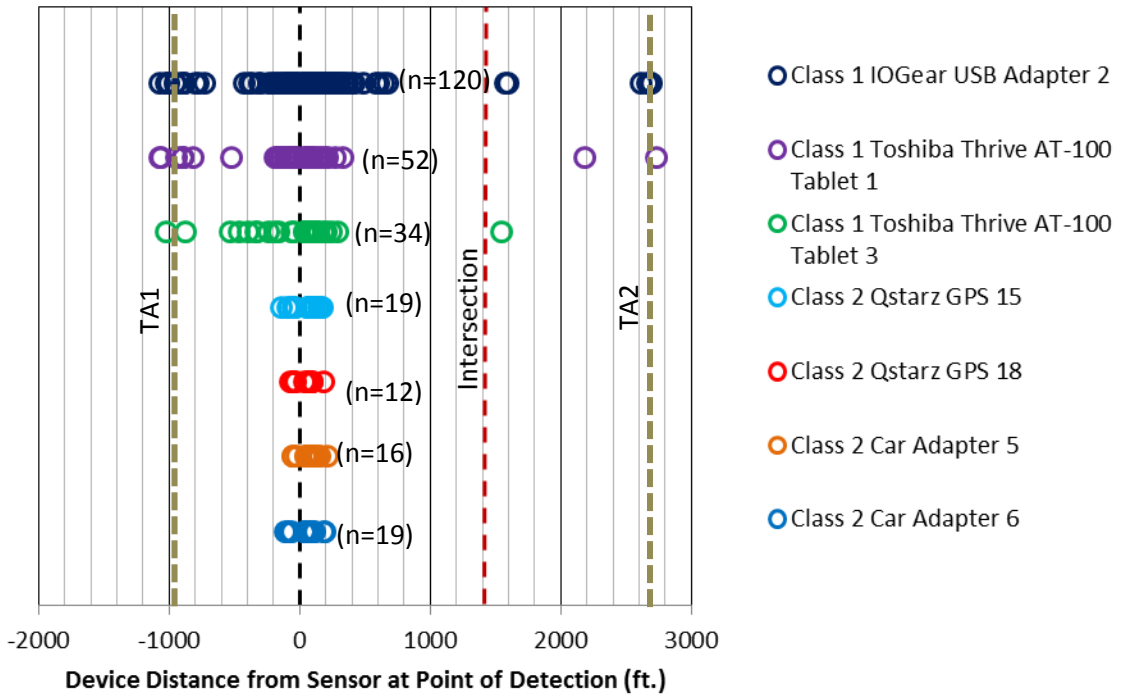

Figure 41 All detections by the midblock sensor

Table 9 provides a summary of the corresponding intersection detection range results. The average records per run does not account for the runs when the device missed detection. Furthermore, the value of the average offset is calculated relative to the eastbound direction. A positive range for eastbound represents downstream detections and a negative range for the eastbound represents upstream detections. The westbound values are switched, with positive values representing upstream detections, and negative values representing downstream detections.

The Class 2 device detections at the midblock sensor show less scatter than the Class 1 detections at the midblock sensor, with most detections taking place within a 200 foot range in either direction from the sensor. Several detections for the Class 1 devices are present at TA1 and TA2, which are off the corridor, and are filtered for the next sections of results. Furthermore, the Class 2 devices are detected at most only once per run through the corridor, whereas the Class 1 devices, when detected, are detected an average of more than two times at the midblock sensor.

Table 9 14th St. Midblock All Detections Summary

Device	Class	No. Records	No. Runs Detected (out of 27)	Average Records per Run*	Average Offset (ft.)	Average Offset (Abs. Value)
Class 1 IOGear USB Bluetooth Adapter 2	1	120	26	2.48	363.32	96.52
Class 1 Toshiba Thrive AT-100 Tablet 1	1	52	20	2.13	321.97	-49.67
Class 1 Toshiba Thrive AT-100 Tablet 3	1	34	14	2.03	250.30	-26.31
Class 2 QStarz GPS 15	2	19	18	1	96.90	46.80
Class 2 QStarz GPS 18	2	12	11	1	71.90	34.82
Class 2 Car Adapter 5	2	16	14	1	85.25	67.05
Class 2 Car Adapter 6	2	19	17	1	79.34	41.65

* For those runs when a detection occurred

Figure 42 shows all of the detections for the intersection Bluetooth sensor, and Table 10 provides a summary of the corresponding intersection detection range results.

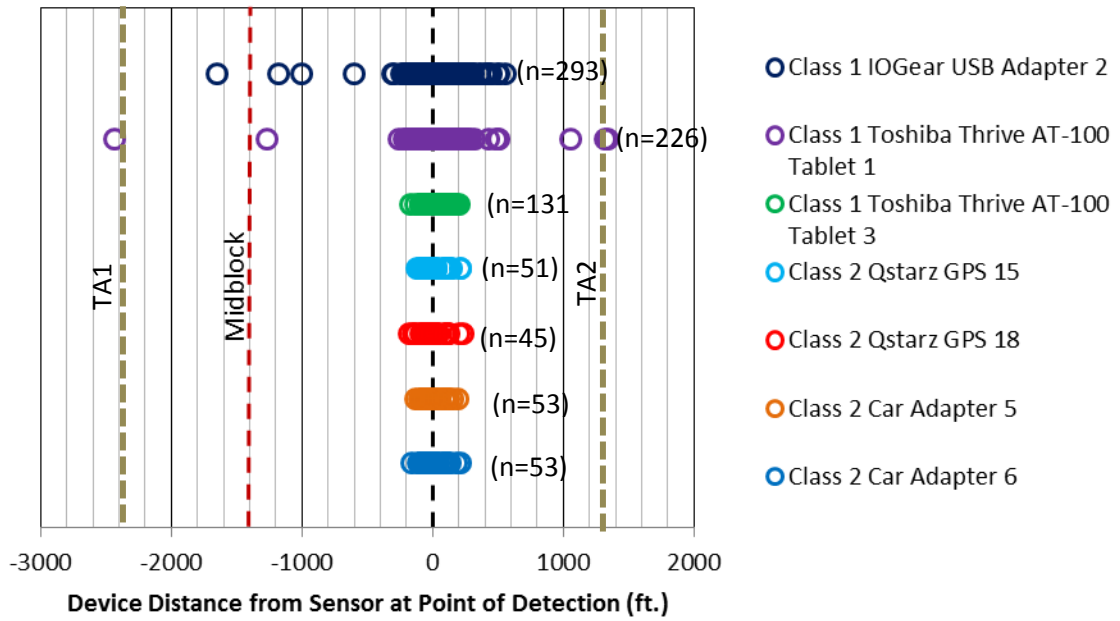

Figure 42 All detections by the intersection sensor

Table 10 14th St. Intersection All Detections Summary

Device	Class	No. Records	No. Runs Detected (out of 27)	Average Records per Run*	Average Offset (ft.)	Average Offset (Abs. Value)
Class 1 IOGear USB Bluetooth Adapter 2	1	293	27	5.06	116.60	36.79
Class 1 Toshiba Thrive AT-100 Tablet 1	1	226	27	4.12	121.73	16.82
Class 1 Toshiba Thrive AT-100 Tablet 3	1	131	27	3.67	58.85	19.88
Class 2 QStarz GPS 15	2	51	27	1.61	64.65	0.512
Class 2 QStarz GPS 18	2	45	27	1.64	65.11	-10.37
Class 2 Car Adapter 5	2	53	27	1.49	61.59	-5.79
Class 2 Car Adapter 6	2	55	27	1.51	60.39	-1.75

* For those runs when a detection occurred

The intersection detections for the Class 2 devices and Toshiba Tablet 3 show very little scatter, and are all concentrated within a 200 foot detection range around the intersection sensor. Similar to the midblock detections, the Class 1 devices show some variability for intersection detections, and have detections at TA1 and TA2, which are again filtered for the next sections of results. The intersection detections show on average more detections per run than for the midblock detections. This is likely due to the stop-and-go nature of the intersection traffic operations. The slowing/stopping of the vehicles maintained the device in the sensor's field of view for a longer period of time, most often more than one cycle, allowing for an average increase in the number of detections per run. Conversely, the vehicles passing the midblock sensor were always in free flow in the eastbound and westbound directions.

6.2.1.2.2 Eastbound All Detections

Figure 43 below shows all eastbound detections for the midblock sensor, and Table 11 provides a summary of corresponding midblock sensor detection range results. Following, Figure 44 shows all eastbound detections for the intersection sensor, and Table 12 provides a summary of the corresponding intersection detection range results. These results follow the corridor span modification, showing detections only 800 feet west of the midblock sensor. After a close inspection of the results, those detections that are taking place outside of the expected 300 foot detection range are typically part of a Class 1 detection "string", which consists of repeat detections within the same 11.24 second sensor inquiry cycle.

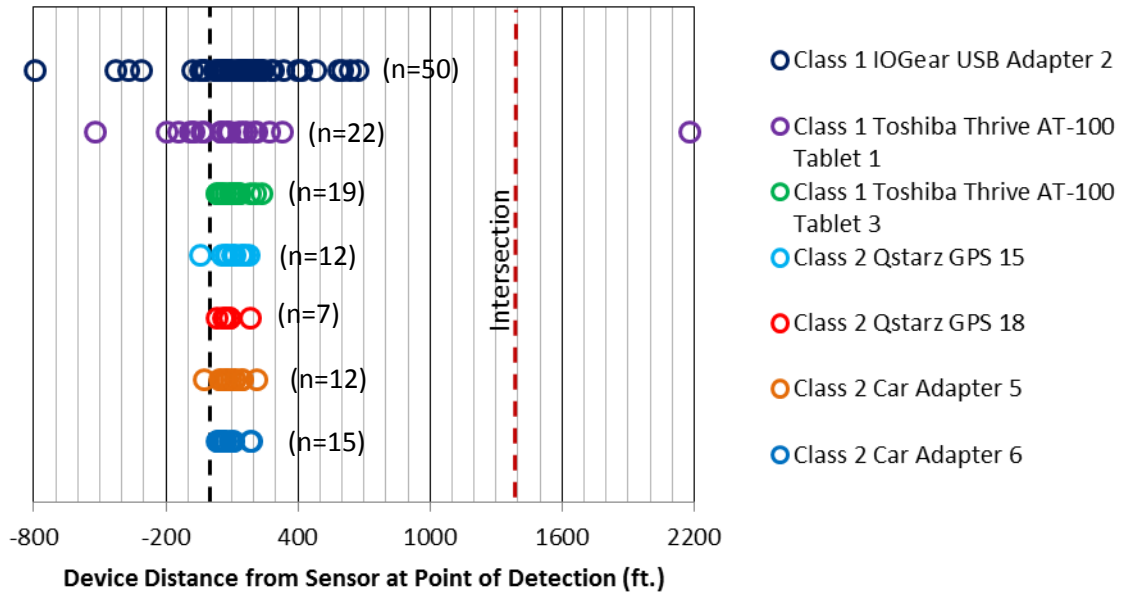

Figure 43 All Eastbound detections by the midblock sensor

Table 11 14th St. Midblock Eastbound All Detections Summary

Device	Class	No. Records	No. Runs Detected (out of 27)	Average Records per Run*	Average Offset (ft.)	Average Offset (Abs. Value)
Class 1 IOGear USB Bluetooth Adapter 2	1	50	20	2.54	133.67	218.61
Class 1 Toshiba Thrive AT-100 Tablet 1	1	22	13	2.20	128.82	235.82
Class 1 Toshiba Thrive AT-100 Tablet 3	1	19	12	2.03	101.99	101.99
Class 2 QStarz GPS 15	2	12	12	1	96.73	104.26
Class 2 QStarz GPS 18	2	7	7	1	82.99	82.99
Class 2 Car Adapter 5	2	12	12	1	90.81	95.78
Class 2 Car Adapter 6	2	15	15	1	76.63	72.63

* For those runs when a detection occurred

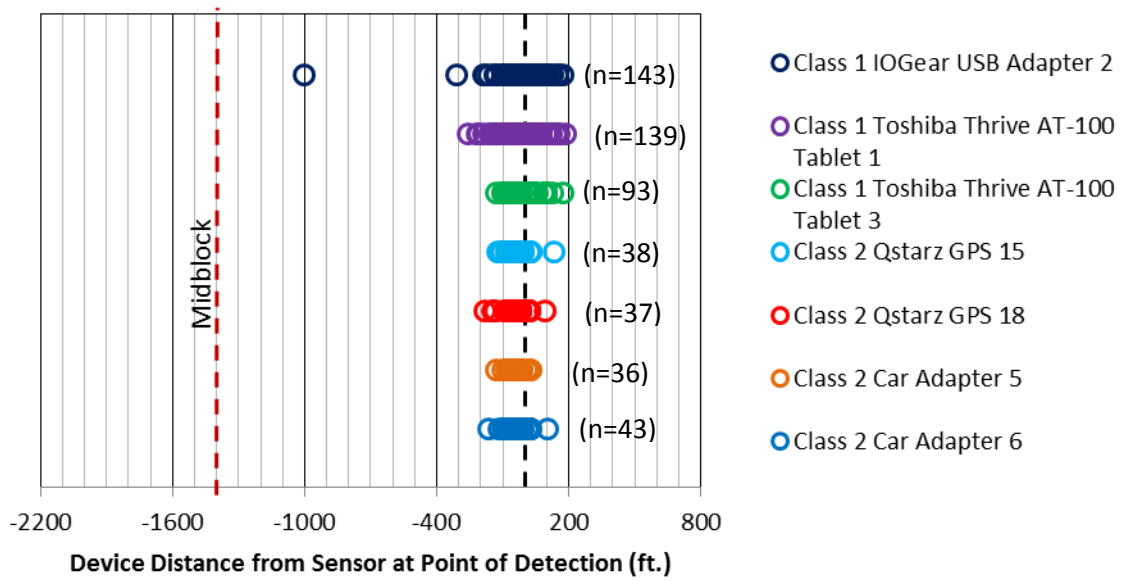

Figure 44 All Eastbound detections by the intersection sensor

Table 12 14th St. Intersection Eastbound All Detections Summary

Device	Class	No. Records	No. Runs Detected (out of 27)	Average Records per Run*	Average Offset (ft.)	Average Offset (Abs. Value)
Class 1 IOGear USB Bluetooth Adapter 2	1	143	26	5.06	-13.07	54.64
Class 1 Toshiba Thrive AT-100 Tablet 1	1	139	26	4.14	-26.41	61.34
Class 1 Toshiba Thrive AT-100 Tablet 3	1	93	22	3.73	-7.98	40.62
Class 2 QStarz GPS 15	2	38	22	1.61	-36.74	47.09
Class 2 QStarz GPS 18	2	37	20	1.64	-39.55	52.24
Class 2 Car Adapter 5	2	36	25	1.52	-44.74	47.44
Class 2 Car Adapter 6	2	43	25	1.51	-32.91	46.56

* For those runs when a detection occurred

The eastbound detections are more often occurring downstream of the sensor at the midblock (after the sensor), and upstream of the sensor at the intersection (on the approach to the sensor). The high presence of detections upstream of the intersection sensor is most likely derived from the stop and slow scenarios mentioned earlier. For the eastbound direction, 17 out of 27, or 63% of the runs passing the intersection sensor presented an increased opportunity for device detection on the approach to the sensor where the stopping/slowing was occurring.

6.2.1.2.3 Westbound All Detections

Figure 45 below shows all westbound detections for the midblock sensor, and Table 13 provides a summary of the corresponding midblock detection range results.

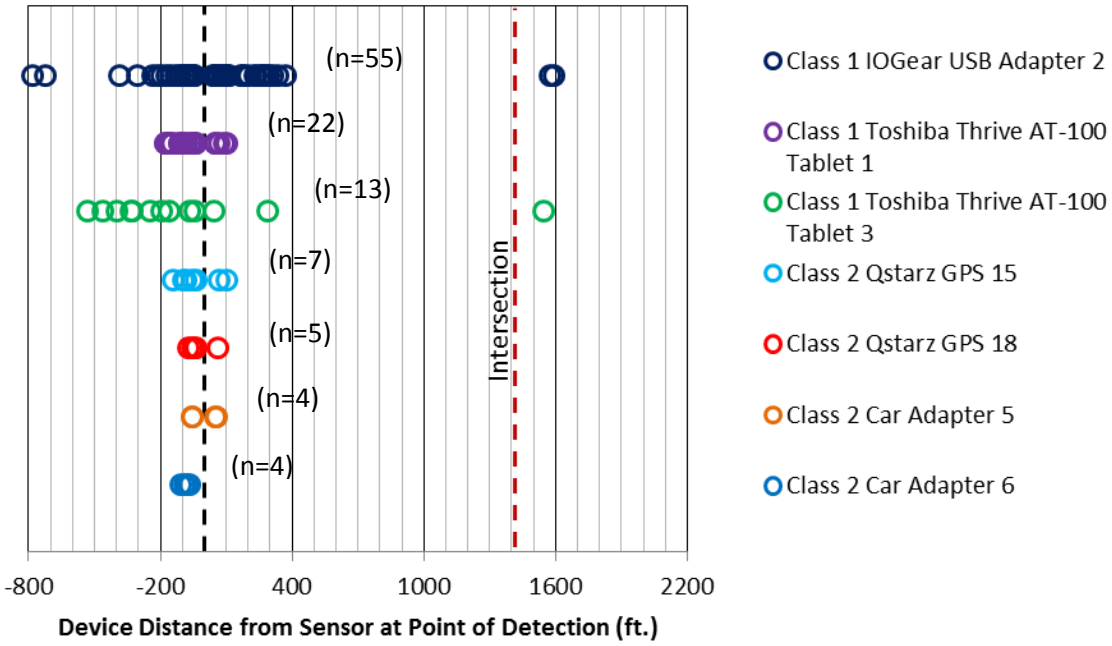

Figure 45 All Westbound detections by the midblock sensor

Table 13 14th St. Midblock Westbound All Detections Summary

Device	Class	No. Records	No. Runs Detected (out of 27)	Average Records per Run*	Average Offset (ft.)	Average Offset (Abs. Value)
Class 1 IOGear USB Bluetooth Adapter 2	1	55	21	2.48	69.63	221.32
Class 1 Toshiba Thrive AT-100 Tablet 1	1	22	13	2.16	-68.76	100.21
Class 1 Toshiba Thrive AT-100 Tablet 3	1	13	6	2.13	-71.29	359.00
Class 2 QStarz GPS 15	2	7	7	1	-38.82	84.29
Class 2 QStarz GPS 18	2	5	5	1	-32.62	56.36
Class 2 Car Adapter 5	2	4	4	1	-4.23	53.67
Class 2 Car Adapter 6	2	4	4	1	-89.50	89.50

* For those runs when a detection occurred

As shown in Figure 45 and Table 13, the westbound midblock detections still experience a large amount of scatter, particularly for the Class 1 devices. The spread is both upstream and downstream of the midblock sensor, but Class 2 devices show a greater likelihood for detection downstream of the midblock sensor. However, the number of records of detection is significantly less for the westbound midblock than the eastbound midblock. This is most likely because the westbound devices are farther from the sensor than the eastbound devices, so their likelihood and frequency of detection decreases.

Next, Figure 46 shows all westbound detections for the intersection sensor, and Table 14 provides a summary of the corresponding intersection detection range results. The westbound intersection detections experience significantly more scatter than the

eastbound intersection detections. Most detection for Class 2 devices are upstream of the sensor, most likely influenced by the 14 out of 27, or 52% stopped or slowed run scenarios. As for the eastbound, the count for the intersection is greater than the count for midblock because of the greater time the devices spent in the sensors field of view during the stopped and slowed traffic movements.

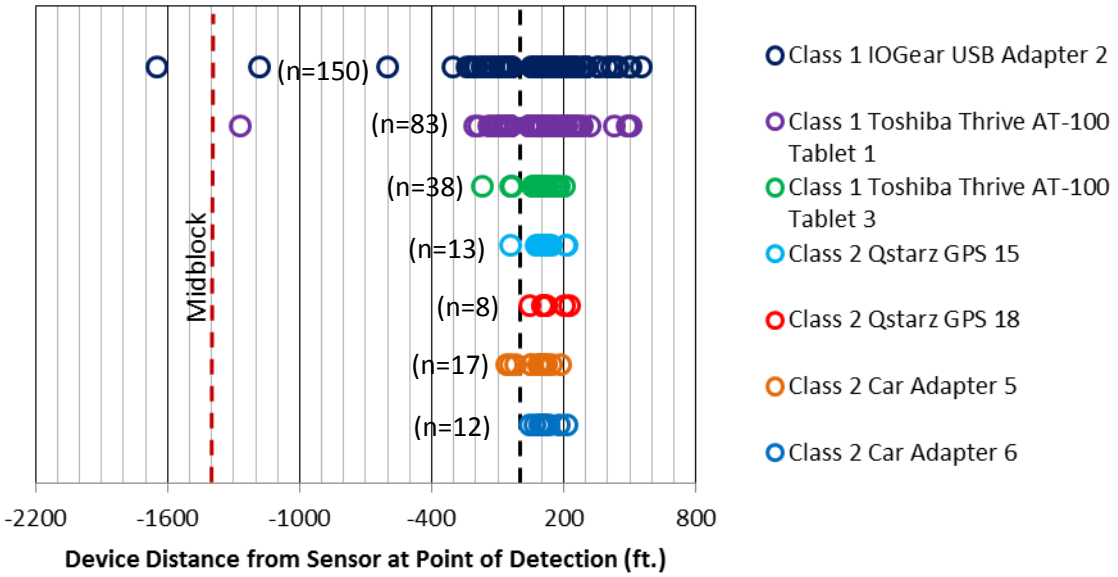

Figure 46 All Westbound detections by the intersection sensor

Table 14 14th St. Intersection Westbound All Detections Summary

Device	Class	No. Records	No. Runs Detected (out of 27)	Average Records per Run*	Average Offset (ft.)	Average Offset (Abs. Value)
Class 1 IOGear USB Bluetooth Adapter 2	1	150	25	5.13	84.34	175.66
Class 1 Toshiba Thrive AT-100 Tablet 1	1	83	23	3.97	74.87	154.70
Class 1 Toshiba Thrive AT-100 Tablet 3	1	38	13	3.50	88.08	103.47
Class 2 QStarz GPS 15	2	13	9	1.54	109.40	115.98
Class 2 QStarz GPS 18	2	8	6	1.69	124.60	124.60
Class 2 Car Adapter 5	2	17	11	1.55	76.71	91.55
Class 2 Car Adapter 6	2	12	11	1.51	109.93	109.93

* For those runs when a detection occurred

6.2.1.2.4 Eastbound First Detection

Figure 47 below shows the first eastbound detections for the midblock sensor detection, and Table 15 provides a summary of the corresponding midblock detection range results. Once again the midblock detections are taking place downstream of the sensor. When considering just the first detection of each run where a detection occurred, there is significantly less scatter than all eastbound detections. The number of records now represents the number of runs out of 27 when a given device was detected. This shows that when the repeat detections are removed from the equation the Class 1 and Class 2 devices perform similarly with respect to the number of runs each device was detected.

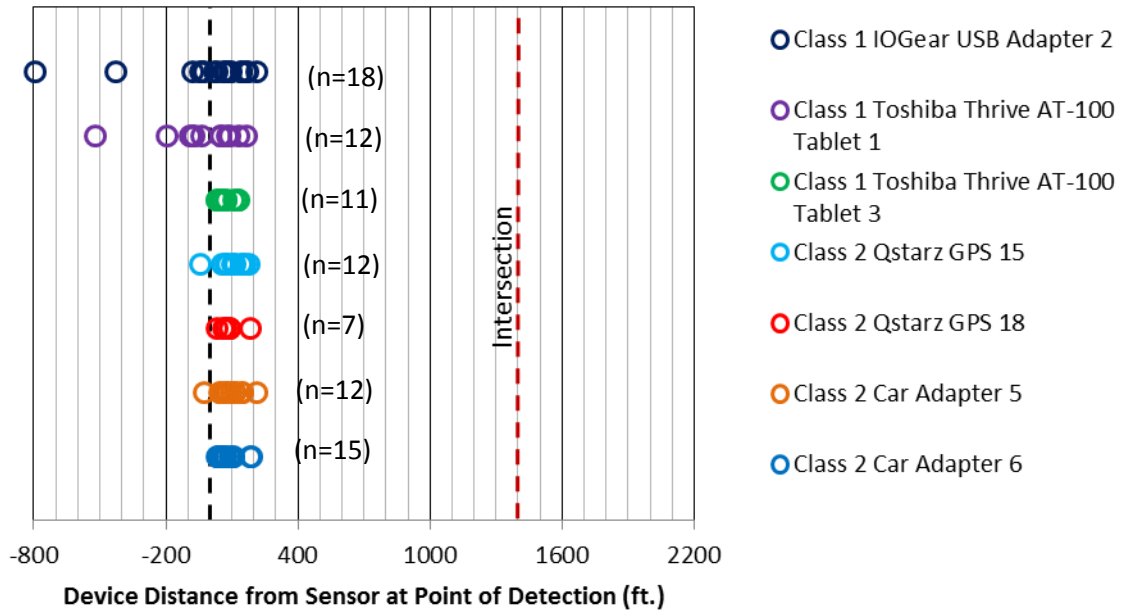

Figure 47 First Eastbound detection in each run by the midblock sensor

Table 15 14th St. Midblock Eastbound First Detections Summary

Device	Class	No. Runs Detected (out of 27)	Average Offset (ft.)	Average Offset (Abs. Value)
Class 1 IOGear USB Bluetooth Adapter 2	1	18	-9.63	148.34
Class 1 Toshiba Thrive AT-100 Tablet 1	1	12	-37.57	129.68
Class 1 Toshiba Thrive AT-100 Tablet 3	1	11	72.33	72.33
Class 2 QStarz GPS 15	2	12	96.73	104.26
Class 2 QStarz GPS 18	2	7	82.99	82.99
Class 2 Car Adapter 5	2	12	90.81	95.78
Class 2 Car Adapter 6	2	15	76.63	72.63

Next, Figure 48 shows the first eastbound detections for the intersection sensor, and Table 16 provides a summary of the corresponding detection range results. Once

again the intersection detections are taking place upstream of the sensor. All devices are detected in a greater portion of the runs for the intersection than the midblock, with GPS 18 missing the most runs at seven. This higher run detection rate is most likely the result of 63% of the runs featuring stopped or slowed traffic scenarios. There is also significantly less scatter for the intersection detection when only the first detection in each run per device is considered as opposed to all eastbound intersection detections.

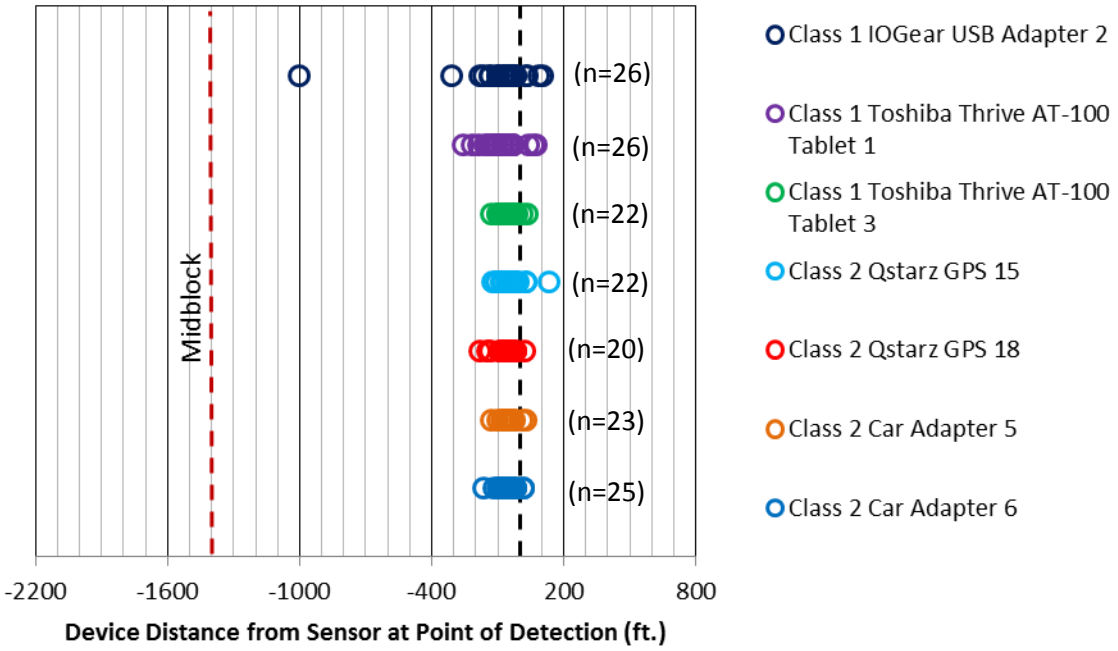

Figure 48 First Eastbound detection in each run by the intersection sensor

Table 16 14th St. Intersection Eastbound First Detections Summary

Device	Class	No. Runs Detected (out of 27)	Average Offset (ft.)	Average Offset (Abs. Value)
Class 1 IOGear USB Bluetooth Adapter 2	1	26	-100.66	118.99
Class 1 Toshiba Thrive AT-100 Tablet 1	1	26	-87.25	100.60
Class 1 Toshiba Thrive AT-100 Tablet 3	1	22	-55.32	59.05
Class 2 QStarz GPS 15	2	22	-43.13	59.38
Class 2 QStarz GPS 18	2	20	-73.14	75.10
Class 2 Car Adapter 5	2	23	-54.18	56.85
Class 2 Car Adapter 6	2	25	-61.43	66.35

6.2.1.2.5 Westbound First Detection

Figure 49 below shows the first westbound detections for the midblock sensor, and Table 17 provides a summary of the corresponding detection range results. The number of records for this case also represents the number of runs out of 27 that a given device was detected. The westbound first detections are distributed around the sensor, but they still show a propensity for detection downstream of the sensor when traveling westbound, as the average offset shows. The number of runs detected for each device shows a great discrepancy in the detection frequency of Class 1 versus Class 2 devices. This is most likely because Class 1 devices are of a higher power class, and thus have a greater ability to communicate across longer distances than Class 2 devices.

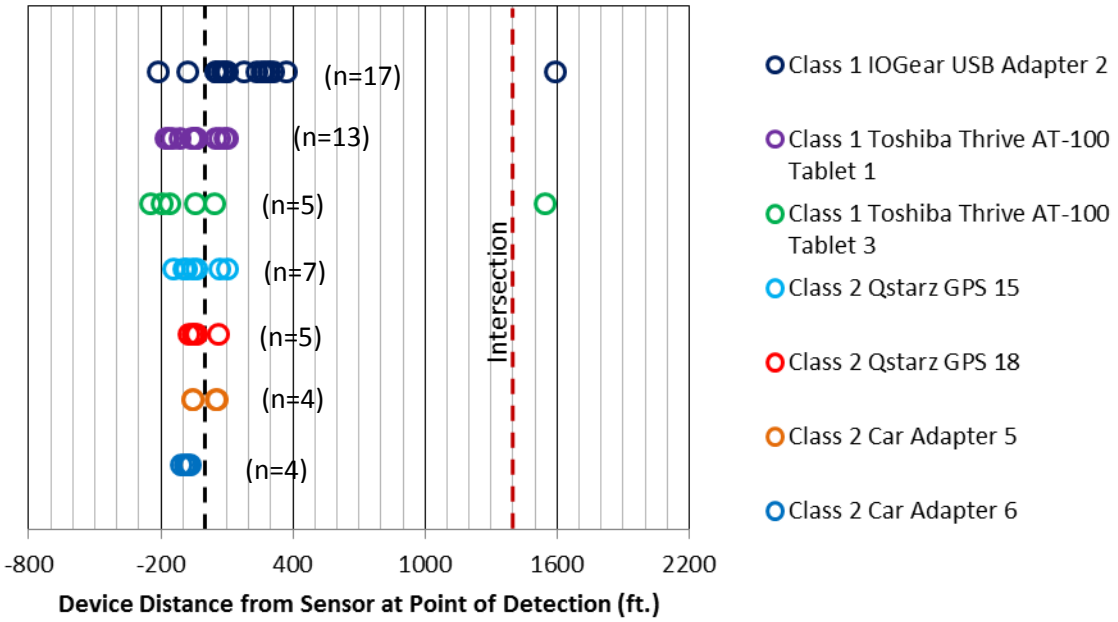

Figure 49 First Westbound detection in each run by the midblock sensor

Table 17 14th St. Midblock Westbound First Detections Summary

Device	Class	No. Runs Detected (out of 27)	Average Offset (ft.)	Average Offset (Abs. Value)
Class 1 IOGear USB Bluetooth Adapter 2	1	17	140.54	175.66
Class 1 Toshiba Thrive AT-100 Tablet 1	1	13	-43.14	89.44
Class 1 Toshiba Thrive AT-100 Tablet 3	1	5	-121.70	138.94
Class 2 QStarz GPS 15	2	7	-38.82	84.29
Class 2 QStarz GPS 18	2	5	-32.62	56.36
Class 2 Car Adapter 5	2	4	-4.23	53.67
Class 2 Car Adapter 6	2	4	-89.50	89.50

Next, Figure 50 shows the first westbound detections for the intersection sensor, and Table 18 provides a summary of the corresponding detection range results. The first

westbound detection takes place in almost all scenarios upstream of the intersection sensor, when the device is first entering the detection window of the sensor. The Class 1 devices still perform well with respect to runs detected for the westbound intersection approach, but the Class 2 device detections at the westbound intersection are less than those for the Class 1, and also less than the first eastbound intersection detections. However, the westbound intersection detection count is still greater than the westbound midblock detection count for Class 2 devices because of the longer time on average the device is spending in the sensor's field of view.

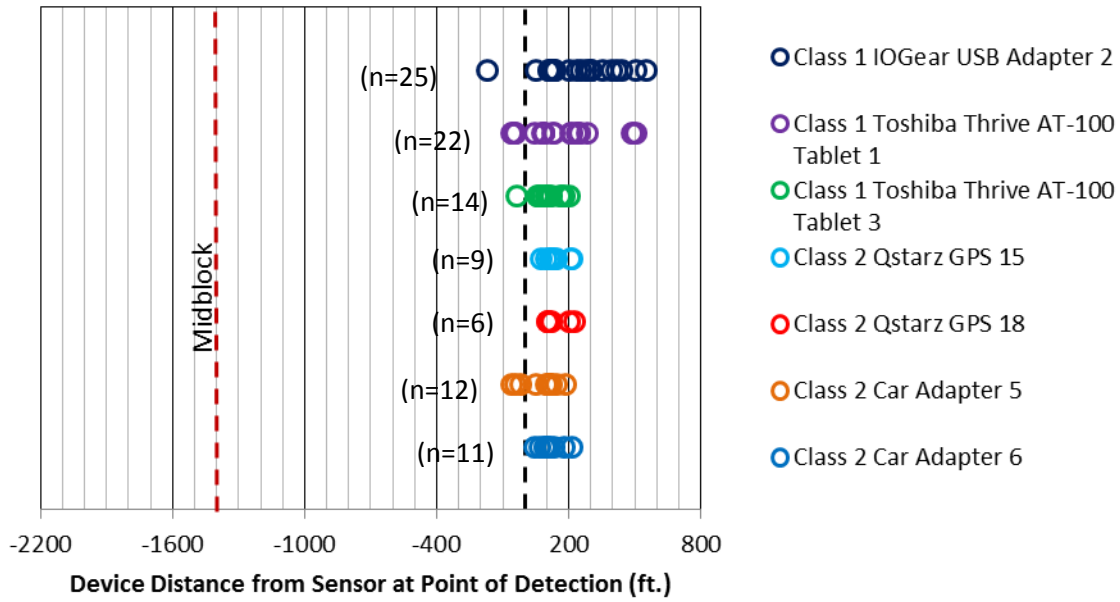

Figure 50 First Westbound detection in each run by the intersection sensor

Table 18 14th St. Intersection Westbound First Detections Summary

Device	Class	No. Runs Detected (out of 27)	Average Offset (ft.)	Average Offset (Abs. Value)
Class 1 IOGear USB Bluetooth Adapter 2	1	25	223.26	236.95
Class 1 Toshiba Thrive AT-100 Tablet 1	1	22	159.31	183.10
Class 1 Toshiba Thrive AT-100 Tablet 3	1	14	101.76	107.42
Class 2 QStarz GPS 15	2	9	132.80	132.80
Class 2 QStarz GPS 18	2	6	141.45	141.45
Class 2 Car Adapter 5	2	12	74.54	95.57
Class 2 Car Adapter 6	2	11	110.38	110.38

6.2.1.2.6 Eastbound Last Detection

Figure 51 shows the last eastbound detections for the midblock sensor, and Table 19 provides a summary of corresponding midblock detection range results. The eastbound last detection count is the same as for the eastbound first detection count. Also, the first and last midblock Class 2 detections are the same because the Class 2 devices always experienced only one detection per run. For the Class 1 devices, where some detections took place upstream of the sensor for the first eastbound, there are more last detections that take place downstream of the sensor.

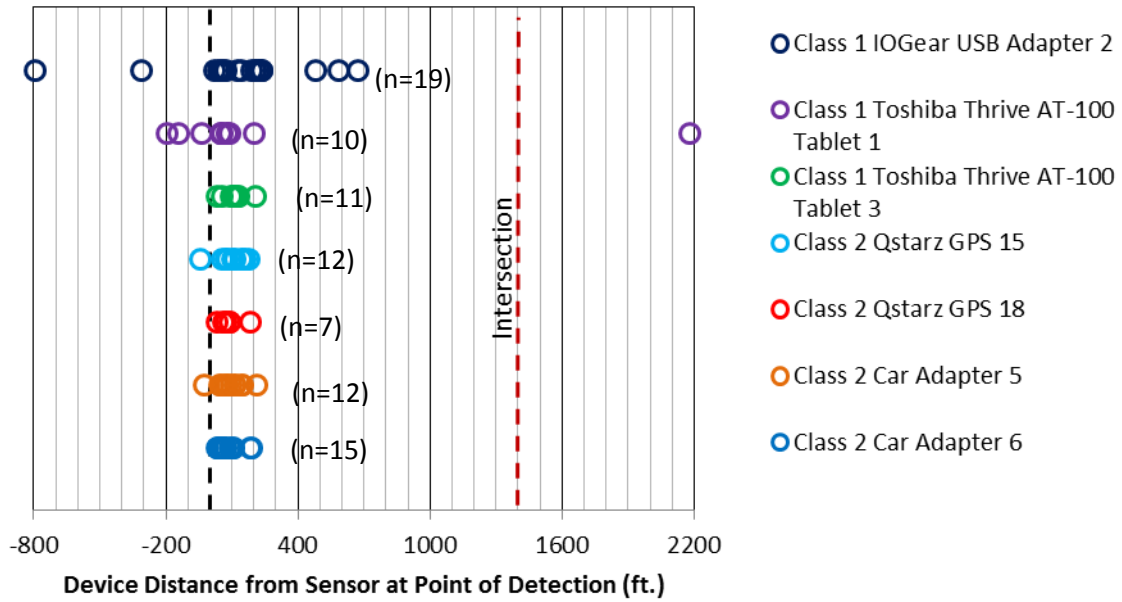

Figure 51 Last Eastbound detection in each run by the midblock sensor

Table 19 14th St. Midblock Eastbound Last Detections Summary

Device	Class	No. Runs Detected (out of 27)	Average Offset (ft.)	Average Offset (Abs. Value)
Class 1 IOGear USB Bluetooth Adapter 2	1	19	137.43	254.16
Class 1 Toshiba Thrive AT-100 Tablet 1	1	10	20.52	96.47
Class 1 Toshiba Thrive AT-100 Tablet 3	1	11	118.07	118.07
Class 2 QStarz GPS 15	2	12	96.73	104.26
Class 2 QStarz GPS 18	2	7	82.99	82.99
Class 2 Car Adapter 5	2	12	90.81	95.78
Class 2 Car Adapter 6	2	15	76.63	72.63

Next, Figure 52 shows the last eastbound detections for the intersection sensor, and Table 20 provides a summary of the corresponding intersection detection range

results. The last detection at the intersection sensor takes place more often downstream of the intersection sensor for Class 1 devices; and upstream of the intersection sensor for the Class 2 devices. There is also more scatter for the midblock detections than for the corresponding intersection detections.

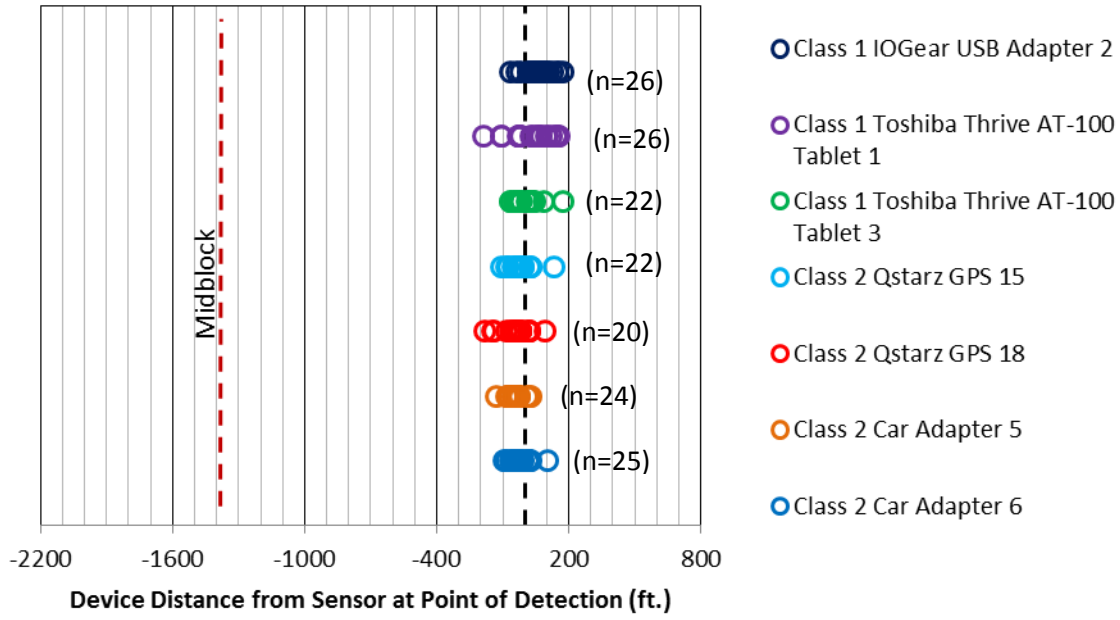

Figure 52 Last Eastbound detection in each run by the intersection sensor

Table 20 14th St. Intersection Eastbound Last Detections Summary

Device	Class	No. Runs Detected (out of 27)	Average Offset (ft.)	Average Offset (Abs. Value)
Class 1 IOGear USB Bluetooth Adapter 2	1	26	59.88	69.61
Class 1 Toshiba Thrive AT-100 Tablet 1	1	26	123.98	168.06
Class 1 Toshiba Thrive AT-100 Tablet 3	1	22	4.50	41.45
Class 2 QStarz GPS 15	2	22	-26.89	44.76
Class 2 QStarz GPS 18	2	20	-42.49	57.91
Class 2 Car Adapter 5	2	24	-46.47	50.51
Class 2 Car Adapter 6	2	25	-24.30	41.19

6.2.1.2.7 Westbound Last Detection

Figure 53 below shows the last westbound detections for the midblock sensor, and Table 21 provides a summary of the corresponding detection range results. The last westbound detections for the midblock sensor are the same count as the first detection, and the Class 2 detections are exactly the same due to their having one detection per run. However, the last detections are more scattered for the Class 1 devices, and are occurring more often downstream of the midblock sensor, rather than on the approach as with the first detection.

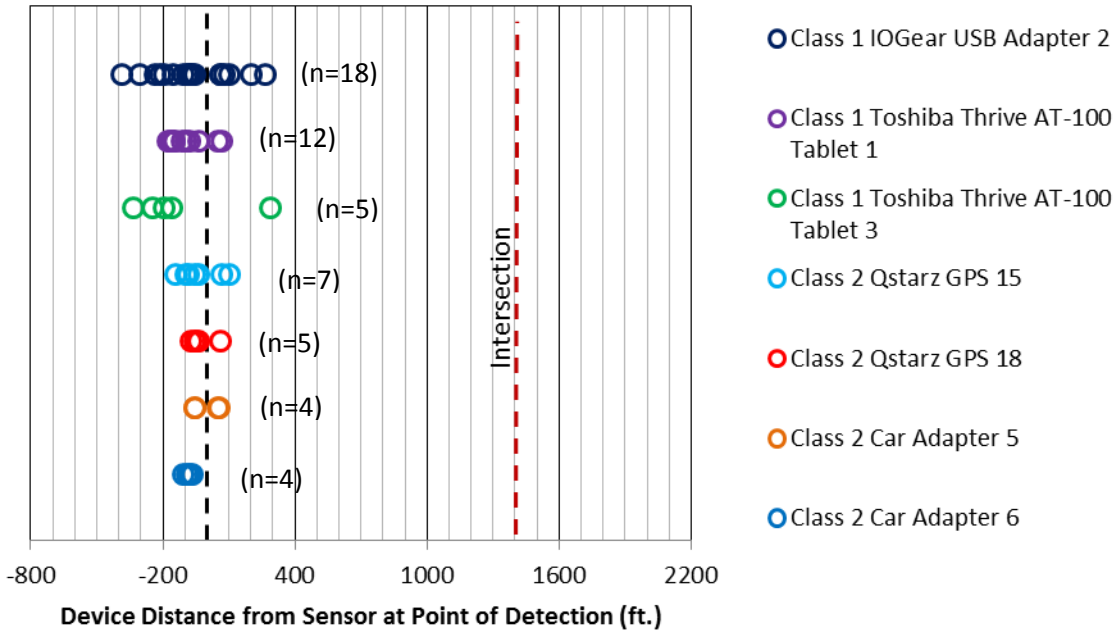

Figure 53 Last Westbound detection in each run by the midblock sensor

Table 21 14th St. Midblock Westbound Last Detections Summary

Device	Class	No. Runs Detected (out of 27)	Average Offset (ft.)	Average Offset (Abs. Value)
Class 1 IOGear USB Bluetooth Adapter 2	1	18	-69.49	153.35
Class 1 Toshiba Thrive AT-100 Tablet 1	1	12	-95.25	113.15
Class 1 Toshiba Thrive AT-100 Tablet 3	1	5	-131.39	246.12
Class 2 QStarz GPS 15	2	7	-38.82	84.29
Class 2 QStarz GPS 18	2	5	-32.62	56.36
Class 2 Car Adapter 5	2	4	-4.23	53.67
Class 2 Car Adapter 6	2	4	-89.50	89.50

Next, Figure 54 shows the last westbound detections for the intersection sensor, and Table 22 provides a summary of the corresponding intersection detection range

results. Whereas the first westbound intersection detections take place mostly before the sensor for the Class 1 devices, the last westbound detections show a strong presence after the sensor, with two detections taking place as far away as the midblock sensor. These detections are most likely the part of a detection "string", and represent the last detection that took place in a given cycle

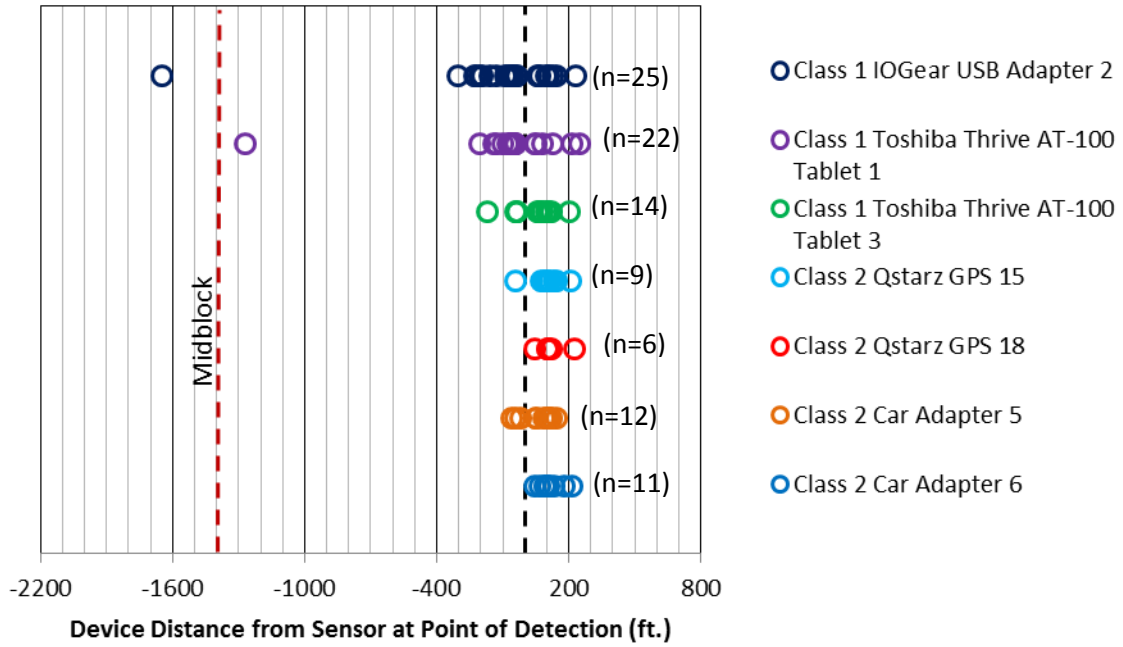

Figure 54 Last Westbound detection in each run by the intersection sensor

Table 22 14th St. Intersection Westbound Last Detections Summary

Device	Class	No. Runs Detected (out of 27)	Average Offset (ft.)	Average Offset (Abs. Value)
Class 1 IOGear USB Bluetooth Adapter 2	1	25	-105.84	186.89
Class 1 Toshiba Thrive AT-100 Tablet 1	1	22	-80.10	147.99
Class 1 Toshiba Thrive AT-100 Tablet 3	1	14	46.62	88.39
Class 2 QStarz GPS 15	2	9	99.31	108.81
Class 2 QStarz GPS 18	2	6	115.73	115.73
Class 2 Car Adapter 5	2	12	61.31	82.34
Class 2 Car Adapter 6	2	11	109.81	109.81

6.2.1.2.8 Detection Range Summary

Intersection detections have consistently less scatter than midblock detections for all detection range calculation methods. Westbound midblock detections have the highest scatter of all detection range categories. In addition, eastbound detection records are also greater than westbound detection records, and intersection is greater than midblock, especially for Class 2 devices. Furthermore, for all detection range calculation scenarios, the majority of detections take place within a 200 foot range of the sensor.

Table 23 below provides a summary of the average detection range based on method of derivation, and sheds light on whether a first-to-first, last-to-last, or overall centroid is the most promising method to use for travel time calculation. Table 23 presents the average detection range without weighing, which is a straight average of the "average offset" values (not absolute value) for each device presented in the above sections of this thesis. This method counts the range of each device as equal.

Furthermore, the Average Possible Range Error is the combined average offset of the intersection and midblock range. See Appendix A for an example of the average detection range calculation.

Table 23 Summary of Detection Range without Weighting

Device	Average Midblock Range (Feet)	Average Intersection Range (Feet)	Average Possible Range Error (Feet)
All	273.63	96.25	177.38
Eastbound All	101.67	-28.77	130.44
Eastbound First	53.18	-67.87	121.05
Eastbound Last	89.03	6.88	82.15
Westbound All	-33.66	95.42	129.08
Westbound First	-27.07	134.79	161.86
Westbound Last	-65.90	35.26	101.16

Table 24 provides a weighted average of the device detections in each calculation method, giving those devices with more detection occurrences more sway in calculating the average range error (which are the Class 1 devices, which inherently experience more variation, and more detection, as the prior results show). Again, the weighted average uses the "average offset" values from the above sections of this thesis, not the absolute value of the average, to retain the true average position of the detection relative to the See Appendix A for an example calculation of the average detection range.

Table 24 Summary of Weighted Detection Range

Device	Average Midblock Range (Feet)	Average Intersection Range (Feet)	Average Possible Range Error (Feet)
All	41.46	19.14	22.32
Eastbound All	112.67	-23.00	135.67
Eastbound First	47.72	-68.89	116.61
Eastbound Last	94.14	10.40	83.74
Westbound All	5.28	84.90	79.62
Westbound First	7.96	148.12	140.16
Westbound Last	-70.19	-2.26	69.93

The results shown in Table 23 and Table 24 show that eastbound all and first detections take place on average downstream of the midblock sensor, and upstream of the intersection sensor. Furthermore, last detections take place farther downstream than the first eastbound midblock detections, and downstream of the intersection sensor. For westbound detections, all and first detections take place upstream of the midblock sensor and upstream of the intersection sensor; and last detections take place downstream of the midblock sensor, and downstream of the intersection sensor, on average.

6.3 I-285 Travel Time Results

6.3.1 Device Detection Window

Paces Ferry Road, Northside Drive and Roswell Road each feature a Class 1 Bluetooth sensor, which reportedly has a standard 300 foot detection range. To explore the wide detection ranges found during the 14th Street test, the research team performed a brief field examination of this property and found the stationary range for the Class 1 custom Bluetooth system sensor to be approximately 287 feet. Therefore, 287 feet

defines the radius of the circle around the sensor representing the device detection window. Each sensor has the same approximate detection radius, but because the position of the sensor relative to the travel lanes is different at each data collection site on I-285 eastbound, the window is slightly different for each location. An understanding of the detection window is important because it describes the length of time a given Bluetooth-enabled device is in a sensor's field of view. The device does not become detectable until crossing over this invisible threshold.

6.3.1.1 Paces Ferry Road Eastbound Detection Window

Paces Ferry Road features four eastbound and four westbound lanes of traffic, with the Bluetooth sensor stationed on the right side of the eastbound traffic. The sensor at Paces Ferry Road is placed approximately 15 feet from the guardrail. The shoulder between the guardrail and the outside lane of traffic is approximately 15 feet wide. Each lane is about 12 feet wide, and the distance from the inside lane to the middle of the concrete barrier separating eastbound and westbound traffic is about seven feet. Therefore, there is about 85 feet from the sensor to edge of eastbound traffic, and 140 feet to the edge of westbound traffic.

The overpass at Paces Ferry Road, which is about 125 feet away from the sensor location, constitutes an obstacle to communication. Table 25 below provides a breakdown of the time a vehicle is within the Paces Ferry Road detection window by lane and traffic speed. Refer to Appendix B for details regarding the calculation of the detection window. Lane 0 is the inside lane, increasing as the lanes move out from the center in either direction. The westbound congested is greyed out because the westbound was in free-flow for the entire AM morning data collection period. Table 25 shows that

as the eastbound traffic experiences more congestion, the westbound traffic spends proportionately less time in the detection window.

Table 25 Paces Ferry Road Eastbound Detection Window by Lane and Speed

			Free-Flow (65 mph)	Congested (40 mph)	Congested (20 mph)
	Lane I.D.	Distance (feet)	Time (sec)	Time (sec)	Time (sec)
Eastbound	3	569	5.97	9.70	19.40
	2	566	5.94	9.65	19.30
	1	561	5.88	9.56	19.12
	0	556	5.83	9.48	18.96
Westbound	0	539	5.65		
	1	530	5.56		
	2	519	5.45		
	3	508	5.25		

6.3.1.2 Northside Drive Eastbound Detection Window

Northside Drive at I-285 features five lanes it the eastbound direction and five lanes in the westbound direction. The same roadway dimensions are taken as in Paces Ferry Road, with the difference lying in the sensor offset from the guardrail, which is about five feet instead of 15 feet. Table 26 below provides a breakdown of the time a vehicle is within the detection window by lane and traffic speed. The ratio of eastbound to westbound time present in the detection window at Northside Drive is very close to Paces Ferry Road. As the congestion increases, and speed decreases, the volume of vehicles present in the detection window at any one time increases. As a result, the presence of devices should increase.

Table 26 Northside Drive Eastbound Detection Window by Lane and Speed

			Free-Flow (65 mph)	Congested (40 mph)	Congested (20 mph)
	Lane I.D.	Distance (feet)	Time (sec)	Time (sec)	Time (sec)
Eastbound	4	572	6.00	9.75	19.50
	3	569	5.97	9.70	19.40
	2	565	5.93	9.64	19.27
	1	560	5.87	9.54	19.08
	0	555	5.82	9.46	18.92
Westbound	0	538	5.64		
	1	528	5.54		
	2	520	5.45		
	3	505	5.30		
	4	492	5.16		

6.3.1.3 Roswell Road Eastbound Detection Window

Roswell Road at I-285 also has five lanes each in the eastbound and westbound directions. The same roadway dimensions are taken for Roswell Road as for Paces Ferry Road and Northside Drive, except the Bluetooth sensor offset from the eastbound guardrail is approximately ten feet. Table 27 provides a summary of the length and time of detection window for different lane and speed combinations. For moderate congestion, the westbound traffic is in the detection zone approximately 35% of the time, and for a high congestion zone the westbound traffic is in the detection window approximately 21% of the time. Again these results are very similar to Paces Ferry Road and Northside Drive detection window ratios.

Table 27 Roswell Road Detection Window by Lane and Speed

			Free-Flow (65 mph)	Congested (40 mph)	Congested (20 mph)
	Lane I.D.	Distance (feet)	Time (sec)	Time (sec)	Time (sec)
Eastbound	4	571	5.99	9.73	19.47
	3	568	5.96	9.69	19.37
	2	563	5.91	9.60	19.19
	1	558	5.85	9.51	19.02
	0	552	5.79	9.41	18.82
Westbound	0	534	5.60		
	1	524	5.50		
	2	513	5.38		
	3	500	5.24		
	4	486	5.10		

6.3.2 Day 1: Friday September 7th, 2012

Figure 55 below shows the Bluetooth travel time plot for vehicles traveling on I-285 eastbound from Paces Ferry Road to Northside Drive after 8:00 am on the morning of Friday, September 7th, 2012. The records are the result of the detections by one custom Bluetooth sensor at each site, separated into the eastbound and westbound direction. Table 28 provides a summary of the Bluetooth detection results for Day 1. The Bluetooth eastbound travel times filtered for this day are all travel times greater than 30 minutes, and the peak travel time is calculated for the first 60 minutes of collection. One out of 64 (1.6%) eastbound data points and one out of 15 (6.7%) westbound data points are removed from the analysis.

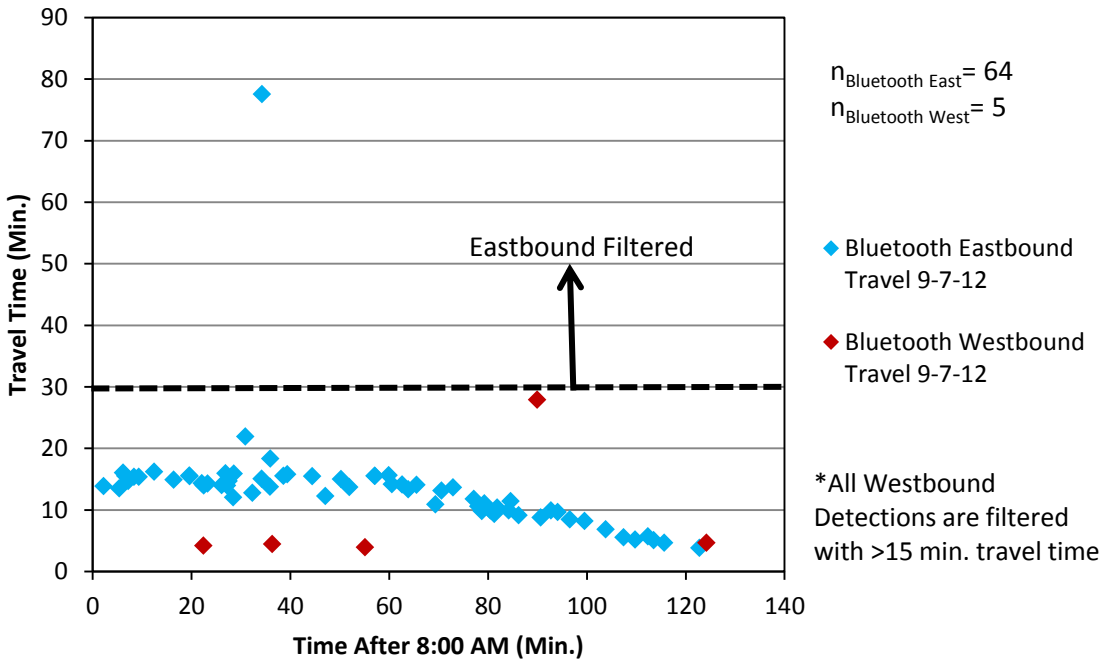

Figure 55 Bluetooth Eastbound to Westbound Travel Time Comparison (all data) from Paces Ferry Road to Northside Drive on I-285 E on 9-7-12

Table 28 I-285 Day 1 Bluetooth Travel Time Summary

Corridor Segment	**Paces Ferry Road→ Northside Drive**	
	Unique Detections	*Match Rate*
Paces Ferry Road	312	22.1%
Northside Drive	564	12.23%
Total Pairs	69	8.5%
EB Pairs	64	7.9%
WB Pairs	5	0.6%
EB%/WB % of Matched Pairs	92.8% / 7.2%	
Time Period	8:00am to 10:15am (2 hr. 15 min.)	
Distance (Miles)	4.3 mi	
EB Peak Travel Time, filtered data (Min.)	15.0 min (17 mph)	
WB Off-Peak Travel Time, filtered data (Min.)	4.3 min (60 mph)	

Northside Drive most likely has almost twice the number of unique detections as Paces Ferry Road because this half of the corridor experienced a large ingress of traffic at the I-75 interchange traveling eastbound on I-285 (where the Paces Ferry Road devices most likely exited at I-75). In addition, the Bluetooth sensor at Paces Ferry Road was positioned about 20 feet further from the closest travel lane in the interest of safety. This farther distance shortened the window where device-detection could occur. The Paces Ferry Road sensor was also positioned closer to the overpass, which may have reduced the detection window for the Bluetooth sensor; and there was also a light pole within close proximity that may have caused additional interference. Furthermore, travel time matches are largely dictated by the site with the least detections, Paces Ferry Road in this case. Thus, while the Northside Drive sensor detected more devices than the Paces Ferry Road sensor the match rate is lower because of the limited data for matching oppurtunities at Paces Ferry Road.

Figure 56 provides a comparison of the Bluetooth eastbound travel time and the ALPR eastbound travel time for Day 1 of the I-285 travel time test series. The ALPR travel time is derived from 180 uniquely matched plates between Paces Ferry Road and Northside Drive, compared to 64 matched Bluetooth MAC addresses. The reason why the start and end of the ALPR travel time readings are not consistent with the Bluetooth readings is because the ALPR system was setup after the Bluetooth, and continued longer than the Bluetooth due to the Bluetooth powering off from excessive heat exposure. In addition, the large amount of scatter present in the ALPR data is most likely due to not filtering out license plate reads that were in fact not plates, such as signs on the backs of vehicles that could have been present on many different vehicles.

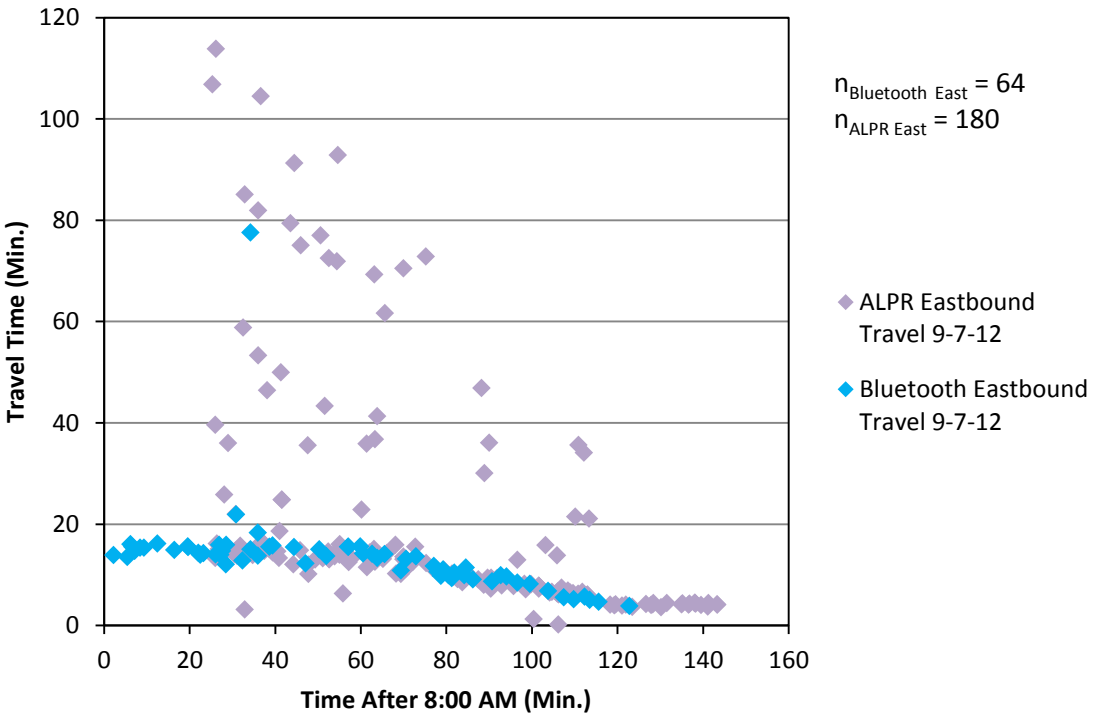

Figure 56 Bluetooth and ALPR Travel Time Comparison (all data) from Paces Ferry Road to Northside Drive on I-285 E on 9-7-12

6.3.3 Day 2: Wednesday September 12th, 2012

Figure 57 below shows the travel time from Northside Drive to Roswell Road after 7:30 AM on Wednesday, September 12th, 2012. The records are the result of the detections by one custom Bluetooth sensor at each site, separated into the eastbound and westbound direction. The westbound travel time presents a baseline for what the free-flow non-congested travel time is for the corridor, which is 3.3 minutes. Table 29 provides a summary of the Bluetooth detection results for Day 2. The Bluetooth eastbound travel times filtered for this day are all travel times greater than 20 minutes, and the peak travel time is calculated for the first 30 minutes of collection. Three out of 266 (1%) eastbound points and two out of 15 (13%) westbound points are removed.

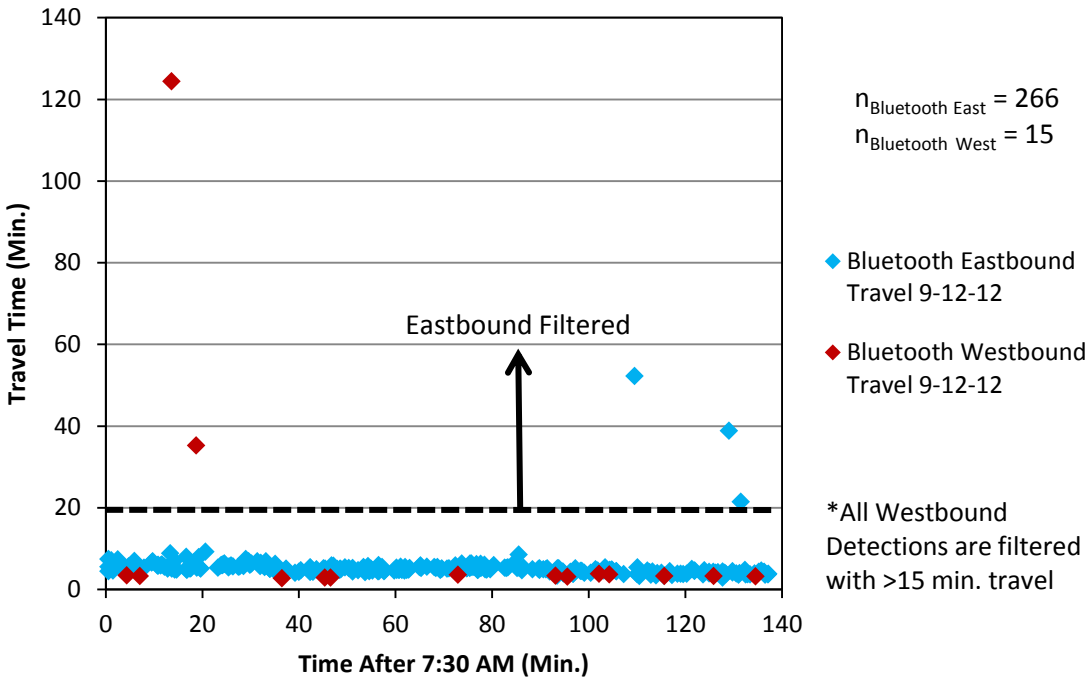

Figure 57 Bluetooth Eastbound to Westbound Travel Time Comparison (all data) from Northside Drive to Roswell Road on I-285 E 9-12-12

Table 29 I-285 Day 2 Bluetooth Travel Time Summary

Corridor Segment	**Northside Drive→ Roswell Road**	
	Unique Detections	*Match Rate*
Northside Drive	699	40.2%
Roswell Road	610	46.1%
Total Pairs	281	27.3%
EB Pairs	266	25.9%
WB Pairs	15	1.4%
EB%/WB % of Matched Pairs	94.7% / 5.3%	
Time Period	7:30am to 9:50am (2 hr. 20 min.)	
Distance (Miles)	3.3 mi	
EB Peak Travel Time, filtered (Min.)	5.9 min (34 mph)	
WB Off-Peak Travel Time, filterd (Min.)	3.3 min (60 mph)	

Northside Drive and Roswell Road see a much higher aggregate match rate than the Paces Ferry Road and Northside Drive pairing, as well as higher individual site match rates. In addition, the detection counts of Northside Drive and Roswell Road are very similar, which is expected because the only opportunity to exit the corridor is at Riverside Drive between these two sites, which leads to residential area. Following, Figure 58 provides a comparison of the Bluetooth and ALPR eastbound travel times. The ALPR travel time is derived from 1924 uniquely matched license plates between Northside Drive and Roswell Road, compared to 266 Bluetooth unique MAC address pairs.

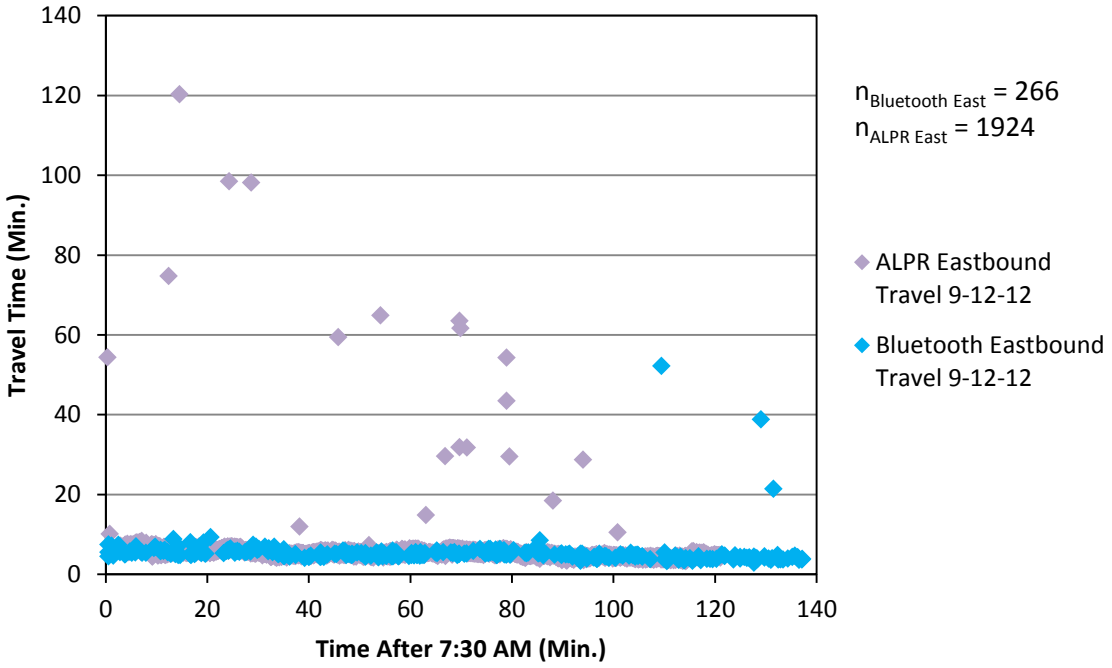

Figure 58 Bluetooth and ALPR Travel Time Comparison (all data) from Northside Drive to Roswell Road on I-285 E on 9-12-12

6.3.4 Day 3: Friday September 14th, 2012

The travel time for Day 3 has three variations: (1) the travel time from Paces Ferry Road to Northside Drive; (2) the travel time from Northside Drive to Roswell

Road; and (3) the travel time from Paces Ferry Road to Roswell Road. The reason for showing the travel times in these segments is to show how the entire corridor travel time compares to the travel time along sections of the corridor.

6.3.4.1 Paces Ferry Road to Roswell Road

Figure 59 below shows the travel time from Paces Ferry Road to Roswell Road, again captured by one custom Bluetooth sensor at each site, for the time after 7:20 AM on Friday, September 14th, 2012. The records separated into the eastbound and westbound direction. The Bluetooth eastbound travel times filtered for this day are all travel times greater than 20 minutes, and the peak travel time is calculated for times 40 minutes through 80 minutes after the start of the data collection period. Therefore, three out of 89 eastbound data points are removed, leaving 97% of the eastbound data points for travel time calculation. Conversely, two out of 11 westbound data points are removed, leaving 82% of the westbound data points for travel time calculation.

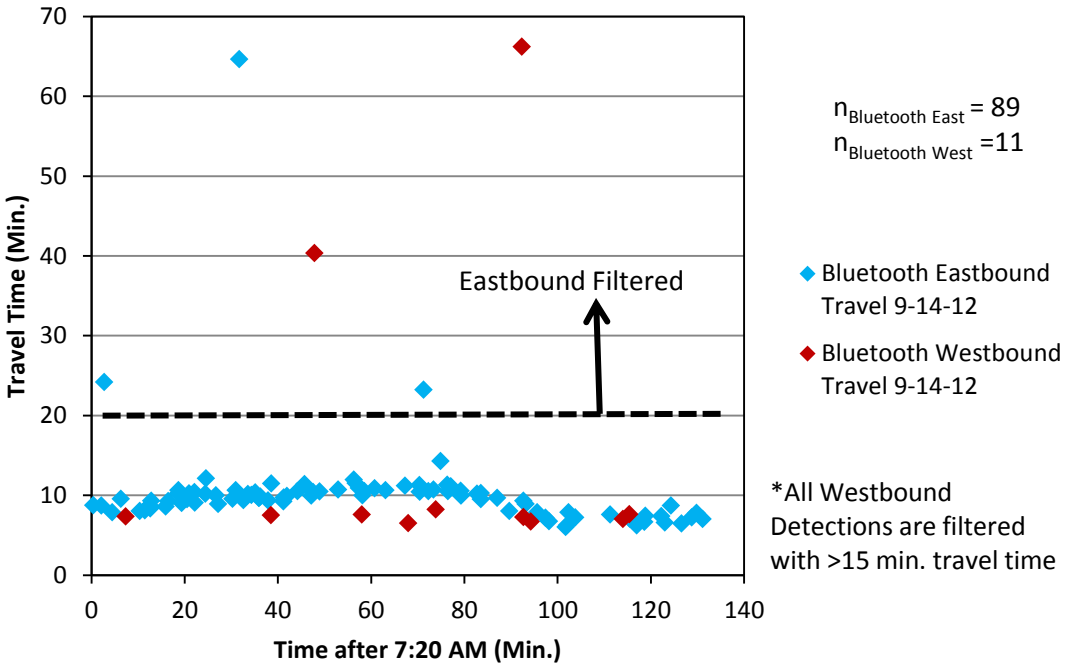

Figure 59 Bluetooth Eastbound to Westbound Travel Time Comparison (all data) from Paces Ferry Road to Roswell Road on I-285 E on 9-14-12

6.3.4.2 Paces Ferry Road to Northside Drive

Figure 60 shows the travel time from Paces Ferry Road to Northside Drive captured by one Bluetooth sensor after 7:20 AM on Friday, September 14, 2012. The records are the result of the detections by one Bluetooth sensor at each site, separated into the eastbound and westbound direction. The number of unique MAC addressed matches is greater for this day than Day 1 of the I-285 travel time test series. The Bluetooth eastbound travel times filtered for this day are all travel times greater than 20 minutes, and the peak travel time is calculated for times 40 minutes through 80 minutes after the start of the data collection period. Therefore, five out of 95 (5.3%) eastbound data points and two out of 11 (18.1%) westbound data points are removed out of the travel time calculation.

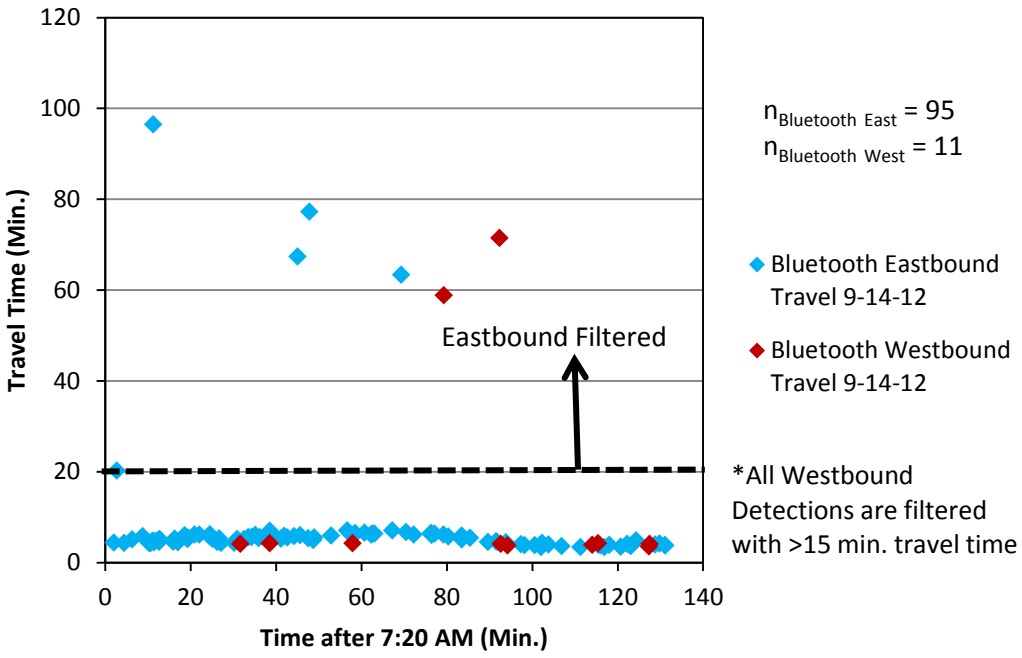

Figure 60 Bluetooth Eastbound to Westbound Travel Time Comparison (all data) from Paces Ferry Road to Northside Drive on I-285 E on 9-14-12

6.3.4.3 Northside Drive to Roswell Road

Figure 61 below shows the Bluetooth travel time from Northside Drive to Roswell Road after 7:20 AM on Friday, September 14, 2012. The records are the result of the detections by one custom Bluetooth sensor at each site, separated into the eastbound and westbound directions. The Bluetooth eastbound travel times filtered for this day are all travel times greater than 20 minutes, and the peak travel time is calculated for times 40 minutes through 80 minutes after the start of the data collection period. Therefore, three out of 282 (1%) eastbound data points, and four out of 30 (13.3%) westbound data points are filtered out of the travel time calculation.

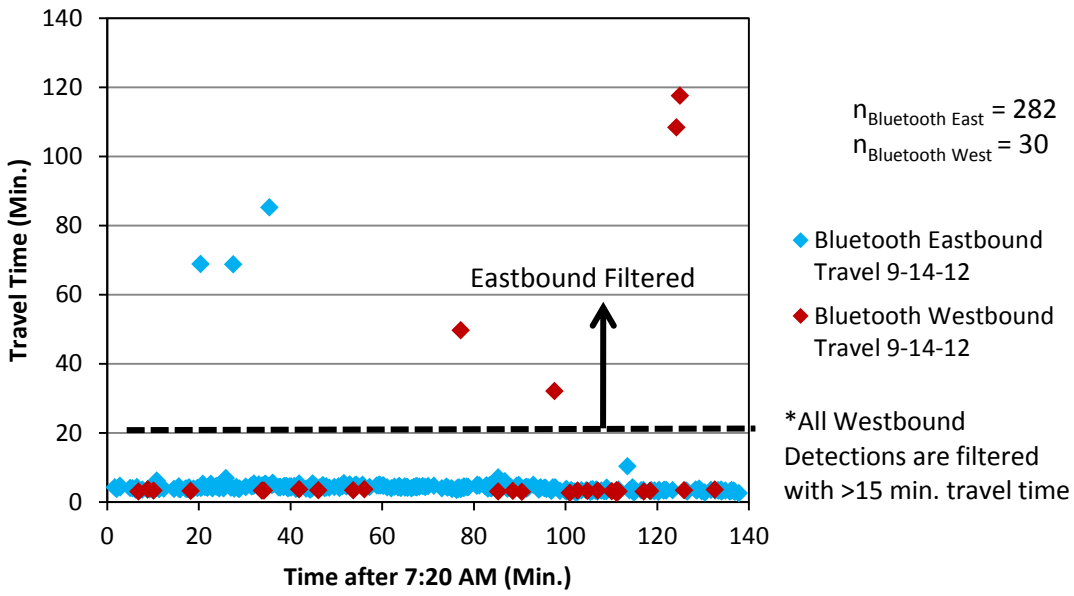

Figure 61 Bluetooth Eastbound to Westbound Travel Time Comparison (all data) from Northside Drive to Roswell Road on I-285 E 9-14-12

Next, Figure 62 provides a comparison of the Bluetooth and ALPR eastbound travel times. The ALPR travel time is derived from 908 uniquely matched license plates compared to 282 matched MAC addresses for Bluetooth. The travel time for the Bluetooth and ALPR technologies display similar trends.

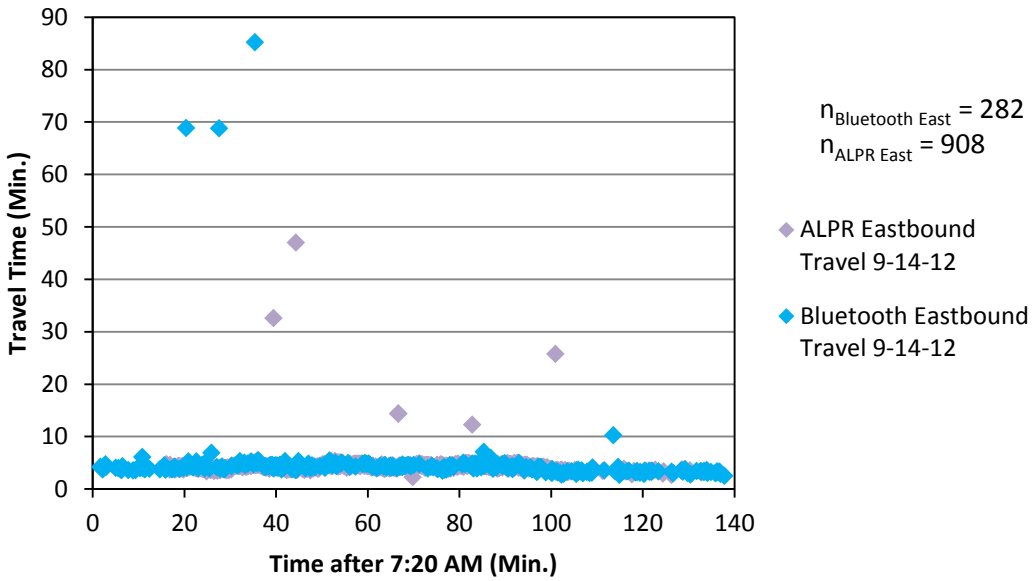

Figure 62 Bluetooth and ALPR Travel Time Comparison (all data) from Northside Drive to Roswell Road on I-285 E on 9-14-12

6.3.4.4 Day 3 Summary

The Northside Drive to Roswell Road segment has the greatest aggregate match rate of the three segments observed at 30.2%. This high match rate is achieved by the lack of a major interchange between Northside Drive and Roswell Road, and this corridor also has the shortest distance of 3.3 miles. Conversely, there is a major interchange between Paces Ferry Road and Northside Drive (and by consequence Paces Ferry Road and Roswell Road) at I-75. Table 30 provides a summary of the travel time results from Day 3 of the I-285 deployment series. There was not a substantial delay observed along the Paces Ferry Road to Roswell Road corridor for Friday, September 14th, 2012, but the breakdown does provide insight into where the most delay is occurring. Furthermore, of the total pairs detected in each segment, there are 99 common MAC pairs for all sites.

Table 30 I-285 Day 3 Bluetooth Travel Time Summary

Corridor Segment	Paces Ferry Rd.→ Roswell Rd.	Paces Ferry Rd.→ Northside Dr.	Northside Dr. → Roswell Rd.
	Unique Detections (Match Rate)		
Paces Ferry Road	388 (25.8%)	388 (27.3%)	
Northside Drive		688 (15.4%)	688 (45.3%)
Roswell Road	658 (15.2%)		658 (47.4%)
Total Pairs	100 (10.6%)	106 (10.9%)	312 (30.2%)
EB Pairs	89 (9.4%)	95 (9.8%)	282 (27.3%)
WB Pairs	11 (1.2%)	11 (1.1%)	30 (2.9%)
EB%/WB % of Matched Pairs	89.0% / 11.0%	89.6% / 10.4%	90.4% / 9.6%
Time Period	7:20am to 9:40am (2 hr. 20 min.)	7:20am to 9:36am (2 hr. 16 min.)	7:20am to 9:40am (2 hr. 20 min.)
Distance (Miles)	7.6 mi	4.3 mi	3.3 mi
EB Peak Travel Time, filtered (Min.)	10.8 min (42 mph)	6.1 Min (42 mph)	4.3 min (46 mph)
WB Off-Peak Travel Time, filtered (Min.)	7.3 min (62 mph)	4.0 min (65 mph)	3.2 min (62 mph)

For the first three days of I-285 travel time measurement, about 90% of the unique MAC address matches are for vehicles traveling in the eastbound direction (side closest to sensor), and about 10% of the unique MAC address matches represent Bluetooth-enabled devices in westbound vehicles for all sites on each day. For the three days of I-285 travel time data collection, the eastbound traffic was congested and slow-moving (average speed 40 mph), putting the eastbound vehicles in the detection window for about 75% more time than the westbound traffic (average speed 63 mph). The one anomaly to this conclusion is the second day breakdown down between eastbound and

westbound matches is roughly 95% and 5%, respectively. In addition, the eastbound devices were closer, giving them an advantage in the competition for detection. Another important observation is the consistency in detection count between the three sites. Northside Drive and Roswell Road consistently have very similar detection counts, with Roswell Road slightly smaller than Northside Drive; and both these sites have between 1.7 and 1.8 times the number of unique detections as Paces Ferry Road.

6.3.6 I-285 Cycle Detection Pattern and Corridor Congestion

This thesis explores how the cycle detection pattern varies under congested and non-congested traffic to assess whether there is a trend towards earlier cycle detection, later cycle detection, patterned cycle detection, or random cycle detection in the two traffic conditions. The reason for considering first and last detections is to observe whether the first detections are concentrated in the beginning of the cycle and the last detections in the later end of the cycle. The only day where significant congestion was monitored was on Day 1 of the I-285 Travel Time test series. The congestion was present from approximately 8 AM to 9 AM. Figure 63 below compares the cycle detection pattern for first device detection and last device detection in congested traffic for Day 1 at Paces Ferry Road. Following, Figure 63 shows the cycle detection pattern for first and last detections for Day 1 at Northside Drive. The detections shown are not limited to only those detections leading to MAC address matches.

The results indicate that there is not a pattern of detection for congested traffic, and the detections are not concentrated towards the beginning of the cycle for the first detections. The most likely cause for this scatter is that the devices may not be present in

the sensor detection window from the start of the cycle, causing the device to be detected towards the middle or end of the cycle.

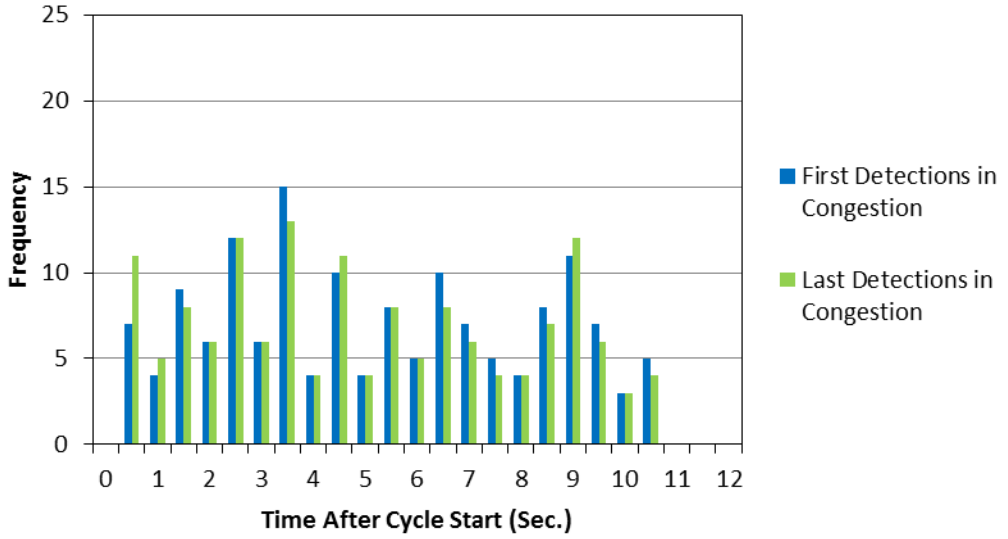

Figure 63 Cycle detection pattern in congestion at Paces Ferry Road (0.5 Sec. bins)

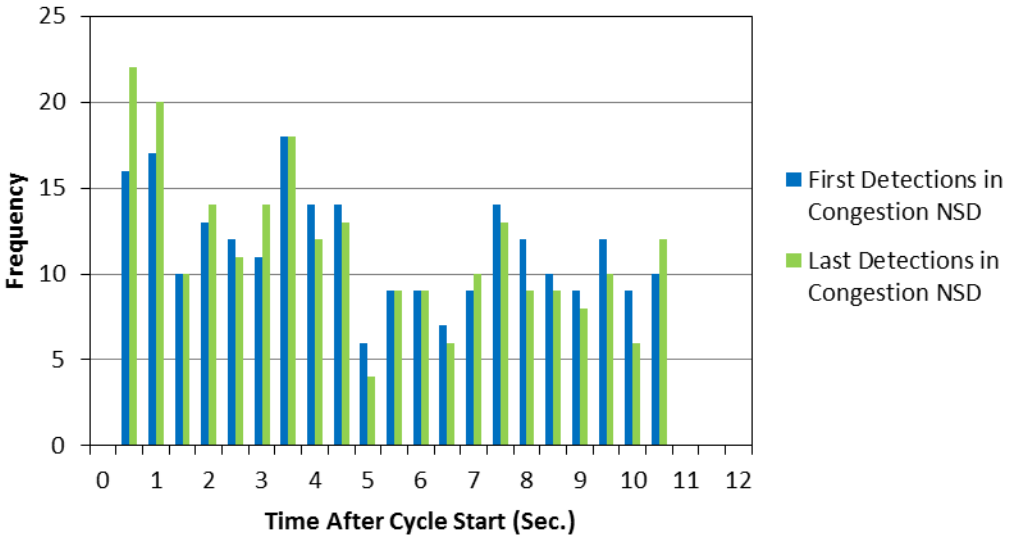

Figure 64 Cycle detection pattern in congestion at Northside Drive (0.5 Sec. bins)

The only day where consistent free flow traffic was observed for the I-285 travel time test series was during Day 2. There is a very minor delay on the corridor from Northside Drive to Roswell Road for the two hour data collection period, but to keep with the trend of the previous congested cycle detection patter, the focus is on detections from the last hour of data collection from 8:45 AM to 9:45 AM. Figure 65 shows the cycle detection pattern for Northside Drive, and Figure 66 shows the cycle detection pattern for Roswell Road, with both providing a comparison of first and last detection trends.

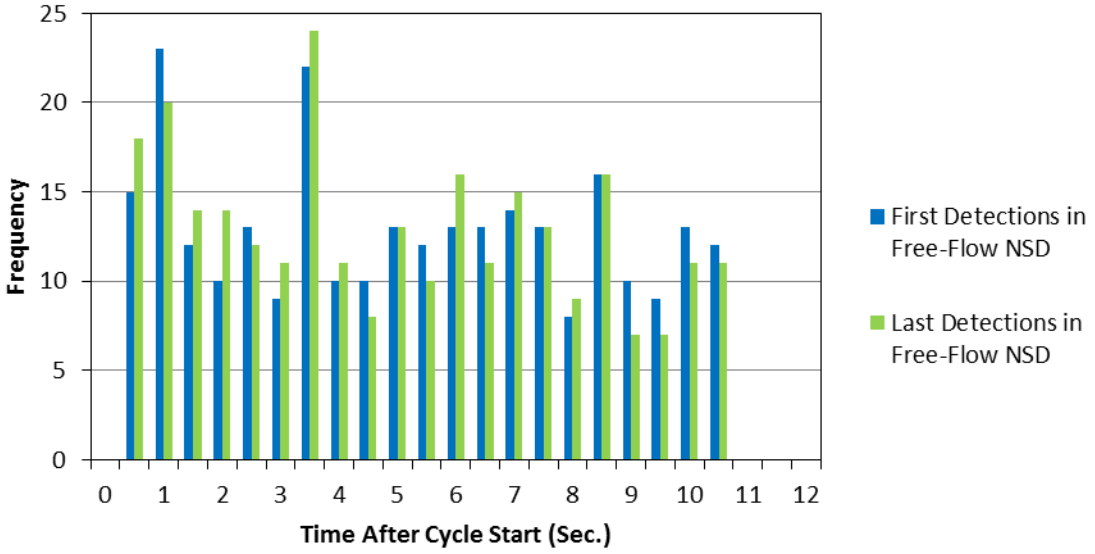

Figure 65 Cycle detection pattern in free-flow at Northside Drive on Day 2 (0.5 Sec. bins)

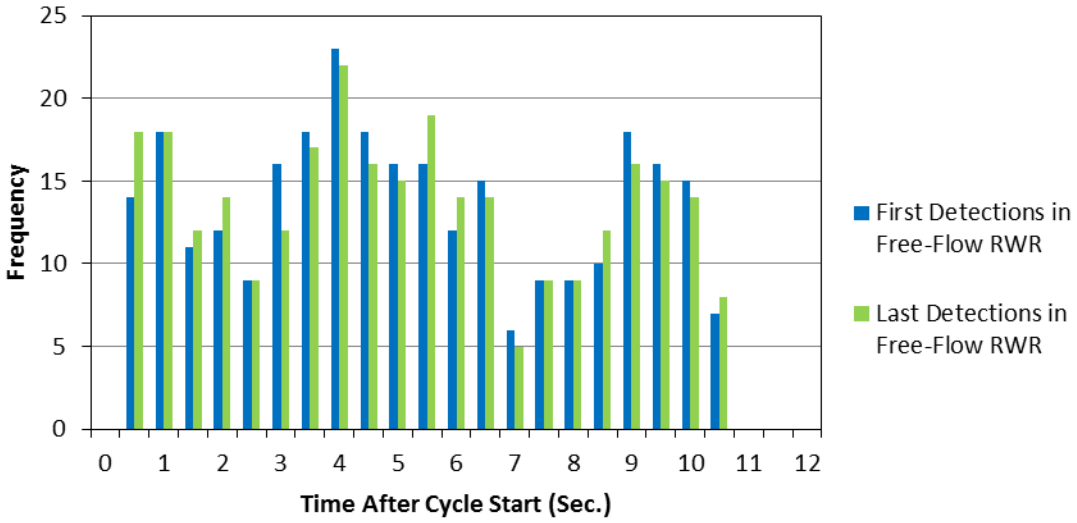

Figure 66 Cycle detection pattern in free-flow for Roswell Road on Day 2 (0.5 Sec. bins)

Just as for the congested traffic, there does not seem to be a concentration of detections towards the beginning of the cycle for the first detections in free flow traffic. Rather, the last detections are showing a higher concentration in the beginning of the cycle than the first detections for Northside Drive and Roswell Road. These results show that an inquiry cycle length of 10.24 seconds is sufficient to capture the discoverable devices in the vehicle population, because there is no unused time where detections are not occurring throughout the cycle duration.

6.4 I-285Work Zone Travel Time Results

6.4.1 Day 1: Saturday September 29, 2012

Figure 67 below shows the travel time from Riverside Drive to Paces Ferry Road for time after 7:14 AM on Saturday, September 29, 2012. The records are the result of the detections by one Bluetooth sensor placed on the right side of westbound traffic at

each site, separated into the eastbound and westbound direction. As a reminder, the data collection for this day was intended to capture an active work zone featuring westbound lane closures. However, on the day of data collection the active lanes closures were in the eastbound direction, opposite the sites selected. Therefore, although the westbound traffic was closer to the Bluetooth sensors, the goal was to capture as many eastbound work zone travel time data points as possible. This proved difficult, however, because although the work zone was active eastbound at Riverside Drive, the work zone was not active eastbound at Paces Ferry Road, which reduced the probably of capturing substantial work zone travel time.

Table 31 provides a summary of the Day 1 Work Zone travel time results. The Bluetooth eastbound (work zone) travel times filtered for this day are all travel times greater than 40 minutes, and the work zone travel time (eastbound) is calculated as an average of all filtered times for the entire data collection period. Therefore, three out of 11 (27%) eastbound work zone travel time points, and three out of 32 (9.4%) westbound non-work zone travel time points are filtered out of the travel time calculation.

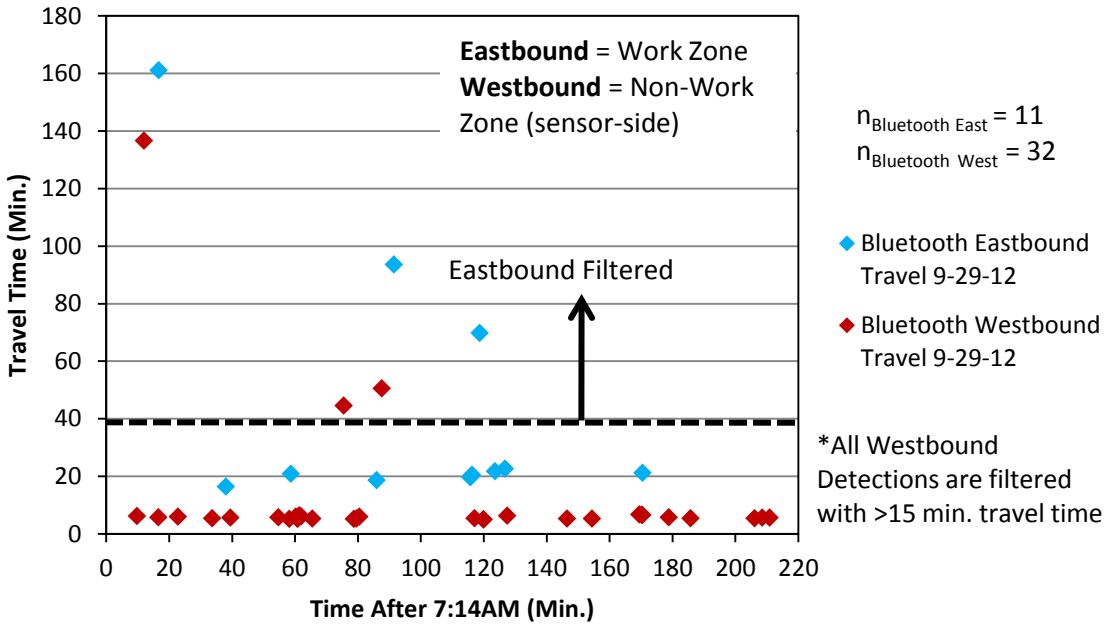

Figure 67 Work Zone Bluetooth Eastbound to Westbound Travel Time Comparison (all data) from Riverside Drive to Paces Ferry Road on I-285 W on 9-29-12

Table 31 I-285 Work Zone Day 1 Bluetooth Travel Time Summary

Corridor Segment	**Riverside Drive→ Paces Ferry Road**	
	Unique Detections	*Match Rate*
Riverside Drive	422	10.2%
Paces Ferry Road	248	17.3%
Total Pairs	43	6.9%
EB Pairs	11	1.8%
WB Pairs	32	5.1%
EB%/WB % of Matched Pairs	74.4% / 25.6%	
Time Period	7:14am to 10:51am (3 hr. 37 min.)	
Distance (Miles)	5.9 mi	
EB Work Zone Travel Time, filtered (Min.)	20.2 min (18 mph)	
WB Free-Flow Travel Time, filtered (Min.)	5.7 min (62 mph)	

For the first day of intended work zone travel time capture, the westbound devices account for approximately 75% of unique MAC address matches (side closest to sensor), and the eastbound for 25% of unique MAC address matches. For the first day of attempted work zone data collection, the westbound traffic (sensor side) was more sparse and moving more quickly (about 63 mph) than the eastbound traffic at Riverside Drive (about 18 mph); but at Paces Ferry Road the eastbound and westbound traffic was equally sparse and in free-flow (about 63 mph). This places the eastbound traffic in the detection window for about 3.5 times the westbound traffic time at Riverside Drive, but the amount of shared window time was comparable for eastbound and westbound at Paces Ferry Road. Therefore, because of the free-flow at Paces Ferry Road eastbound, the potential for collecting downstream work zone travel time was reduced. This outcome is evident in the preceding results.

Next, Figure 68 shows the travel time derived from the ALPR system detection records. These travel time records very closely mirror the travel time trend from the Bluetooth sensors, and consist of 90 unique license plate matches for vehicles traveling in the westbound direction, compared to 32 matched Bluetooth MAC addresses.

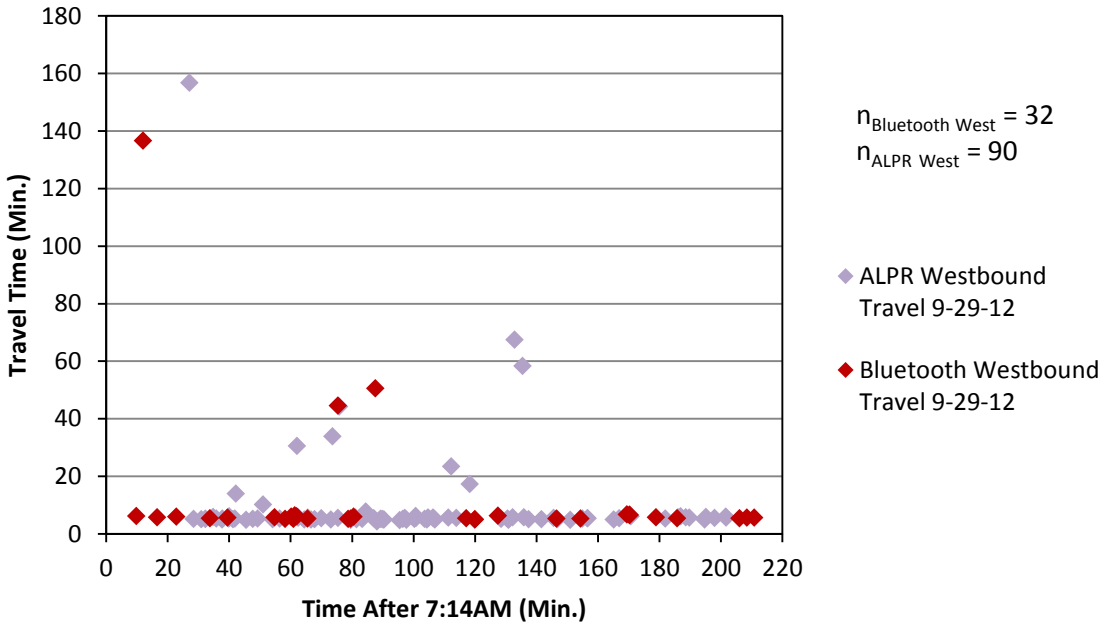

Figure 68 Bluetooth and ALPR Travel Time Comparison (all data) from Riverside Drive to Paces Ferry Road on I-285 W on 9-29-12

6.4.2 Day 2: Saturday October 20, 2012

Figure 69 below shows the Bluetooth work zone travel time measured by one custom sensor at eastbound Paces Ferry Road and Northside Drive for the time after 9:25 AM on Saturday, October 20, 2012. The travel time is separated into the eastbound and westbound directions. The active lane closures were present in the eastbound direction, so the Bluetooth sensors were able to directly capture the work zone travel time during this day of data collection. Table 32 provides a summary of the travel time statistics for the second day of active work zone data collection. There is no base filtering for this day of data collection because no extreme travel time values are present for the eastbound or westbound directions; and the work zone Bluetooth travel time is calculated as an average of all eastbound travel times for the entire data collection period.

Initially, an extra step of filtering was executed for this day of data collection to weed out those vehicles that were backed up about 0.5 miles before the Northside Drive eastbound off-ramp. MAC addresses were filtered out that saw more than six detections at Northside Drive, derived from the shorter Class 1 headway of one record per second, taken over the six second span when a free flow device is within the sensor detection window at Northside Drive, as Table 26 presented earlier. There were 52 unique MAC addresses that met these criteria at Northside Drive, 36 of which were also detected at Paces Ferry Road. In order to assess whether the MAC addresses re-detected less than or equal to six times, and those detected greater than six times produced statistically different travel times, a Chi Squared test was performed. Appendix C presents the findings of the Chi Squared test, which shows that there is not a statistical significance between the MAC addresses detected less than or equal to six times, and those detected more than six times, using an alpha significance of 0.05. Because there is no statistical significance in the travel times generated by these two groups, the travel times generated from greater than six MAC address repetitions were added back to the original dataset.

However, the sample size available for the Chi Squared test was so small (188 less than or equal to six, and 36 greater than six) that although the results could not demonstrate a statistical difference, the results are inconclusive. Future efforts will test the significance of these two frequency distributions as a larger dataset becomes available, and will also explore whether other potential portioning of the data should be considered.

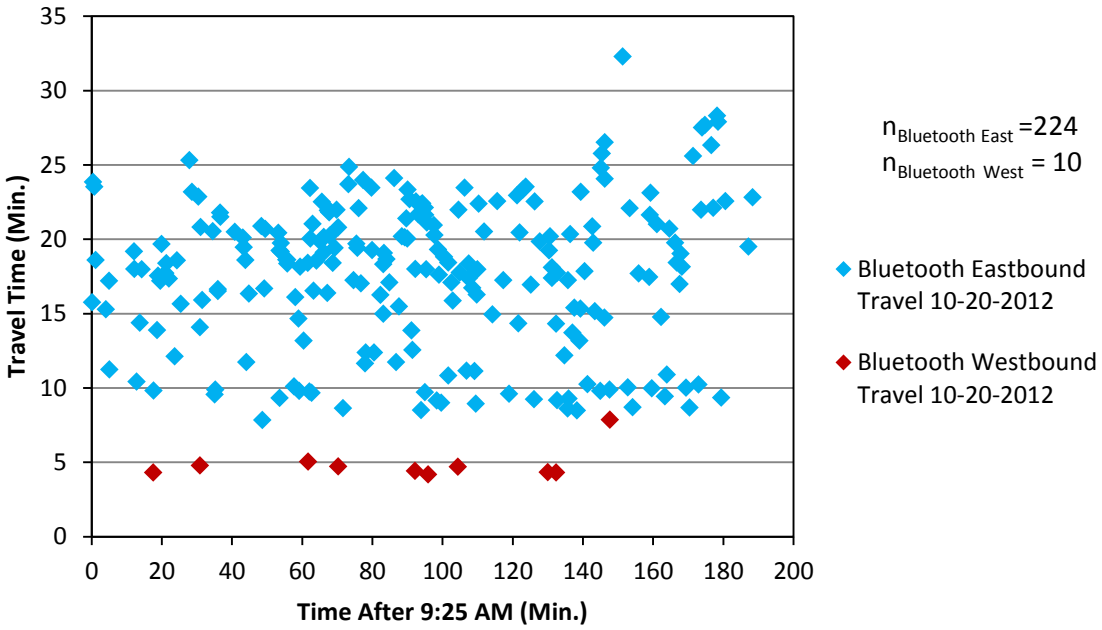

Figure 69 Work Zone Bluetooth Eastbound to Westbound Travel Time Comparison (all data) from Paces Ferry Road to Northside Drive on I-285 E on 10-20-12

Table 32 I-285 Work Zone Day 2 Bluetooth Travel Time Summary

Corridor Segment	**Paces Ferry Road → Northside Drive**	
	Unique Detections	*Match Rate*
Paces Ferry Road	445	52.6%
Northside Drive	595	39.3%
Total Pairs	234	29.0%
EB Pairs	224	27.8%
WB Pairs	10	1.2%
EB%/WB % of Matched Pairs	95.7%/4.3%	
Time Period	9:25am to 10:52am (3 hr. 27 min.)	
Distance (Miles)	4.3 mi	
EB Work Zone Time (Min.)	17.7 min (15 mph)	
WB Free-Flow Travel Time (Min.)	4.9 min (53 mph)	

For the second day of work zone data collection, eastbound devices account for approximately 95% of unique MAC address matches (side closest to sensor), and the westbound for 5% of unique MAC addresses matches. The Paces Ferry Road eastbound traffic was stop and go in significant congestion, and the Northside Drive off-ramp eastbound was stop and go in significant congestion (despite the Northside Drive I-285 corridor traveling in free flow). Furthermore, the westbound traffic at each site was in free flow. This presents a huge advantage for eastbound detection over westbound detection, which the results portray.

Figure 70 below shows the eastbound ALPR travel times, derived from 203 exact plate matches, compared to the eastbound Bluetooth travel times, derived from 224 unique MAC address matches. It appears that work zones have an inherently variable travel time. Both the Bluetooth and ALPR data show an average travel time of 17.7 minutes in the work zone corridor.

The results also show what appears as a bimodal travel time, with a strong presence of a ten minute travel time, as well as a 15 to 20 minute travel time for the entire data collection period as measured by the Bluetooth sensors. The ALPR reads have no data points in the ten minute travel time, but only in the average 17.7 minute travel time. One possible explanation for this is that those vehicles with a ten minute travel time were present in the left-most lane, or outside lanes, in the start of the work zone, and were not caught into congestion until the end of the construction taper. The ALPR cameras are less likely to detect plates in the outside lanes if there are vehicles in the inside lanes blocking the view of the cameras. However, Bluetooth can detect devices in all lanes. Further investigation is required to determine what lanes the vehicles were in when

detected by the ALPR system, and whether this played a role in the travel time trend evident in the results.

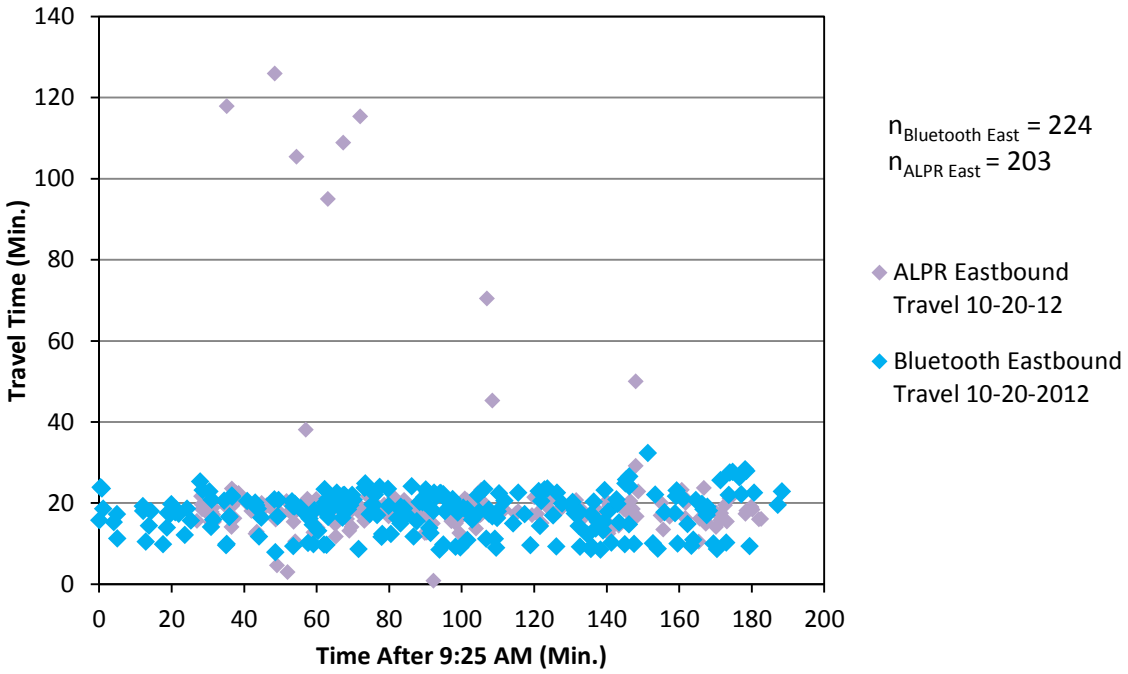

Figure 70 Work Zone Bluetooth and ALPR Travel Time Comparison (all data) from Paces Ferry Road to Northside Drive on I-285 E on 10-20-12

Chapter 7: Conclusions

7.1 Discussion of Results

The findings presented in this thesis provide additional insight into the performance of Bluetooth-enabled devices as well as Bluetooth sensors in various controlled and uncontrolled environments. The controlled indoor tests of Bluetooth device and sensor characteristics shed light on the unique detection properties of Class 1 and Class 2 Bluetooth enabled devices, and how those patterns of detection change with the introduction of multiple Bluetooth sensors. The 14th Street tests allowed the research team to measure the average detection range of various Class 1 and Class 2 devices around both a midblock and intersection sensor, but further statistical analysis is needed to translate this detection range into a travel time error. The non-work zone travel time tests on I-285 demonstrated that side-fire Bluetooth sensors provide an accurate measure of corridor travel time, and the active work zone travel time tests reinforced this finding. The following sections provide a brief discussion of the results presented in this thesis, and how the findings show that Bluetooth technology is a reliable method of real-time work zone travel time.

7.1.1 Detection Range Summary

The detection range test results show that Class 1 devices have more detection per run, a greater detection range, greater variability in their detection location, and are distributed both upstream and downstream of the Bluetooth sensors for all detection range calculation methods. Class 2 devices typically have fewer detections per run (one detection per run at the midblock location, often no detection) than Class 1 devices; less

variable detection, no extreme detection range values, and their detections are often concentrated downstream of the midblock sensor and upstream the intersection sensor for the eastbound direction of travel (i.e. the direction closer to the sensor).

The average detection range error is much lower than the potential 600 foot distance error between two sensors along a corridor, defined by the 300 foot transmission range properties of Class 1 devices. Although extreme distances were present, upwards of 1000 feet, 69% (out of 272) of all device detections for the midblock sensor and 91% (out of 854) of all device detections for the intersection sensor were within a 200 foot range.

7.1.2 Travel Time Summary

For this effort, the likelihood of achieving a MAC address pair depends on two variables: (1) traffic speed and (2) traffic proximity to the sensor. The potential third variable is the multitude of competing devices also in proximity to the sensor, but future efforts will have to demonstrate this influence, as the findings of this thesis are inconclusive in this regard. The findings demonstrate that detections increase as speed decreases and as sensor proximity increases. More detection increases the likelihood of a MAC address match and resulting travel time pair. Moreover, a travel time pair becomes more likely as the ingress and egress points along a corridor are minimized. The results show that the rate of pairing data between Paces Ferry Road and Northside Drive is significantly less than between Northside Drive and Roswell Road on the same day of travel, with 89 eastbound matches compared to 282 due to the likely departure of devices at the I-75 interchange.

An additional factor influencing travel time generation is that the sensors may not detect all devices within range. One reason for this lack of detection is because a device enters and exits a sensor's detection window before detection can occur (i.e. the device is not present in the sensor's detection window for the entire sensor cycle duration). The lack of sufficient capacity for detection is likely not the cause of a missed detection, because the results find that fifty devices, composed for 25 Class 1 and 25 Class 2 devices, do not reach the level of saturation of a single Bluetooth sensor.

7.2 Limitations of Research Study

The research team encountered several obstacles when designing the research to meet the ultimate goal of this thesis, which was to provide a method of measuring real-time travel time in an active work zone. The main factors that limited the scope of this study are the personnel requirements associated with multiple Bluetooth sensor stations, and the safe access to ideal deployment locations. The following sections detail how these factors specifically influenced the scope of the research conducted for this thesis.

7.2.1 Personnel Requirements

Access to an adequate number of research assistants places a constraint on acquiring an optimal number of deployment locations. About three individuals are needed to provide adequate staff support to each site and assist with the setup and takedown of the Bluetooth equipment. The average number of URA available for each day of deployment was about six, which is just enough for two Bluetooth stations, in addition to the GRA leaders. Two stations are not ideal for a large scale deployment to cover a 15 mile work zone corridor. About six stations, or one every three miles plus one at the end of the corridor, would have been sufficient to provide a real-time corridor

travel time, and capture vehicles before and after major egress and ingress points along the corridor. In addition to the limited number of available URAs for each day of data collection, the number of trained GRAs was always either two or three. One GRA is required at each data collection site to oversee the equipment setup, and ensure that the data collection proceeds safely and according to schedule. The limit of properly trained GRAs put an additional constraint on deploying at the optimal number of sites. While some of these constraints are specific to the research environment, it is expected that a regular field implementation of Bluetooth equipment will require additional personnel requirements, in terms of man-hours and training, in roadway projects.

An additional personnel constraint was present in the lack of personnel to assist with the processing of the overpass video for a ground truth travel time calculation. Because of the lack of available personnel, and the lengthy processing requirements, the video ground truth travel time data was not available in time for integration into this thesis. However, the ALPR sensors were able to provide a reasonable measure of ground truth travel time for the Bluetooth sensors.

7.2.2 Safe Access to Ideal Deployment Locations

In addition to the lack of sufficient personnel, the ability to safely access those sites most ideal for placing a Bluetooth device provided a further constraint. As discussed throughout this thesis, a Bluetooth sensor works most effectively when not within a 200 to 300 foot range of possible sources of interference. The interference comes from vehicles passing on a nearby overpass, vehicles passing on nearby streets or freeway on/off ramps, and also from overhanging vegetation or solid obstructions like poles and signs. The ideal location would avoid all of these interferences. However, it is

difficult to find safe locations along a freeway that are accessible via a sidewalk that is not within 200 feet of an overpass or on/off ramp.

The second aspect of ideal location is the ability to access the location at all with a sidewalk. The ideal location would be on either side of a major interchange to capture vehicles before they exit the corridor and as they get on the corridor. The ideal location would be to setup along the off-ramp from I-285 onto I-75 and SR-400, but there is no way to access this location safely, and the location is also not protected by a wall or guardrail, which is another requirement to meet the safety standards of deployment. The safety of project personnel and the traveling public was given highest importance when selecting potential data collection sites. Future deployments may consider using equipped construction vehicles that can be parked on the shoulder to increase the accessibility of optimal deployment locations. While again some of these constraints were specific to deployment as part of a research project, the use of this equipment in regular field construction projects will require workers near the active travel way and potential create some additional risks.

7.3 Feasibility of Bluetooth for Travel Time Measure in Work Zones

Unlike other vehicle detection technologies on the market such as ALPR, loop detectors, and infrared cameras, Bluetooth technology is not a fine-point mechanism. When a Bluetooth sensor detects a Bluetooth-enabled device in the traffic stream, the device may very well have come from any traffic stream within a 300 foot radius of the Bluetooth sensor. Although this property limits the ability of Bluetooth to solve work zone traffic management issues such as queue length buildup, the property allows for a more versatile application to travel time measurement. One benefit to Bluetooth not

being a fine point mechanism is that when mounted in side fire, vehicles in closer lanes of traffic will not block the inquiry signal transmission to farther lanes, or to traffic flowing in the opposite direction. The results demonstrate this property by showing that of all the detections by a sensor mounted closer to the eastbound traffic, between 5% and 25% of the total detections were for westbound devices.

Bluetooth experiences a favorable travel time match rate at individual sites in the range of 12% to 47%. In addition, the aggregate match rate increases significantly between sensor locations as the number of egress points and sensor separation are minimized along the corridor, from a minimum observed 6% when sensors were divided by the I-75 corridor to a maximum observed 30% aggregate match rate with no major interchange along the corridor. This provides evidence that the number of travel time measurements is contingent upon the placement of Bluetooth sensors, with optimal placement occurring both before major egress points and after major ingress points. Overall, Bluetooth appears as a viable method of work zone travel time measure when optimally located to capture ingress and egress traffic due to the high MAC address match rate and consequent travel time measurements, the ability to detect across lanes of traffic, as well as the ability to provide travel time measurements for more than one direction of travel.

7.4 Further Research

There are at least three steps of interest in further exploration of this research. The first is to develop an algorithm to model the correlation between traffic speed, closeness of traffic to a Bluetooth sensor, and the presence of competing devices on device detection potential. If a direct correlation is found, this would allow for the most

ideal deployment of Bluetooth sensor to meet the demands of the work zone corridor, and to most optimally detect travel times for both direction of a corridor.

The second step in the further research is to measure the travel time on adjacent corridors to the work zone to investigate how the work zone directly impacts congestion on alternative routes. An additional component to this investigation is the ability to provide alternative route recommendations to motorists to properly inform traveler decisions, and to measure the portion of traffic that diverts in response to these suggestions. By providing specific alternative route options through CMSs or an online server, the overall congestion of the work zone and surrounding area may be mitigated. Of course, this would require many more Bluetooth stations, and thus the ability to overcome the current limitations of this research including personnel availability, and safe access to ideal sensor locations.

The final step of the further research is creating a link to an on-line server that travelers can access when planning trips. Currently, the custom Bluetooth sensors are great for collecting and post-processing data for travel time, but they do not provide a direct upload of travel time information. Having a system that met the real-time uplink needs would allow the research team to study how an accurate measure of travel time on a roadway, provided in advance to users before they begin their trips, affects driver travel behavior.

Appendix A – Calculation of Detection Range

The All Eastbound detection category will be used as an example to portray how the un-weighted and weighted detection range values are calculated. First, Table 33 gives the modified results of the All Eastbound detections for the midblock sensor.

Table 33 All Eastbound Detections for the Midblock Sensor

	A	B	C	D	E	F
1	**Device**	**No. Records**	**No. Runs Detected (out of 27)**	**Average Offset (ft.)**	**Average Offset (Abs. Value)**	**Total Offset (ft.) - NEW**
2	*Class 1 IOGear USB Bluetooth Adapter 2*	50	20	133.67	218.61	6683.5
3	*Class 1 Toshiba Thrive AT-100 Tablet 1*	22	13	128.82	235.82	2834.04
4	*Class 1 Toshiba Thrive AT-100 Tablet 3*	19	12	101.99	101.99	1937.81
5	*Class 2 QStarz GPS 15*	12	12	96.73	104.26	1160.76
6	*Class 2 QStarz GPS 18*	7	7	82.99	82.99	580.93
7	*Class 2 Car Adapter 5*	12	12	90.81	95.78	1089.72
8	*Class 2 Car Adapter 6*	15	15	76.63	72.63	1149.45

The un-weighed detection range is calculated from the following equation:

$$\text{Average Un - Weighed Detection Range} = \text{Average (D2 : D8)} = \mathbf{101.66\ feet}$$

The first step in the weighted detection range is entering a new column (F), equal to the B entry for each row multiplied by the D entry for each row. Then, the average weighted detection range is calculated from the following equation:

$$\text{Average Weighted Detection Range} = \frac{\text{Sum(F2 : F8)}}{\text{Sum(B2 : B8)}} = \mathbf{112.67\ feet}$$

Appendix B – Detection Window Calculation

Figure 71 below provides a visual aid for the calculation of an approximate sensor detection window, assuming a circular detection pattern, using the outside eastbound lane at Paces Ferry Road as an example.

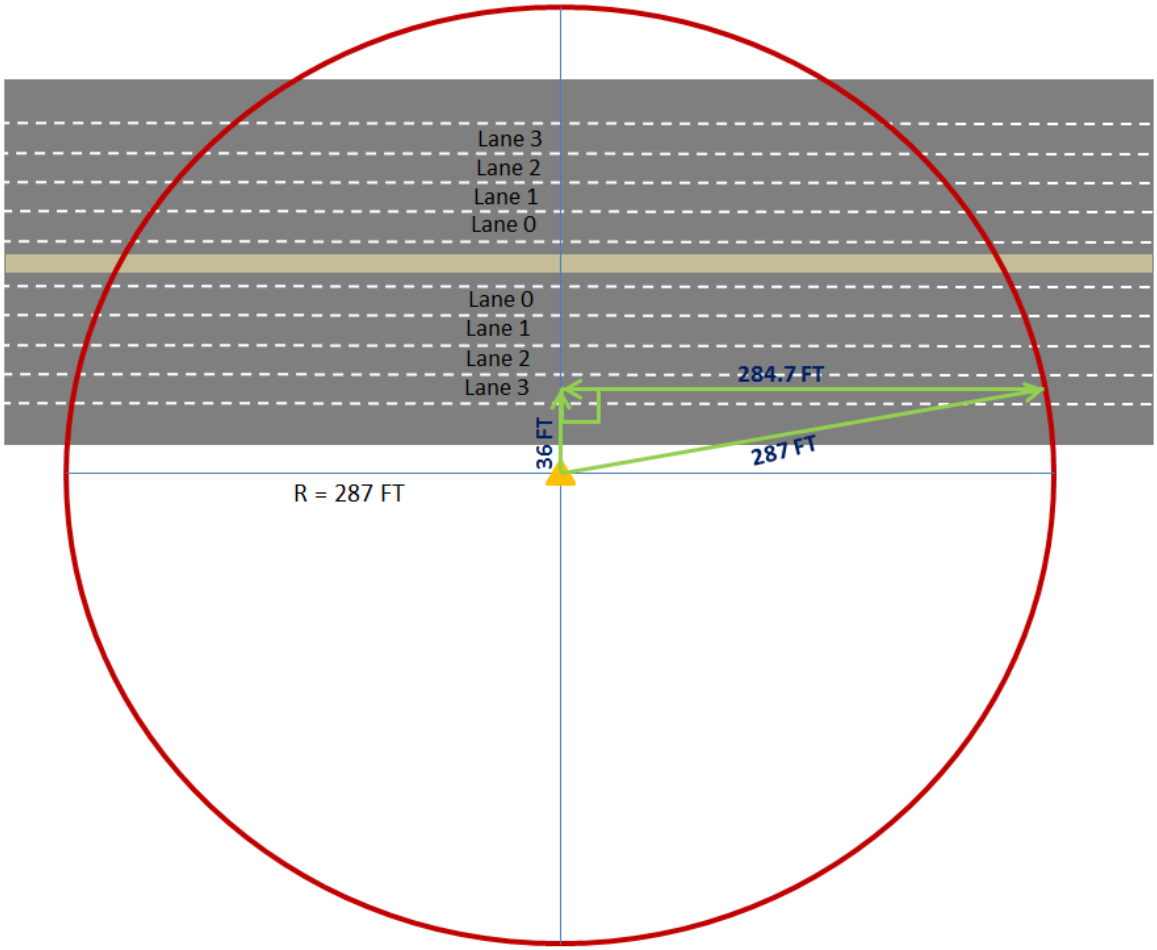

Figure 71 Paces Ferry Road Detection Window Visual Aid, not to scale (NTS)

Knowing the sensor offset from the edge of the roadway, and that each lane and outside shoulder are 12 feet and 15 feet wide, respectively, allows for the 36 foot

measurement from the sensor to the middle of the inside lane. Then, the Pythagoras Theorem allows for the calculation of the horizontal piece of the triangle. Doubling this value gives the approximate distance that the lane spends in the sensor detection window. This assumes that the antennae range is symmetric in either direction given that the antenna points directly at the road. Then, giving different travel speeds, the time a lane is spending in the detection window for different levels of congestion may be calculated. By summing these times for all the eastbound lanes and all the westbound lanes separately, one can calculate the proportion of time each direction spends in the sensor's detection window.

Appendix C – Chi Squared Test for MAC Address Detection Frequency

The first step in the Chi Squared test is to define the null and alternative hypotheses.

H_o = MAC addresses detected ≤6 times and MAC addresses detected >6 times **DO NOT** produce different travel times

H_o = MAC addresses detected ≤6 times and MAC addresses detected >6 times **DO** produce different travel times

After defining the null hypothesis, the travel time must be broken up into bins so that each bin has at least five records to qualify the Chi Squared test. Figure 72 shows the travel time distribution for the two groups identified in the null hypothesis.

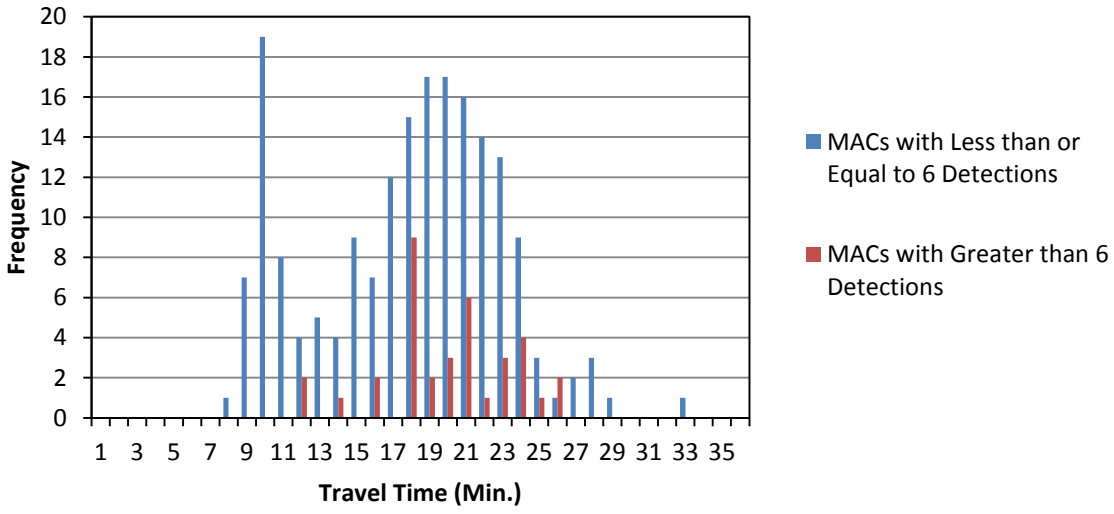

Figure 72 Travel Time Distribution Comparing Effect of MAC Address Frequency

Table 34 below shows the travel time broken into appropriate bins, as well as the observed values for ≤6 and >6 MAC address repetitions for each bin. The table also shows the sum values for each row and column, which combine to produce the expected values via the equation shown below.

Table 34 Observed Values for MAC Frequency Categories

Travel Time Bins	MACs with ≤6 Repetitions	MACs with >6 Repetitions	Sum
0-16	64	5	69
17-18	27	9	36
19-20	34	5	39
21-22	30	7	37
23-35	33	10	43
Sum	188	36	N=224

$$\text{Expected Value} = \frac{\text{Row Total} \times \text{Column Total}}{\text{Total N}}$$

Table 35 shows the expected values for the same bin and MAC frequency combinations.

Table 35 Expected Values for MAC Frequency Categories

Travel Time Bins	MACs with ≤6 Repetitions	MACs with >6 Repetitions
0-16	57.91	11.09
17-18	30.21	5.79
19-20	32.73	6.27
21-22	31.05	5.95
23-35	36.09	6.91

Next, the following equation shows how the Chi Squared value was calculated for each individual cell and Table 36 shows the individual cell values.

$$\text{Chi Squared} = \sum \frac{(\text{Observed} - \text{Expected})^2}{\text{Expected}}$$

Table 36 Individual Cell Chi Square Values

Travel Time Bins	MACs with ≤6 Repetitions	MACs with >6 Repetitions
0-16	0.640	3.344
17-18	0.342	1.786
19-20	0.049	0.256
21-22	0.036	0.187
23-35	0.264	1.381

By summing all the cell values, there is a final Chi Square value of 8.825. There are five bin divisions, so (n-1) or four degrees of freedom are taken for this scenario. Using an alpha sensitivity of 0.05, and four degrees of freedom, the Chi Squared table gives a value of 9.488. Because 8.825 is less than 9.488, the null hypothesis is accepted, and the two groups of ≤6 and >6 MAC address repetitions are not significantly different. Given the small sample size, the Chi Squared test could not show that the two samples are statistically significant, so this test should be repeated when a larger sample size is available.

References

1. "Bluetooth Tutorial – Baseband" Palowireless Bluetooth Resource Center, Accessed from http://palowireless.com/bluearticles/baseband.asp

2. Johnson Consulting (2004) "Bluetooth – An Overview: How Networks Are Formed and Controlled," Accessed from http://www.swedetrack.com/images/bluet10.htm

3. G. Zaruba, *et al.*, (2004) "Simplified Bluetooth Device Discovery – Analysis and Simulation" The University of Texas at Arlington, Proceedings of the 37th Hawaii International Conference on System Sciences, Accessed from http://crystal.uta.edu/~zaruba/Publications/C20.pdf

4. G. Kewney, (2004) "High Speed Bluetooth Comes a Step Closer: Enhanced Data Rate Approved," Access from http://www.newswireless.net/index.cfm/article/629

5. S. Quale, *et al.*, (2010) "Arterial Performance Measures with Media Access Control Readers; Portland, Oregon, Pilot Study" Transportation Research Board of the National Academies, Washington, D.C. Transportation Research Record No. 2192, pg. 185-193

6. Motorola (2008) "Bluetooth Radio Performance Technical Brief: Rugged Bluetooth Scanners" Access from

7. M. Loy, *et al.*, (2005) "ISM-Band and Short Range Device Regulatory Compliance Overview" Texas Instruments, Application Report SWRA048, Accessed from http://www.ti.com/lit/an/swra048/swra048.pdf

8. Semtech International AG (2006) "FCC Regulations for ISM Band Devices: 902-928 MHz" AN1200.04, Wireless and Sensing Products, Accessed from http://www.semtech.com/images/datasheet/fcc_part15_regulations_ag.pdf

9. University of Maryland (2008) "Bluetooth Traffic Monitoring Technology; Concept of Operation and Deployment Guidelines" Center for Advanced Transportation Technology

10. R. Woodings, *et al.*, (2001) "Rapid Heterogeneous Connection Establishment: Accelerating Bluetooth Inquiry Using IrDA" Department of Computer Science, Bringham Young University, Accessed from http://mcl.cs.byu.edu/downloads/IrDA_Assisted_BT_Discovery.pdf

11. "Bluetooth Tutorial – Bluetooth Glossary" Palowireless Bluetooth Resource Center, Accessed from http://www.palowireless.com/infotooth/glossary.asp

12. L. Harte, (2010) “Introduction to Bluetooth: Technology, Market, Operation, Profiles, and Services,” Second Edition, Athos Publishing, Fuquay-Varina, North Carolina

13. “Bluetooth Radio Layer Tutorial” Palowireless Bluetooth Resource Center, Accessed from http://www.palowireless.com/infotooth/tutorial/radio.asp

14. D. Chakraborty, *et al.*, (2006) "Discovery and Delay Analysis of Bluetooth Devices," 7th International Conference on Mobile Data Management, Accessed from http://ieeexplore.ieee.org/stamp/stamp.jsp?tp=&arnumber=1630650

15. B. Peterson, *et al.*, (2006) “Bluetooth Inquiry Time Characterization And Selection”, IEEE Transactions On Mobile Computing, Vol. 5, No. 9. Accessed from http://ieeexplore.ieee.org/stamp/stamp.jsp?tp=&arnumber=1661527

16. Federal Highway Administration FHWA (2004) “Intelligent Transportation Systems in Work Zones: A Case Study: Work Zone Travel Time System”, Accessed from http://ops.fhwa.dot.gov/wz/technologies/arizona/arizona.pdf

17. Ontario Ministry of Transportation (2011) “Saddle up with Bluetooth: MTO First in Canada to use Bluetooth for Travel Time Monitoring” Ontario’s Transportation Technology Transfer Digest, Summer 2011, Vol. 17, Issue 3, Access from http://www.mto.gov.on.ca/english/transtek/roadtalk/rt17-3/index.shtml#a3

18. A. Voigt, (2011) “Collecting External Data Using Bluetooth Technology”, Texas Transportation Institute, Houston, TRB 90th Annual Meeting, Session 175, PowerPoint Presentation

19. “Bluetooth Radio Communications” Stevens Water Monitoring Systems, Inc., Accessed from http://www.stevenswater.com/telemetry_com/bluetooth_info.aspx

20. (2012) “XRange2000” Mind Vision Consulting, BlueMagnet, Accessed from http://www.bluemagnet.com/xrange2000.html

21. A. Haghani, *et al.*, (2010) “Data Collection of Freeway Travel Time Ground Truth with Bluetooth Sensors” Transportation Research Record: Journal of the Transportation Research Board, No. 2160

22. (2011) “Bluetooth Versions”, SP Commerce LLC, Accessed from http://bluetomorrow.com

23. J. Porter, D. Kim, and M. Magana (2011) “Wireless Data Collection Systems for Real-Time Arterial Travel Time Estimates” RS 500-410, Oregon Department of Transportation and Oregon Transportation Research and Education Center

24. S.M. Baker (2010) “Bluetooth Technology to be Standard in More Than 90 Percent of Automobiles by 2016” Kirkland, WA, November 18th, 2010, Accessed from http://www.bluetooth.com/Pages/Press-Releases-Detail.aspx?ItemID=117

25. Governors Highway Safety Association (2012) “Cell Phone and Texting Laws”, State Laws and Funding, Accessed from http://www.ghsa.org/html/stateinfo/laws/cellphone_laws.html

26. C. Monsere, *et al.,* (2006) “Validating Dynamic Message Sign Freeway Travel Time Messages with Ground Truth Geospatial Data” Transportation Research Record No. 1959

27. J.S. Wasson, *et al.*, (2008) “Real-Time Travel Time Estimates Using Media Access Control Matching” ITE Journal, June 2008.

28. L. Tudor, *et al.,* (2003) “Deployment of Smart Work Zone Technology in Arkansas” Transportation Research Record No. 1824, Accessed from http://trb.metapress.com/content/e2655n7753500257/fulltext.pdf

29. R. Varon, (2010) “Sensors Use Bluetooth to Compute Travel Times on Ike”, ABC 7 News, Chicago, IL, Accessed from http://abclocal.go.com/wls/story?section=resources/traffic&id=7473453

30. R.J. Haseman, *et al.,* (2010) “Real-Time Measurement of Travel Time Delay in Work Zones and Evaluation Metrics Using Bluetooth Probe Tracking”, Transportation Research Record No. 2169

31. C.A. Quiroga and D. Bullock (1998) “Determination of Sample Sizes for Travel Time Studies” ITE Journal, August 1998, Accessed from http://www.ite.org/membersonly/itejournal/pdf/JHA98A92.pdf

32. Texas A&M Transportation Institute (2012) “TTI-Designed Information System Helps Keep I-35 Travelers Informed”, September 28, 2012, Accessed from http://tti.tamu.edu/2012/09/28/tti-designed-information-system-helps-keep-i-35-travelers-informed/

33. H.T. Zwahlen and A. Russ (2002) “Evaluation of the Accuracy of a Real-Time Travel Time Prediction System in a Freeway Construction Work Zone” Transportation Research Record No. 1803, Paper No. 02-2371

34. Federal Highway Administration (2008) “Comparative Analysis Report: The Benefits of Using Intelligent Transportation Systems in Work Zones”, U.S.

Department of Transportation, Report Number FHWA-HOP-09-002. Accessed from http://ops.fhwa.dot.gov/wz/its/wz_comp_analysis/comp_anl_rpt_08.pdf

35. Vehicle Detector Clearinghouse (2007) "A Summary of Vehicle Detection and Surveillance Technologies Used In Intelligent Transportation Systems" Federal Highway Administration, Accessed from http://www.fhwa.dot.gov/policyinformation/pubs/vdstits2007/vdstits2007.pdf

36. T. Notbohm, et al., (2001) "Smart Work Zone Deployment Initiative Summer 2001 Travel Time Prediction System (TIPS)" Wisconsin Evaluation, Accessed from http://www.eng.mu.edu/~drakopoa/web_documents/TIPS/Tipswisconsin.pdf

37. S. Du, et al., (2012) "Automatic License Plate Recognition (ALPR): A State of the Art Review" IEEE Transactions on Circuits and Systems for Video Technology, Accessed from http://ieeexplore.ieee.org/stamp/stamp.jsp?tp=&arnumber=6213519

38. Y. Malinovskiy, et al., (2009) "Field Experiments on Bluetooth-based Travel Time Data Collection" University of Washington, Accessed from http://staff.washington.edu/yegorm/Papers/2009_TRB_Bluetooth.pdf

39. J. Barcelo, et al., (2010) "Travel Time Forecasting and Dynamic Origin-Destination Estimation for Freeways Based on Traffic Monitoring" Transportation Research Record No. 2175, Accessed from http://trb.metapress.com/content/17x1v88n6p8363p1/fulltext.pdf

40. S. Box (2011) "Arterial Roadway Traffic Data Collection Using Bluetooth Technology" Master's Thesis, Georgia Institute of Technology

41. DVDVideoSoft "Free Video to JPG Convertor" Accessed from http://www.dvdvideosoft.com/products/dvd/Free-Video-to-JPG-Converter.htm

42. K. D'Ambrosio (2011) "Methodology for Collecting Vehicle Occupancy Data on Multi-Lane Interstate Highways: A GA 400 Case Study" Master's Thesis, Georgia Institute of Technology